Liquid Phase Heterogeneous Catalysis - Deeper Insight; Novel Transient Response Technique with ESI-MS as a Detector

Dejan Radivojević

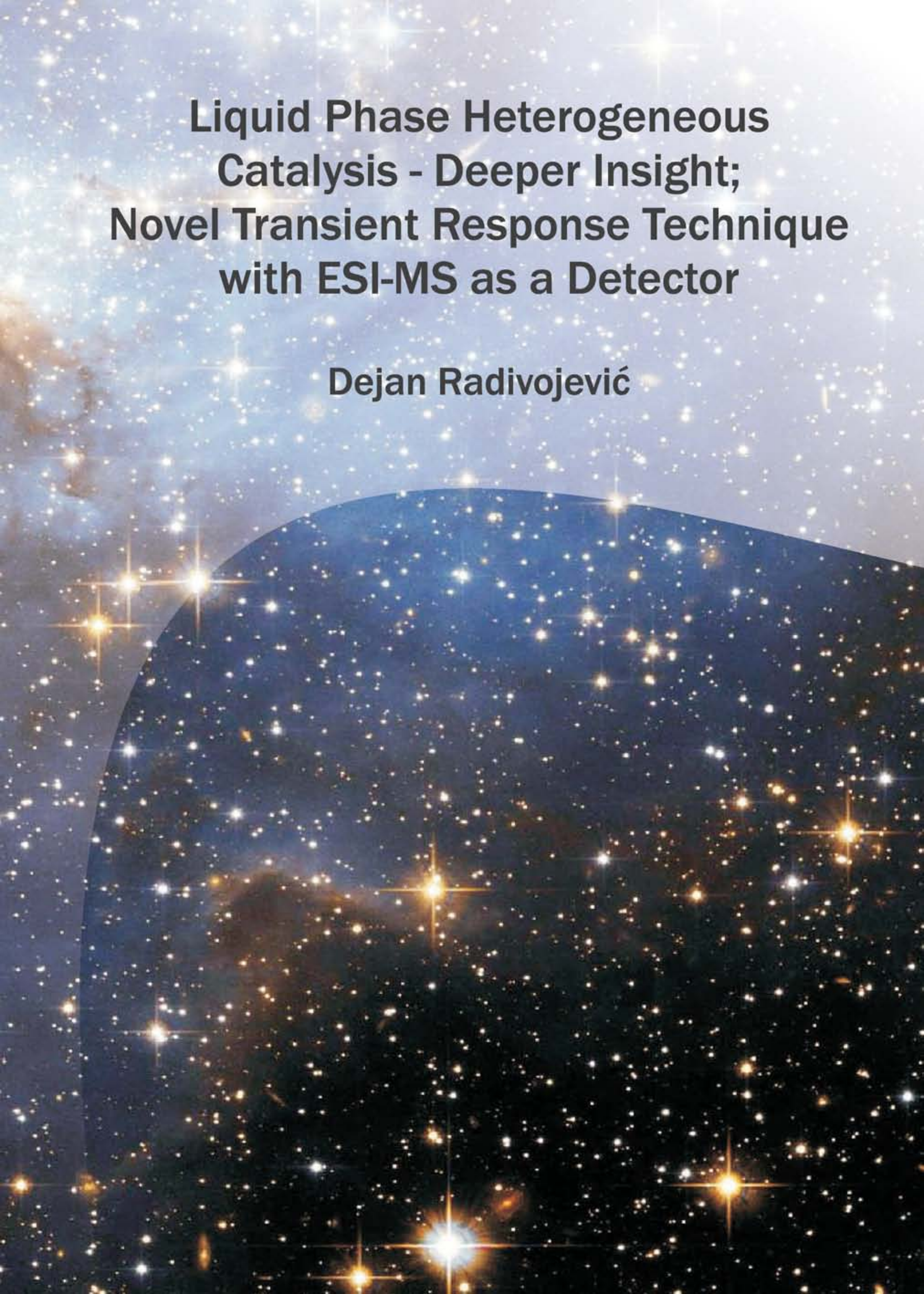

Liquid phase heterogeneous catalysis — deeper insight; Novel transient response technique with ESI-MS as a detector

Samenstelling promotiecommissie:

Rector Magnificus, voorzitter	Universiteit Twente
Prof. dr. ir. L. Lefferts, promotor	Universiteit Twente
Dr. ir. K. Seshan, assistent-promotor	Universiteit Twente
Prof. dr. ir. M. Wesseling	Universiteit Twente
Prof. dr. ir. W. P. M. van Swaaij	Universiteit Twente
Prof. dr. ir. J. G. E. Gardeniers	Universiteit Twente
Prof. dr. ir. J. C. Schouten	Universiteit Eindhoven
Prof. dr. C. Hardacre	University of Belfast
Dr. ir. H. Oevering	DSM

Publisher:
Gildeprint, Enschede, The Netherlands

ISBN 978-90-365-2667-8

Author email: `dejan_radivojevic@yahoo.com`

LIQUID PHASE HETEROGENEOUS CATALYSIS — DEEPER INSIGHT; NOVEL TRANSIENT RESPONSE TECHNIQUE WITH ESI-MS AS A DETECTOR

PROEFSCHRIFT

ter verkrijging van
de graad van doctor aan de Universiteit Twente,
op gezag van de rector magnificus,
prof. dr. W. H. M. Zijm,
volgens besluit van het College van Promoties,
in het openbaar te verdedigen
op vrijdag 23 mei 2008 om 15.00 uur
door

Dejan M. Radivojević

geboren op 11 juli 1972
te Kraljevo (Servië)

Dit proefschrift is goedgekeurd door de promotors:

Prof. dr. ir. L. Lefferts

en de assistent-promotor

Dr. ir. K. Seshan

Шта је Љубав? Није опипљива, мерљива а често није ни очигледна. Битна је јер сви причају о њој; вредна је јер је сви желе. Ја замишљам Љубав као катализатор у нама који може да учини човека способним да дотакне звезде.

Посвећено мојим највољенијима — Људини, Лики, Секи и Мари

Contents

1

Introduction

Development of heterogeneous catalysts for the liquid phase processes requires detailed knowledge about phenomena that occur on the catalyst surface during the catalytic reaction in liquid phase. Transient response technique with detectors that can perform continuous, rapid, multi-component and simultaneous detection are ideal for such studies. However, there are hardly any transient techniques available that allow experimental investigation of the adsorption of reactants, intermediates and probe-molecules from liquid phase on the surface of catalysts. The existing liquid phase detectors are not able to detect more than one specie simultaneously and rapidly, making the more detailed study of the catalytic reaction mechanisms impossible. Development and application of a transient response technique for studies of adsorption and catalytic reactions over heterogeneous catalysts in liquid phase with ESI-MS as detector can be an option to overcome the problem.

1.1 Catalysis in modern world

PROCESSES IN THE CHEMICAL INDUSTRY convert readily available starting materials to more valuable product molecules. Catalytic materials are used in these processes to accelerate chemical transformations so that reactions proceed in a highly efficient manner, achieving high yields of desirable products and avoiding unwanted by-products. Compared to classical stoichiometric procedures, catalysts often allow more economical and environment-friendly production. Approximately 85–90 % of the products of the chemical industry are made applying catalytic processes. The annual turnover of the catalysts market in 2007 was close to $13.5 billion, increasing annually with of 5 % [1]. Catalysts are indispensable in three main fields of application [2]:

1. Production of transportation fuels
2. Production of bulk and fine chemicals
3. Abatement of pollution in end-of-pipe solutions (automotive and industrial exhaust)

Within these application areas, environmental catalysts [3] are the largest segment of the catalyst market due to increasingly strict legislation concerning emissions [4]. One of the trends in catalysis is including increasing use of sophisticated tools to study and characterize catalytic materials [5].

1.2 Multiphase catalytic processes

Chemical operations are increasingly carried out as multiphase processes [6, 7], particularly in aqueous phase, because use of water as a solvent offers advantages over organic solvents [8], i.e. low cost and availability, safety in use and less negative impact on the environment.

Typical multiphase heterogeneous catalytic process in slurry phase can be broken down into several steps (Figure 1.1):

1. transfer of gaseous reactant from the bulk phase to the gas/liquid interface (diffusion) and
2. from there to the bulk liquid phase (adsorption and diffusion)
3. transfer of both reactants (gas and liquid) from bulk liquid to the external surface of the catalyst particle (diffusion through stagnant external film surrounding catalyst particle)

4. transfer of reactants into the porous catalyst (internal diffusion)
5. adsorption of reactants
6. surface reaction
7. desorption and transfer of product(s) by
   (a) internal and
   (b) external diffusion to bulk liquid or gas phase [9, 10].

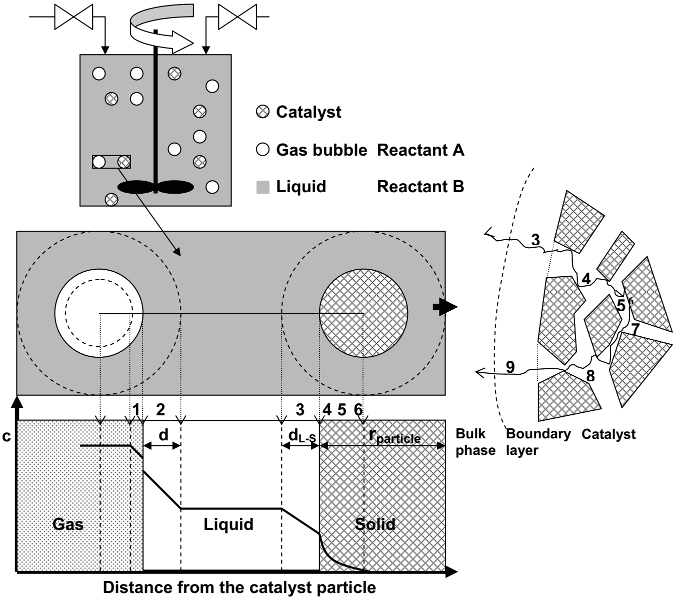

Figure 1.1: *Concentration profile for a heterogeneously catalyzed chemical reaction*

In case mass transfer is slow compared to the reaction rate, concentration gradients will occur, especially in the pores of a heterogeneous catalyst. Concentration gradients may prevent optimal operation because the active catalytic sites experience different concentrations and part of the active sites operates under nonoptimal conditions. Thus, selectivity of multiphase catalytic reactions can be affected by mass transfer limitation. As an example, D'Arino et al. [11] studied the influence of intraparticle diffusion and local buffering during selective hydrogenation of nitrites and nitrates from aqueous solution over Pt and Pd based catalysts. It was reported that it is essential to maximize accessibility of all reactants to the active catalytic sites dispersed throughout the internal pore structure of the catalyst, in order to maximize the selectivity towards nitrogen. The concentration gradient in the pores of a catalyst particle is minimized when the Thiele modulus (quantifies the ratio of the reaction to the diffusion rate in the particle, Eq.1) approaches zero:

$$\phi = L \cdot \sqrt{\frac{k_v \cdot C^{n-1} \cdot \tau}{\epsilon \cdot D_{mol}}} \tag{1.1}$$

L - diffusion path, k_v - volumetric rate coefficient, C - reactant concentration, n - the order of the reaction, τ - tortuosity, ϵ- porosity and D_{mol} - diffusion coefficient. This can be achieved via shortening the diffusion path L, (i.e. using small catalyst particles) and via increasing the pororsity of the particles ϵ, which will in general also result in a decrease in the tortuosity τ. Unfortunately, application of small particles in a fixed bed causes large pressure drops and the use of slurry reactors is preferable, resulting in disadvantages such as attrition of the catalyst particles causing a loss of active materials, need for relative expensive and non-robust filtration units and erosion of the equipment.

Decreasing pressure drop by using shallow beds (pancake shape) is not a solution because of misdistribution (channeling) of the liquid flow. That is the driver for current developments of new, more accessible catalytic structures that have lower pressure drops and better mass transfer properties e.g. thin layers of catalyst on monoliths and foam materials [12]. Additional advantages can be obtained by using highly porous thin layers on monoliths and foams, e.g. based on carbon-nano-fibers. Particles and layers consisting of carbon nanofibers are promising catalyst supports because of the combination large pore volume (0.5–2 cm^3/g) and extremely open morphology, on one hand, and significant high surface area (100–200 m^2/g), on the other hand [13]. Structured catalyst supports based on CNFs (Figure 1.2), have a structure similar to the inverse structure of a conventional porous support material.

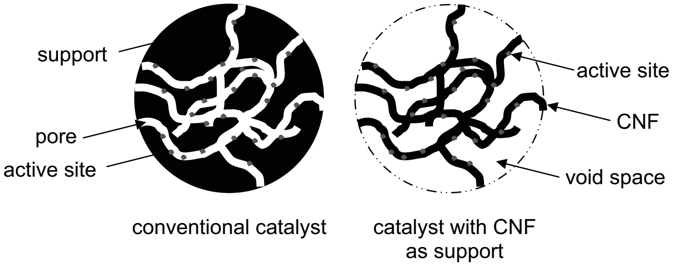

Figure 1.2: *Catalyst with conventional (left) and CNF (right) as a support*

Superior performance of monolith reactors was credited to improved mass transfer due to Taylor flow: gas bubbles and liquid slugs flow consecutively through the monolith channels [14]. Gas-solid mass transfer is enhanced because only a thin liquid film separates the gas from the catalyst [15].

1.3 Tools and methods to study heterogeneous catalysts in gas and liquid phase

Improvement of catalysts and understanding of reaction mechanisms for gas phase reactions has been enormously enhanced by the availablity of powerful characterization tools as well as methods that allow characterization in-situ or operando [16]. Unfortunately, most techniques require vacuum or low pressure and can not be used in liquid phase directly; these techniques need to be tuned for application in liquid phase in order to deal with the solvent, being present in high excess by definition. An example of successful modification of a characterization technique to enable experiments in liquid phase is Infra-Red (IR) spectroscopy in Attenuated Total Reflection (ATR) [17, 18] mode. Next to spectroscopic tools, different methods (i.e. steady state or transient) are applied frequently to obtain kinetic and mechanistic information.

Measurement of reaction kinetics and determination of rate expressions and constants are usually carried out in steady-state experiments. The benefit of steady-state experiments is that these are simple for analysis and highly relevant for industrial production processes where a continuous flow is passed through the reactor. Under steady state conditions all elementary steps, i.e. adsorption, surface reaction and desorption, are progressing at the same rate. Unfortunately, information obtained from steady state kinetic analysis provides lumped kinetic data without details about elementary steps and short-lived reaction intermediate species, except for the rate-determining elementary step. Compared with steady-state measurements, transient experiments can provide more information. As a matter of fact, it allows to evaluate the residence time and the surface accumulation of the reaction intermediates and may also provide information on possible competition in adsorption/desorption steps with co-reacting molecules. Transient methods can be applied to determine surface coverages via material balances while reactivity of the pre-adsorbed surface species can be studied in titration type experiments. Furthermore, a broad window concentrations of reactants, intermediates and products can be explored in a single experiment. The transient kinetic analysis is based on the principle

1. of perturbing a steady-state established on a working catalyst by changing abruptly one or more variables such as feed concentration, molar flow rate, pressure or temperature, and

2. of following the relaxation of the system.

Various authors reviewed transient response techniques applied in heterogeneous catalysis in gas phase [19–24]. In general, the experimental set-up consists of a reactor, a switching valve and a rapid analyzer (Figure 1.3). Flow reactors used in the transient experiments are preferably either a plug-flow (tubular) reactor [25] or a perfectly backmixed (tank) reactor [26], providing relatively easy interpretation and analysis of the transient response data. Experimental equipment is usually equipped with switching valves to introduce well defined step or pulse changes. Finally, the setup must be equipped with an analyzer that can perform continuous analysis of the reaction components. On-line monitoring of the reactor outlet should have sufficient time resolution.

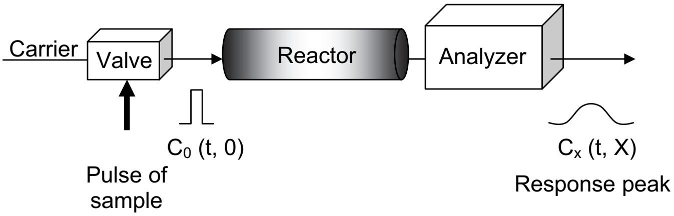

Figure 1.3: *Transient response set-up*

For example, transient methods applied with rapid reactions requires sub-milisecond time resolution. That can be achieved with the Temporal Analysis of Products (TAP) technique [27]. In the case of TAP a very narrow pulse of reactant is injected to a reactor system, which is evacuated at the other end. Mass transport takes place in the Knudsen diffusion regime and the output pulse reflects the mass transport and intrinsic reaction kinetics. However, TAP is costly technique, and analysis of the results require complicate modeling; furthermore, conditions (low pressure) during the experiments are usually quite different from process conditions, especially in the case of processes in liquid phase.

Another specific transient response technique is Steady State Transient Kinetic Analysis (SSITKA) [23, 28]. In SSITKA the system is first operated in steady state and then one of the reactants is suddenly switched to an isotopically labeled compound. The rate of exchange, monitored by mass spectrometry, reveals the intrinsic reaction kinetics as well as identification of those elementary steps that are kinetically relevant.

Transient experiments were not much used in liquid phase heterogeneous catalysis due to lacking suitable fast analysis techniques. The liquid phase detectors that have been used (i.e. UV-Vis [29–31], RI [32, 33]) are not able to detect more than one specie, which is actually limiting the technique so far to adsorption and diffusion studies, while catalytic reactions were not possible to study in detail. The only transient study of a catalytic reaction was reported by Toukoniitty et al. [34] who used Gas Chromatography (GC) to study hydrogenation of dione over Pt/SiO_2 catalyst. Obvious limitation in this case was relatively slow sampling of the effluent from the reactor, every 5 minutes. Mass Spectrometry (MS), a powerful detector able to detect multiple components simultaneously in gas phase, is not in common use in liquid phase. Main difficulty is to maintain high vacuum (10^{-6}–10^{-8} mbar), necessary for proper operation of MS, despite the introduction of a liquid. For that reason, various interfaces have been developed [35] that can remove solvent from analyte species, like Electro-Spray Ionization (ESI) or Atmospheric Pressure Chemical Ionization (APCI) for applications in HPLC-MS technology [36, 37]. To the best of our knowledge, transient techniques using MS equipped with ESI as a detector to analyze a liquid-stream leaving the reactor has not been described before. Goal of the present study is to develop and explore this technique using ESI-MS as a detector, to perform simultaneous identification and quantification of species. Furthermore, the ability of the new technique will be explored with two catalytic reaction systems in aqueous phase:

1. catalytic reduction of nitrite (NO_2^-) over a Pt/SiO_2 catalyst and

2. catalytic oxidation of glucose over Pt supported on carbon.

1.3.1 ESI process

The electrospray ionization interface removes solvent and ionizes analyte species (Figure 1.4a) from the liquid sample. The ionization process consists of three main steps [38] (Figure 1.4b): droplet formation, droplet shrinkage, and vaporization (formation of gas-phase ions). A sample flows through the capillary, which is kept at a high potential. When a sample approaches the capillary tip a so-called Taylor cone is formed, followed by the formation of a cloud of highly charged, fine droplets.

At the same time, hot nitrogen flows in normal direction to the cloud to evaporate solvent from the droplets. The charged droplets fly towards the mass spectrometer driven by both pressure and potential gradients. While flying to the detector, the droplets shrink due to evaporation of the solvent, which causes the charge density on the droplets surface to rise to a critical value. When the Coulombic repulsion forces exceed the surface tension forces, the droplets explode into smaller droplets (Coulombic explosion). The continuous solvent evaporation will eventually lead to the formation of desolvated, partially solvated and associated analyte ions.

Nitrogen and other dissolved gasses can not be detected with ESI-MS due to the soft ionization nature of interface. In order to arrive at an universal transient technique for liquid phase experiments allowing detection of both organic compounds

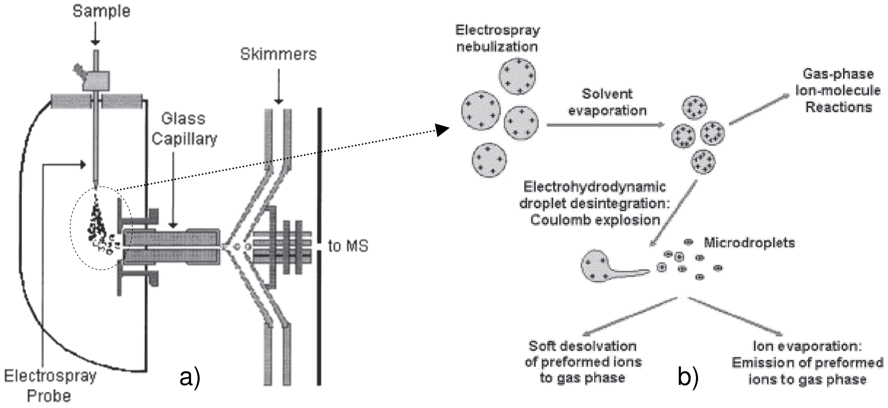

Figure 1.4: *Schematic of ESI-MS: a) liquid phase interface and b) ESI process*

and ions (ESI-MS) as well as dissolved gases a separate gas analyzer is necesary. Therefore, development of an analyzer similar to Membrane Inlet Mass Spectrometry (MIMS) [39] is another goal of the present study.

1.4 Outline of this thesis

This thesis focuses on development and application of a transient response technique for studies of heterogeneous catalysts in liquid phase with ESI-MS as detector that can perform on-line multi-component simultaneous analysis of reacting systems.

In *Chapter 2* we explored tailored preparation methods for Pt/SiO_2 catalysts. Pt-precursors suitable for the preparation of catalytic reactors at temperatures below 150 °C will be presented. This is important because microstructured reactors are preferred in order to prevent the pressure-drop over the reactor and polymer based microstructured reactors, with limited temperature stability, is one option to achieve this.

In *Chapter 3*, development and demonstration of the transient technique equipped with ESI-MS analyzer will be described. Capabilities and unique opportunities of the novel technique will be shown with multi-component and simultaneous quantitative detection of reacting and adsorbing species over Pt/SiO_2 and Pt/CNF/Ni catalysts.

Detection of dissolved gases is necessary and *Chapter 4* will describe development and demonstration of analyser based on MIMS. Capabilities and opportunities of the analyzer will be shown with H_2–O_2 and O_2–H_2 titrations using liquid phase over EuroPt-1, Pt/SiO_2 and Pt/CNF/Ni catalysts in order to determine amounts of Pt available for reaction.

Chapter 5 describes preparation of a novel structured reactor, suitable for transient operation, by incorporating mono-dispersed Pt/SiO_2 catalyst particles into an EVAL polymer porous matrix.

Finally, in *Chapter 6* results are summarized and concluding remarks are presented.

References

[1] A. E. Comyns. Future fuel cells? *Focus on Catalysts*, 2003(8), 1 (2003).

[2] I. Chorkendorff and J. W. Niemantsverdriet. *Concepts of Modern Catalysis and Kinetics.* Wiley-VCH Verlag GmbH&Co. KgaA, Weinheim, 1 edition (2003).

[3] `http://www.nacatsoc.org`

[4] Air quality guidelines for particulate matter, ozone, nitrogen dioxide and sulfur dioxide - Summary of risk assessment. Technical report, World Health Organization, Geneva (2005).

[5] C. H. Bartholomew and R. J. Farrauto. *Fundamentals of industrial catalytic processes.* John Wiley & Sons, Inc., Publication (2006).

[6] M. P. Dudukovic, F. Larachi and P. L. Mills. Multiphase reactors — revisited. *Chemical Engineering Science*, 54, 1975–1995 (1999).

[7] C. G. M. van de Moesdijk. *The catalytic reduction of nitrate and nitric oxide to hydroxylamine: kinetics and mechanism.* Ph.D. thesis, University of Eindhoven, The Netherlands (1979).

[8] P. T. Anastas, L. G. Heine and T. C. Williamson. *Green Chemical Syntheses and Processes.* American Chemical Society, Washington, D.C (2000).

[9] R. A. van Santen, P. W. N. M. van Leeuwen, J. A. Moulijn and B. A. Averill, editors. *Catalysis: An Integrated Approach.* Elsevier Science B. V. (1999).

[10] H. S. Fogler. *Elements of chemical reaction engineering.* Prentice-Hall Inc., New Jersey, USA, 3 edition (1999).

[11] M. D'Arino, F. Pinna and G. Strukul. Nitrate and nitrite hydrogenation with Pd and Pt/SnO_2 catalysts: the effect of the support porosity and the role of carbon dioxide in the control of selectivity. *Applied Catalysis B: Environmental*, 53, 161–168 (2004).

[12] C. P. Stemmet, J. N. Jongmans, J. van der Schaaf, B. F. M. Kuster and J. C. Schouten. Hydrodynamics of gas-liquid counter-current flow in solid foam packings. *Chemical Engineering Science*, 60, 6422–6429 (2005).

[13] J. K. Chinthaginjala, K. Seshan and L. Lefferts. Preparation and Application of Carbon-Nanofiber Based Microstructured Materials as Catalyst Supports. *Industrial & Engineering Chemical Research*, 46, 3968–3978 (2007).

[14] F. Kapteijn, J. J. Heiszwolf, T. A. Nijhuis and J. A. Moulijn. Monoliths in multiphase catalytic processes. *CATTECH*, 3, 24–41 (1999).

[15] A. Cybulski and J. A. Moulijn. *Structured Catalysts and Reactors.* Marcel Dekker, New York, 1 edition (1998).

[16] J. W. Niemantsverdriet. *Spectroscopy in Catalysis: An Introduction.* Wiley-VCH, 2 edition (2000).

[17] T. Bürgi and A. Baiker. In Situ Infrared Spectroscopy of Catalytic Solid-Liquid Interfaces Using Phase-Sensitive Detection: Enantioselective Hydrogenation of a Pyrone over Pd/TiO_2. *Journal of Physical Chemistry B*, 106, 10649–10658 (2002).

[18] S. D. Ebbesen, B. L. Mojet and L. Lefferts. In situ ATR-IR study of CO adsorption and oxidation over Pt/Al_2O_3 in gas and aqueous phase: Promotion effects by water and pH. *Journal of Catalysis*, 246, 66–73 (2007).

[19] H. Kobayashi and M. Kobayashi. Transient Response Method in Heterogeneous Catalysis. *Catalysis Review: Science and Engineering*, 10, 139–176 (1974).

[20] T. Furusawa, M. Suzuki and J. M. Smith. Rate Parameters in Heterogeneous Catalysis by Pulse Techniques. *Catalysis Reviews — Science and Engineering*, 13(1), 43–76 (1976).

[21] C. O. Bennett. Transient Method and Elementary Steps in Heterogeneous Catalysis. *Catalysis Reviews-Science and Engineering*, 13(2), 121–148 (1976).

[22] C. O. Bennett. Experiments and processes in the transient regime for heterogeneous catalysis. *Advances in Catalysis*, 44, 329 (2002).

[23] C. Mirodatos. Use of isotopic transient kinetics in heterogeneous catalysis. *Catalysis Today*, 9, 83–95 (1991).

[24] P. L. Mills and J. L. Lerou. Transient response methods for assisted design of gas phase heterogeneous catalysts: experimental techniques and mathematical modelling. *Catalysis Review: Science and Engineering*, 9(1–2), 1–96 (1993).

[25] M. Kobayashi and H. Kobayashi. Application of transient response method to the study of heterogeneous catalysis; I. Nature of catalytically active oxygen on manganese dioxide for the oxidation of carbon monoxide at low temperatures. *Journal of Catalysis*, 27, 100–107 (1972).

[26] C. O. Bennett, M. B. Cutlip and C. C. Yang. Grandientless reactors and transient methods in heterogeneous catalysis. *Chemical Engineering Science*, 27, 2255–2264 (1972).

[27] J. T. Gleaves, J. B. Ebner and T. C. Kueschler. Temporal analysis of products (TAP) — a unique catalyst evaluation system with submillisecond time resolution. *Catalysis Review — Science and Engineering*, 30, 49–116 (1988).

[28] J. Happel. *Isotopic Assessment of Heterogeneous Catalysis.* Academic Press, Orlando (1986).

[29] V. Hejtmánek and P. Schneider. Diffusion of large molecules in porous glass. *Chemical Engineering Science*, 49(16), 2575–2584 (1994).

[30] Y. Lin and Y. H. Ma. A comparative chromatographic study of liquid adsorption and diffusion in microporous and macroporous adsorbents. *Industrial & Engineering Chemical Research*, 28, 622–630 (1989).

[31] Z. Kiraly, A. Mastalir, A. Csaszar, H. Demir, D. Uner and G. H. Findenegg. Liquid chromatography as a novel method for determination of the dispersion of supported Pd particles. *Journal of Catalysis*, 245, 267–271 (2007).

[32] J. F. Denayer, A. Bouyermaouen and G. V. Baron. Adsorption of Alkanes and Other Organic Molecules in Liquid Phase and in the Dense Vapor Phase: Influence of Polarity, Zeolite Topology, and External Fluid Density and Pressure. *Industrial & Engineering Chemical Research*, 37, 3691–3698 (1998).

[33] G. H. Jonker. *Hydrogenation of edible oils and fats.* Ph.D. thesis, University of Groningen (1999).

[34] E. Toukoniitty, J. Wärnå, T. Salmi, P. Mäki-Arvela and D. Y. Murzin. Application of transient methods in three-phase catalysis: hydrogenation of a dione in a catalytic plate column. *Catalysis Today*, 79(1–4), 383–389 (2003).

[35] D. C. Harris. *Quantitative Chemical Analysis.* W. H. Freeman & Co., 6 edition (2003).

[36] `http://www.agilent.com`

[37] `http://www.waters.com`

[38] P. Kebarle and Y. Ho. *Electrospray Ionization Mass Spectrometry — Fundamentals, Instrumentation and Applications (On the Mechanism of Electrospray Mass Spectrometry).* John Wiley & Sons, Inc. (1997).

[39] T. M. Kana, C. Darkangelo, M. D. Hunt, J. B. Oldham, G. E. Bennett and J. C. Cornwell. Membrane Inlet Mass Spectrometer for Rapid High-Precision Determination of N_2, O_2, and Ar in Environmental Water Samples. *Analytical Chemistry*, 66, 4166–4170 (1994).

2

Preparation of well-dispersed Pt/SiO$_2$ catalysts using low-temperature treatments

In Chapter 2 methods to prepare platinum on silica catalyst using temperatures as low as possible are explored. Therefore, thermal stability in both oxidizing and reducing atmosphere of eight different precursors was studied with thermo-gravimetric analysis (TGA-MS). Based on these data, the precursors were tested to prepare silica supported catalysts, resulting in relationship between the thermal stability of the precursors, the procedures of impregnation, reduction and calcination with the final dispersion on silica. Platinum precursors decomposed more easily in reducing than in oxidizing environment, due to thermochemistry. Catalysts prepared by using ion-exchange and direct reduction in hydrogen resulted in highly dispersed platinum particles on silica. $PtCl_x$ *and* PtO_x *species, when present during catalyst preparation, cause sintering of platinum at temperatures higher than 250 °C (*$PtCl_x$*) and 350 °C (*PtO_x*), respectively. These species can be converted more easily in hydrogen than in air.* $PtCl_4$, $H_2PtCl_6 \cdot 6\,H_2O$ *and* $H_2Pt(OH)_6$ *are suitable as precursors for achieving high platinum dispersion, keeping temperatures below 150 °C.*

Parts of this chapter are published in

1. *Applied Catalysis A: General*, 301, 51–58, (2006)
2. *Studies in Surface Science and Catalysis*, 162, 529–536, (2006)

2.1 Introduction

Supported platinum catalysts are used in a variety of heterogeneously catalyzed reactions for commercial applications [1]. Application of heterogeneous catalysis in liquid phase has been and will be increasingly important in bulk chemistry, fine chemistry and environmental process technologies. However, there are hardly any techniques available that allow studying the adsorption of reactants, intermediates and probe-molecules from liquid phase on the surface of catalysts. Work in our laboratory is in progress to develop new experimental techniques that allow operando spectroscopy and transient operation in liquid phase catalytic reactors.

In order to study reactions in liquid phase, it is essential to have a reactor module, which

- provide a sufficient number of catalytic sites,
- minimizes any concentration gradients,
- provides mechanical stability to the catalyst bed,
- minimizes interference with the spectroscopic technique of choice and
- minimize chromatographic effects of the support in the transient experiment.

Polymer reactors and supports are promising in this respect. E.g., silica foam in a polymer cartridge (offered by Merck of the type Chromolith as a novel high performance liquid chromatography (HPLC) column [2]) is suitable as a reactor for transient experiments because the high surface area silica foam can act as support with relatively low pressure drop. However, thermal stability of this HPLC column is limited to low temperatures because of the polymer housing (< 150 °C). It is therefore essential to use mild temperatures during the deposition of active phase (platinum) in the Chromolith reactor and at the same time

1. achieve complete decomposition of the precursor to form platinum and
2. achieve high platinum dispersion.

Exhaustive information is available on Pt/SiO_2 catalyst, EUROPT-1 [3–5]. In this article we explore low temperature preparation of platinum catalysts on conventional silica and review the effects of

1. nature and chemical composition of the platinum precursor,
2. preparation method and

3. post preparation treatments (calcination, reduction) on the properties of catalysts prepared with eight commonly used platinum precursors.

To our knowledge such a systematic study is not available in the open literature.

2.2 Experimental

2.2.1 Materials

Silica (Aerosil 380, surface area 382 $m^2 \cdot g^{-1}$) support was obtained from Degussa and used as received. Platinum precursors were solved in water viz. $PtCl_4$, $H_2PtCl_6 \cdot 6\,H_2O$, $[Pt^{II}(NH_4)_2]Cl_4$, $[Pt^{IV}(NH_4)_2]Cl_6$, $[Pt^{II}(NH_3)_4](NO_3)_2$, $[Pt^{II}(NH_3)_4](OH)_2$, $H_2Pt(OH)_6$ (Alfa Aesar, purity 99.9 %) or in toluene, $Pt(C_5H_7O_2)_2$ (Aldrich). Doubly de-ionized water or toluene (Merck, purity 99.9 %) was used. The pH of the solutions during preparation was adjusted with 25 % solution of NH_4OH (Merck) and HCl (Merck).

2.2.2 Catalyst preparation

Catalysts were prepared by impregnation/adsorption using aqueous solutions of $PtCl_4$, $H_2Pt(OH)_6$, $H_2PtCl_6 \cdot 6\,H_2O$, $[Pt^{II}(NH_4)_2]Cl_4$, $[Pt^{IV}(NH_4)_2]Cl_6$, $[Pt^{II}(NH_3)_4](NO_3)_2$ and $[Pt^{II}(NH_3)_4](OH)_2$ or solution of $Pt(C_5H_7O_2)_2$ in toluene. Preparation procedure was as follows: 8.0 grams of silica was contacted with 200 ml of de-ionized water or toluene. Required amounts of platinum precursor, to result in 1 wt% Pt/SiO_2 catalyst, was dissolved in 30 ml of water; toluene was used instead water in the case of $Pt(C_5H_7O_2)_2$.

Silica suspension and solution of platinum precursor were stirred separately for 30 minutes. Solution of platinum precursor was added to the silica suspension, and the mixture was covered and stirred overnight at room temperature. The suspension was dried for 3 hours at 60 °C in a rotary evaporator. Dried samples were crushed with a mortar and stored. Preparation using $PtCl_4$ as a precursor was performed at (i) pH 2.6 and (ii) pH 1.5. In the later case, pH was adjusted by adding HCl. In the case of $[Pt^{II}(NH_3)_4](NO_3)_2$ and $[Pt^{II}(NH_3)_4](OH)_2$ the pH of the solution was adjusted to 8.2 by adding NH_4OH, to facilitate ion exchange of the complex cations $[Pt^{II}(NH_3)_4]^{2+}$ with silica surface. The pH was measured using 744 Metrohm pH-meter.

The impregnated support was subjected to calcination/reduction treatment at temperatures directed from thermo-gravimetric analysis (details in the next section). Catalysts were calcined and/or reduced in a stream 40 $ml \cdot min^{-1}$ of 22 % O_2 in N_2 or 50 % H_2 in Ar, respectively. Temperature ramp was 5 $°C \cdot min^{-1}$.

2.2.3 TGA-SDTA of platinum precursors

In order to determine the decomposition temperatures and resulting heat effects of platinum precursors in both oxidizing and reducing environments, thermo-gravimetric analysis together with simultaneous differential thermal analysis were performed (Mettler Toledo TGA/SDTA 851e) under 40 ml·min^{-1} gas flow of either 22 % O_2 in N_2 or 50 % H_2 in Ar in the temperature range from 25 °C to 600 °C at 5 °C·min^{-1}. When appropriate, effluent gases were analyzed by online mass spectroscopy (MS) (Balzer, QMS 422). These experiments were performed using pure platinum precursors instead of impregnated silica because it was not possible to follow weight changes of the catalysts with TGA, due to the low loading of platinum precursor (corresponding to 1 wt% platinum). Catalysts were heat treated at slightly higher temperatures (50 °C) than the decomposition temperatures of the pure precursors, in order to account for possible stabilization of platinum precursor by the support [6].

2.2.4 Characterization

The platinum content in the solutions used for preparation was measured with atomic absorption spectroscopy analysis (AAS) (Varian SpectrAA 10). Platinum and chlorine (samples made with chloride precursors) contents in the catalyst samples were determined with X-ray fluorescence spectroscopy (XRF) (Phillips PW 1480 spectrometer).

BET surface areas of catalysts were ±5 % to that of the silica support material. Platinum metal dispersion was measured with hydrogen chemisorption in a volumetric set-up, using a procedure described elsewhere [7]. The catalyst sample (0.4 gram) was first reduced in hydrogen for 2 hours at the temperature used in the preparation procedure. The system was then evacuated at the same temperature for 1 hour and cooled to 20 °C. Hydrogen sorption was measured at 20 °C from 20 to 80 mbar. The monolayer volume was obtained by extrapolating the linear part of the corrected isotherm to zero pressure. Stoichiometry of $H/Pt = 1$ was assumed for calculating the platinum dispersion [1].

Transmission electron microscopy (TEM) (Phillips CM 30, 300 kV) was used to check the platinum particle size in some of the catalysts. Average platinum particle size was determined based on analysis of about 100 platinum crystallites.

2.3 Results

First, thermal analysis results of platinum precursors are shown below, followed by the results of the catalyst preparation procedure, which was directed by the TGA results.

2.3.1 Thermal analysis

Chlorine containing platinum precursors

$PtCl_4$: Figure 2.1 and Table 2.1 show the TGA and products of decomposition of $PtCl_4$ under oxidizing and reducing conditions. In the case of decomposition of $PtCl_4$ in air, weight loss of 3 %, below 100 °C, is due to moisture. Observed weight losses for the two steps agree well with the following reactions:

$$PtCl_4 \longrightarrow PtCl_2 + Cl_2 \tag{2.1}$$

$$PtCl_2 \longrightarrow Pt + Cl_2 \tag{2.2}$$

In presence of hydrogen, decomposition occurred in agreement with reaction 2.3:

$$PtCl_4 + 2\,H_2 \longrightarrow Pt + 4\,HCl \tag{2.3}$$

$H_2PtCl_6 \cdot 6\,H_2O$: In oxidizing atmosphere, $H_2PtCl_6 \cdot 6\,H_2O$ decomposed in three steps (Fig 2.2, Table 2.1). The weight changes observed are in agreement with the following three reactions:

$$H_2PtCl_6{\cdot}6\,H_2O \longrightarrow PtCl_4 + 2\,HCl + 6\,H_2O \tag{2.4}$$

$$PtCl_4 \longrightarrow PtCl_2 + Cl_2 \tag{2.5}$$

$$PtCl_2 \longrightarrow Pt + Cl_2 \tag{2.6}$$

Obviously, the first two steps are not very well separated in Figure 2.2. However, steps 2.5 and 2.6 in Figure 2.2 occur at temperatures similar to those observed for $PtCl_4$ in Figure 2.1.

In hydrogen, weight loss is in accordance with reaction 2.7:

$$H_2PtCl_6{\cdot}6\,H_2O + 2\,H_2 \longrightarrow Pt + 6\,HCl + 6\,H_2O \tag{2.7}$$

From the results (Figs 2.1, 2.2 and Table 2.1) it is obvious that both precursors ($PtCl_4$ and $H_2PtCl_6 \cdot 6\,H_2O$) have in common that chlorine is retained up to much higher temperatures (up to 520 °C) during decomposition in air as compared to reduction in hydrogen (below 100 °C).

The results of thermal analysis for $[Pt^{II}(NH_4)_2]Cl_4$ and $[Pt^{IV}(NH_4)_2]Cl_6$ are given in Table 2.1 and Figs 2.3 and 2.4. The final decomposition temperature in air was marginally lower (40 °C) for $[Pt^{II}(NH_4)_2]Cl_4$ as compared to $[Pt^{IV}(NH_4)_2]Cl_6$, while in hydrogen, latter complex decomposed at lower temperature and the difference is again not significant (30 °C). The TGA patterns were alike, as one would expect based on the similarity of the two complexes.

Table 2.1: *Decomposition temperatures, observed and calculated weight losses and products of decomposition in hydrogen and in air*

Compound	Decomposition temperature (°C)		Observed weight loss (%)		Theoretical weight loss (%)	Product of decomposition detected with MS	
	In H_2	In air	In H_2	In air		In H_2	In air
Group 1							
$PtCl_4$	25–45	25–350 350–525	44	41	42	HCl	Cl_2
$H_2PtCl_6 \cdot 6\,H_2O$	25–100	25–280 280–350 350–530	61	61	62	HCl, H_2O	HCl, Cl_2, H_2O
$H_2Pt(OH)_6$	25–80	25–100 100–150 150–310 310–490	61	61	33	H_2O	H_2O, O_2
Group 2							
$[Pt^{II}(NH_4)_2]Cl_4$	25–180 180–250	25–280 350–525	48	48	48	NH_3	–
$[Pt^{IV}(NH_4)_2]Cl_6$	25–225	25–350	56	58	56	NH_3	H_2O
Group 3							
$[Pt^{II}(NH_3)_4](NO_3)_2$	25–220	25–230	50	52	50	NH_3, H_2O, NO_x	N_2, NO_x, NH_3
$[Pt^{II}(NH_4)_2](OH)_2$	25–230	25–190 190–270	33	33	33	NH_3, H_2O	N_2, NO_x, NH_3
$Pt(C_5H_7O_2)_2$	25–100	25–220	50	56	50	CH_4, H_2O	CO, H_2O

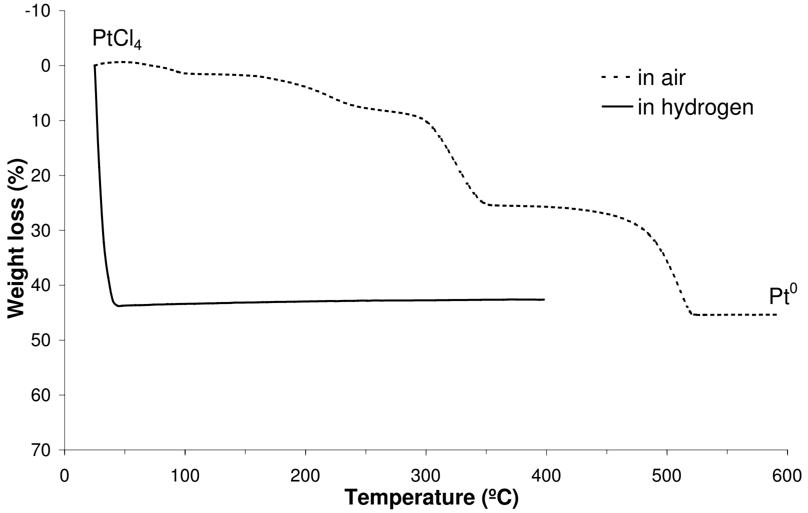

Figure 2.1: *TG Analysis of $PtCl_4$ in gas flow* 40 ml/min 22 % *O_2, in N_2, or* 50 % *H_2 in Ar, heating rate* 5 °C/min , 25 – 600 °C, *P=1bar*

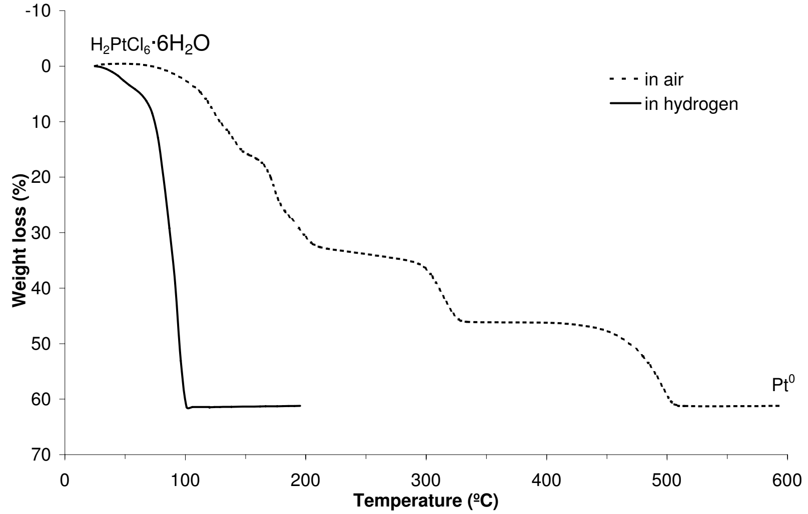

Figure 2.2: *TG Analysis of $H_2PtCl_6 \cdot 6H_2O$ in gas flow* 40 ml/min 22 % *O_2, in N_2, or* 50 % *H_2 in Ar, heating rate* 5 °C/min , 25 – 600 °C, *P=1bar*

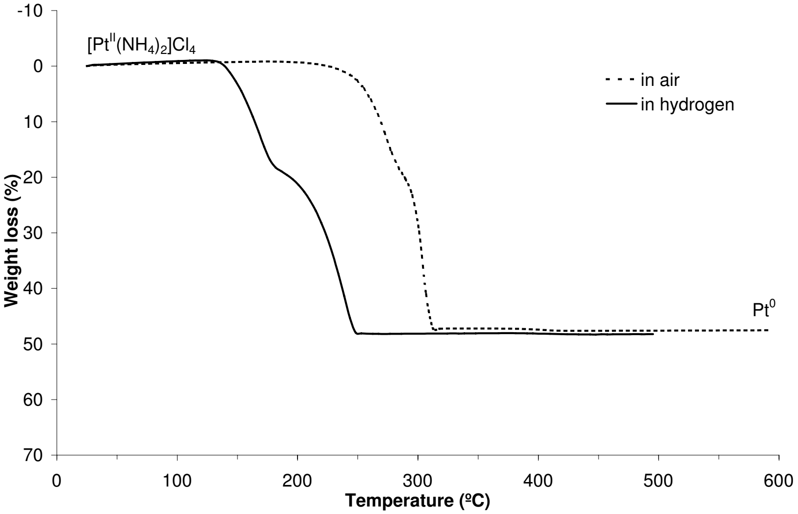

Figure 2.3: *TG Analysis of* $(NH_4)_2Cl_4$ *in gas flow* 40 ml/min 22 % O_2*, in* N_2*, or* 50 % H_2 *in Ar, heating rate* 5 °C/min , 25 – 600 °C, *P=1bar*

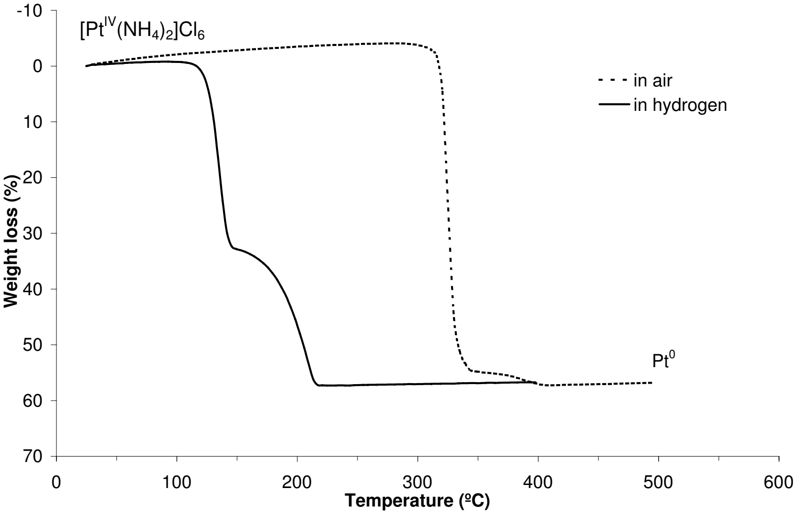

Figure 2.4: *TG Analysis of* $(NH_4)_2PtCl_6$ *in gas flow* 40 ml/min 22 % O_2*, in* N_2*, or* 50 % H_2 *in Ar, heating rate* 5 °C/min , 25 – 600 °C, *P=1bar*

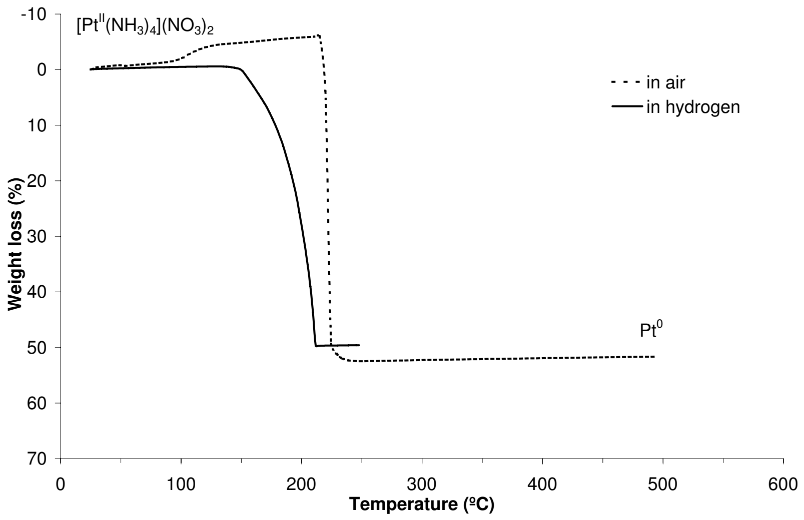

Figure 2.5: *TG Analysis of* $(NH_4)_2Pt(NO_3)_2$ *in gas flow* 40 ml/min 22 % O_2, *in* N_2, *or* 50 % H_2 *in Ar, heating rate* 5 °C/min , 25 – 600 °C, *P=1bar*

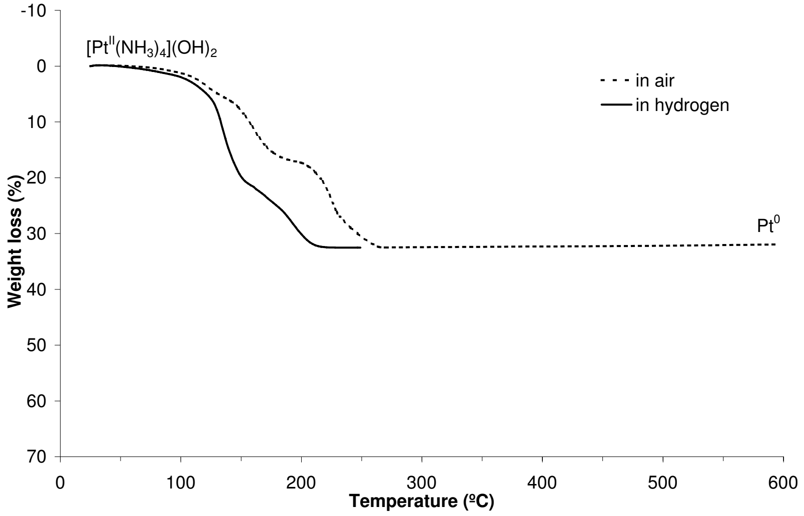

Figure 2.6: *TG Analysis of* $(NH_4)_2Pt(OH)_2$ *in gas flow* 40 ml/min 22 % O_2, *in* N_2, *or* 50 % H_2 *in Ar, heating rate* 5 °C/min , 25 – 600 °C, *P=1bar*

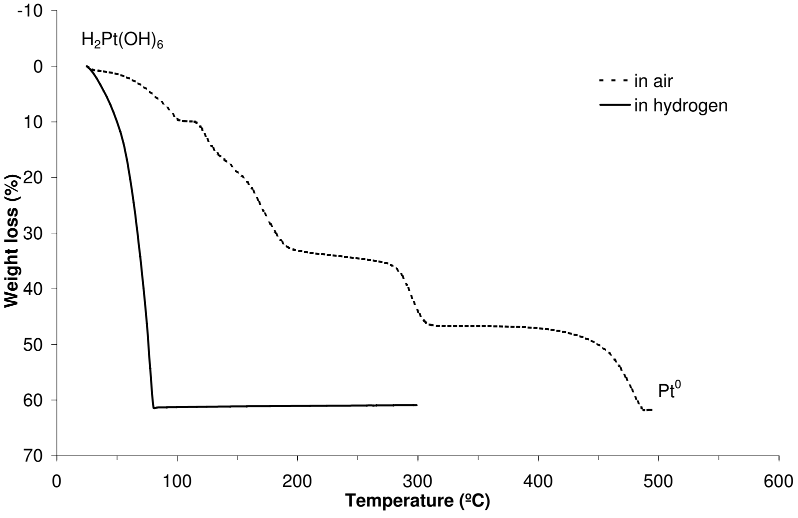

Figure 2.7: *TG Analysis of $H_2Pt(OH)_6$ in gas flow* 40 ml/min 22 % O_2*, in* N_2*, or* 50 % H_2 *in Ar, heating rate* 5 °C/min , 25 – 600 °C, *P=1bar*

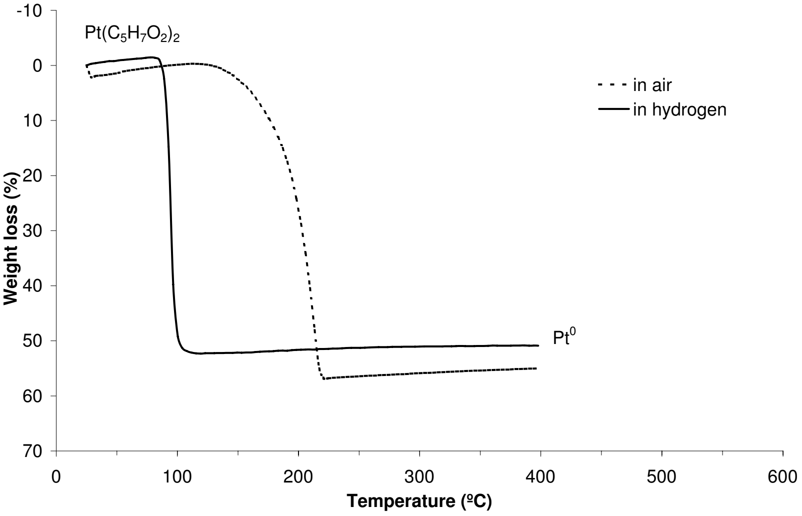

Figure 2.8: *TG Analysis of* $Pt(C_5H_7O_2)_2$ *in gas flow* 40 ml/min 22 % O_2*, in* N_2*, or* 50 % H_2 *in Ar, heating rate* 5 °C/min , 25 – 600 °C, *P=1bar*

Chlorine free platinum precursors

$[Pt^{II}(NH_3)_4](NO_3)_2$: Figure 2.5 and Table 2.1 show TG analysis and decomposition products of $[Pt^{II}(NH_3)_4](NO_3)_2$ in oxidizing and reducing atmospheres. In air, there was a small increase in weight (5 %) in the range 100–215 °C. This probably due oxidation of the sample, but it is not possible to clarify this from the TGA results. SDTA analysis indicated exothermic character of the decomposition reactions in both oxidizing and reducing environments.

$[Pt^{II}(NH_3)_4](OH)_2$: In the case of $[Pt^{II}(NH_3)_4](OH)_2$ SDTA showed endothermic effects below 150 °C and exothermic effects at higher temperatures, in both hydrogen and air. Obtained TGA results (Fig 2.6 and Table 2.1) are in agreement with results obtained by Goguet et al. [8], who studied decomposition of $[Pt^{II}(NH_3)_4](OH)_2$ mixed or exchanged with silica, in reducing and oxidizing environment using mass spectrometry. This author proposed formation of $(NH_3)_2PtO$, ammonia and water under oxygen in the range 90–170 °C (for mixture of silica with platinum precursor). Water observed is due to dehydration of silica. At higher temperatures, remaining ammonia oxidized to form water, nitrogen and NO_x. In hydrogen, formation of $(NH_3)_2PtO$ between 100 and 120 °C is suggested [8] while releasing ammonia and water; ammonia and water are also released at higher temperatures.

It is important to note that in both samples above, i.e. $[Pt^{II}(NH_3)_4](NO_3)_2$ and $[Pt^{II}(NH_3)_4](OH)_2$, oxygen-containing platinum species are stable up to 230 °C and 270 °C during decomposition in air while in hydrogen they are converted at only slightly lower temperatures ($\Delta T < 30\,°C$).

$H_2Pt(OH)_6$: Figure 2.7 and Table 2.1 show TGA and products of decomposition in oxidizing and reducing atmospheres of $H_2Pt(OH)_6$. This compound is highly hygroscopic and thus there was significant difference between experimental weight loss and theoretical for $H_2Pt(OH)_6$ to platinum. For decomposition in air, assuming that the first two steps (< 150 °C) correspond to desorption of sorbed water, the remainig weight loss corresponds to changes accordng to reactions below;

$$H_2Pt(OH)_6 \longrightarrow PtO_2 + 4\,H_2O \tag{2.8}$$

$$PtO_2 \longrightarrow Pt + O_2 \tag{2.9}$$

Also in hydrogen the weight loss measured differed from the expected value (Fig 2.7 and Table 2.1), due to adsorbed water. Decomposition occurred in one rapid step at a much lower temperature than in air. The fact that the weight achieved at 80 °C is equal to the final weight in the presence of oxygen, including the decomposition of PtO_2, proofs that platinum is formed directly according reaction 2.10:

$$H_2Pt(OH)_6 + 4\,H_2 \longrightarrow Pt + 6\,H_2O \tag{2.10}$$

Obviously, oxidic species of platinum are stable up to higher temperatures (490 °C) in oxygen while in hydrogen that is not the case (< 100 °C).

$Pt(C_5H_7O_2)_2$: Figure 2.8 and Table 2.1 show TG analysis and decomposition products in oxidizing and reducing environments of $Pt(C_5H_7O_2)_2$. One-step decomposition is observed in air. Experimental weight loss was higher than the theoretical value for conversion of $Pt(C_5H_7O_2)_2$ to platinum (Fig 2.8, Table 2.1). This is attributed to evaporation of $Pt(C_5H_7O_2)_2$ during calcination, as metallic platinum deposition was observed on the walls of the sample holder, indicating platinum loss due to evaporation. In hydrogen, decomposition occurred in one step and obtained weight loss agreed with theory. Obviously, hydrogen allows reduction of $Pt(C_5H_7O_2)_2$ at temperatures below the onset of evaporation.

It can be deducted from the TG measurements that chlorine and/or oxygen containing platinum species (either present in the precursor or formed during thermal treatment) are less stable and could be removed at lower temperatures in hydrogen than in the presence of oxygen. This is important because presence of chlorine and/or oxygen containing platinum species during heat treatments is known to influence platinum dispersion. A series of supported silica catalysts were prepared. Details of these catalysts are described in the next section.

2.3.2 Catalyst characterization

Details of thermal treatments and characteristics of the catalysts prepared in this study using the precursors discussed above are given in Table 2.2. The calcination and reduction temperatures were chosen 50 °C above those observed for decomposition/reduction during thermal analysis of the platinum precursors.

In general, platinum loadings for the catalysts were in the range intended (1 wt%) i.e., 0.90–1.04 wt% platinum. The single exception was $H_2Pt(OH)_6$; the highly hygroscopic nature caused that less platinum was introduced then intended (0.60 wt%).

Table 2.2 also gives the platinum dispersions measured via hydrogen chemisorption for the various catalysts. In order to cross check these values, TEM photographs were recorded for seven catalysts and platinum particle sizes measured for about 100 particles in each case (Figure 2.9). Platinum dispersions obtained from TEM analysis of catalysts, show reasonable correlation with results obtained from hydrogen chemisorption measurements.

Particle size estimations, based on TEM, for dispersions above 90 % (platinum particle size < 1.2 nm) is obviously less accurate. Most of catalysts subjected to a direct reduction have better or at least the same platinum dispersions as compared to catalysts that were calcined in air first and then reduced (Table 2.2). Catalysts prepared with $[Pt^{II}(NH_4)_2]Cl_4$ and $[Pt^{IV}(NH_4)_2]Cl_6$ showed similar low dispersions for both treatments, with slightly higher dispersion for samples calcined prior to reduction.

Catalyst based on $Pt(C_5H_7O_2)_2$, that was calcined prior to reduction, has higher platinum dispersion. This is due to carbonaceous species deposited on the catalyst during decomposition in hydrogen as demonstrated by the fact that additional oxidation at 270 °C of this sample resulted in higher platinum dispersion (28 %).

Table 2.2: *Platinum loadings and dispersions for catalysts prepared with different platinum precursors, calcined and then reduced or directly reduced, [-] indicates absence of this treatment*

Precursor/ SiO_2[1]	Calcination temperature	Reduction temperature	Pt content	Dispersion from H_2 chemisorption[2]	Dispersion from TEM[3]
	°C	°C	wt %	%	%
$PtCl_4$	-	100	1.02	66 (100)[4]	77
	-	570	1.02	58	-
	570	100	1.04	8	8
$H_2PtCl_6 \cdot 6\,H_2O$	-	150	0.95	75	77
	580	150	0.94	5	8
$H_2Pt(OH)_6$	-	130	0.58	85	-
	250	250	0.58	61	-
	550	130	0.58	5	11
$[Pt^{II}(NH_4)_2]Cl_4$	-	300	0.96	13	-
	360	360	0.90	22	-
$[Pt^{IV}(NH_4)_2]Cl_6$	-	270	0.97	6	-
	400	270	0.98	10	-
$[Pt^{II}(NH_3)_4](NO_3)_2$	-	270	1.08	102	-
	290	290	1.08	100	-
	500	290	1.08	47	-
$[Pt^{II}(NH_4)_2](OH)_2$	-	270	1.07	94	72
	320	320	1.07	93	90
	500	320	1.07	55	-
$Pt(C_5H_7O_2)_2$	-	160	1.00	7	-
	270	270	1.00	35	-

---

[1] Catalysts are named by precursor used

[2] Pt dispersion was determined with assumption H/Pt=1:1 [1]

[3] Equation to calculate dispersion of Pt particles from particle diameter data $D_{isp} = 108/d[\text{nm}]$[1]

[4] Value outside the brackets corresponds to the dispersion of the catalyst made from suspension with pH=2.6 while value of dispersion in brackets corresponds to the catalyst made from suspension mixture with pH=1.5

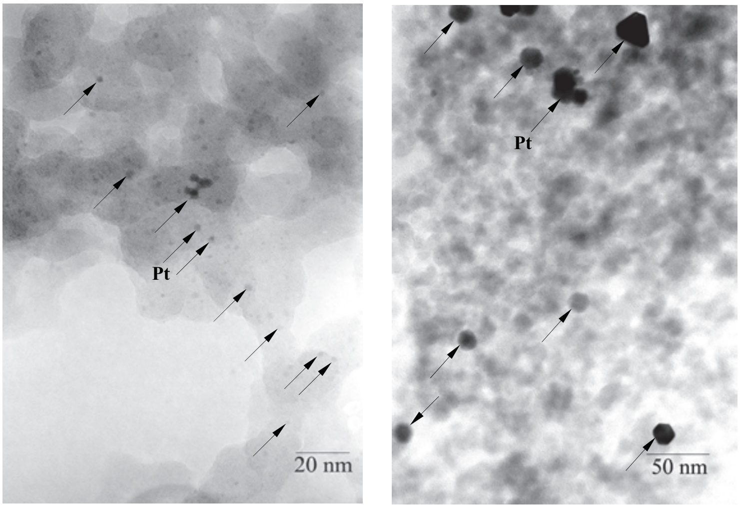

Figure 2.9: *TEM micrographs of* $PtCl_4$ *catalyst (a) after direct reduction at* 100 °C*, (b) after calcination at* 570 °C *followed by reduction at* 100 °C

2.4 Discussion

Aim of this work is to prepare well dispersed platinum catalysts using mild thermal treatments. First, the results of the thermogravimetric study of decomposition of the pure precursors are discussed. Factors that influence platinum dispersion of the resulting catalysts (nature of precursors, preparation method, thermal treatments, ambient, etc.) are discussed next.

2.4.1 TGA of precursors

Thermo-gravimetric studies indicate that platinum precursors decompose at lower temperatures in hydrogen than in air. Three groups of compounds can be distinguished based on the temperatures needed for decomposition and reduction, as indicated in Table 1. The first group of compounds decomposes at low temperatures in hydrogen, which is due to the thermodynamically favorable formation of HCl or water. In air, these reaction pathways are not available; instead, decomposition to chlorine and oxygen/water is only possible and much higher temperatures are necessary. The compounds in group II contain (NH_4^+) ligands; in hydrogen, endothermic ligand elimination will occur, requiring higher temperatures in comparison to reduction of group I compounds. In contrast, in air lower temperatures are sufficient for group II, because oxidation of NH_4^+, to form NO_x, is exothermic and thermodynamically highly favorable. The compounds in group III also need fairly high temperatures in hydrogen because of the same reason as for the group II compounds. In oxygen, even lower temperatures then for group II allow decomposition, resulting in temperatures close to the reduction temperatures. Thus, the trends in the decomposition and reduction temperatures of the precursors can be rationalized based on thermodynamics.

2.4.2 Catalyst preparation; impregnation

The catalysts were prepared by impregnation method, but for three cases, the pH of the impregnation medium was adjusted to facilitate platinum incorporation via ion-exchange. For silica, the point zero charge (PZC), i.e, pH at which surface of oxide is neutral is reported to be around 2.5 [8–11]. Below this pH, the surface is positively charged while above it is negatively charged. Platinum can be present in the precursor solutions as cation (e.g., $[Pt^{II}(NH_3)_4]^{2+}$) or as anions (e.g., $[Pt^{IV}Cl_{(6\text{-}x)}(H_2O)_x]^{(2-x)-}$ (x = 0, 1, 2), and $[Pt^{IV}(OH)_6]^{2-}$). According to Boujday et al. [11], reaction of Pt anionic complex (such as $[Pt^{IV}Cl_6]^{2-}$) with silica surface occurs according to Eqs. 2.11 and 2.12;

$$[Pt^{IV}Cl_6]_2^- + SiOH \longleftrightarrow [Pt^{IV}Cl_5(SiOH)]^- + Cl^- \tag{2.11}$$

$$[Pt^{IV}Cl_6]_2^- + 2\,SiOH \longleftrightarrow [Pt^{IV}Cl_4(SiOH)_2] + 2\,Cl^- \tag{2.12}$$

In the case of Pt in cationic form $[Pt^{II}(NH_3)_4]^{2+}$, reaction with silica surface occurs according to (Eq. 2.13), [6]:

$$2\,(\equiv Si{-}O^-) + [Pt^{II}(NH_3)_4]^{2+} \longleftrightarrow (\equiv Si{-}O^-)_2[Pt^{II}(NH_3)_4]^{2+} \tag{2.13}$$

Based on the type of platinum ionic species and applied pH during preparation, catalysts can be divided into three groups:

1. Catalysts prepared with anionic platinum species at pH ~ 1.5 – 2.6 ($[Pt^{IV}Cl_{(6\text{-}x)}(H_2O)_x]^{(2-x)-}$ (x = 0, 1, 2) and $[Pt^{IV}(OH)_6]^{2-}$)
2. Catalysts prepared with anionic platinum species at pH ~ 3.2 – 4.0 ($[Pt^{IV}Cl_{(6\text{-}x)}(H_2O)_x]^{(2-x)-}$ (x = 0, 1, 2)) and
3. Catalysts prepared with cationic platinum species (e.g., $[Pt^{II}(NH_3)_4]^{2+}$) at pH corrected to 8.2.

Results show (Table 2.2) that conditions favorable for ion exchange result in well dispersed catalysts, as expected. Ion exchange is a specific case of adsorption, allowing molecular scale dispersion of platinum species and stronger interaction between platinum species with silica surface than in the case of impregnation, which operates via pore filling and weak adsorption mechanism [12, 13].

2.4.3 Catalyst preparation; thermal treatment

Generally, the thermal treatments of catalysts have a strong influence on the platinum dispersion. In this section we will discuss the influence of the chemical composition of platinum precursors (chlorine or oxygen, containing) and ambient (oxidizing vs. reducing) on platinum dispersions.

In the case of chlorine containing precursor ($PtCl_4$), a direct reduction at 100 °C is sufficient to remove the chlorine completely and gives a reasonably dispersed platinum catalyst (66 %, Table 2.2). However, in air, much higher temperature (570 °C) is necessary for the removal of all the chlorine (see Figure 2.1, Table 2.1) and the resulting catalyst is poorly dispersed (8 %). Since a direct reduction at 570 °C still gave a well dispersed catalyst (58 %, Table 2.2) it can be concluded that presence of chloride or oxygen species facilitate sintering of platinum and affect particle size during thermal treatments. This is also documented well in literature [6, 12–15].

Figure 2.10, highlights this in the case of chlorine containing Pt precursors; plot of the temperature required to remove chlorine from the catalyst against platinum dispersion (see Table 2.2) show that temperatures above 200–250 °C will lead to poor dispersions when chlorine is present.

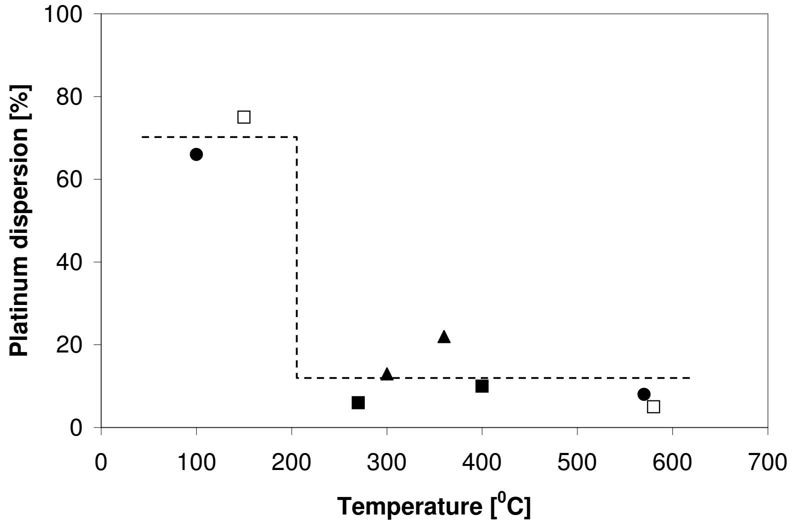

Figure 2.10: *Relationship between platinum dispersion and temperature required to remove chlorine from the catalyst during the preparation:* □– $H_2PtCl_6 \cdot 6H_2O$, ●– $PtCl_4$, ▲ – $[Pt^{II}(NH_4)_2]Cl_4$, ■ – $[Pt^{IV}(NH_4)_2]Cl_6$

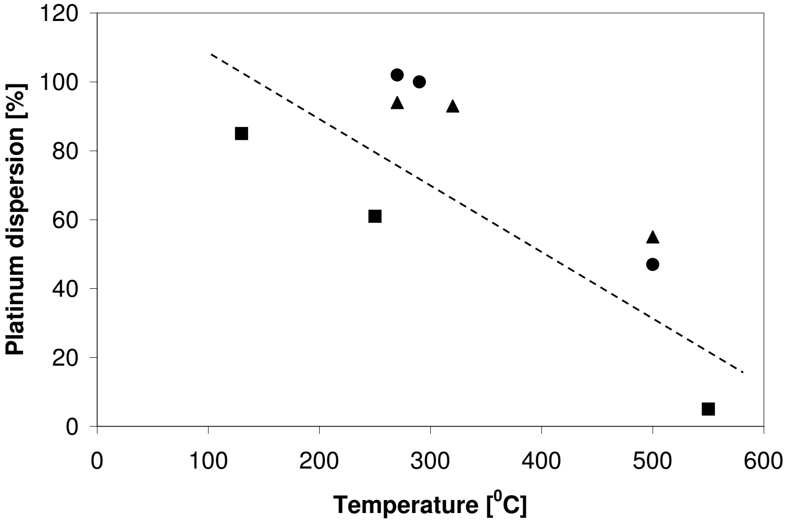

Figure 2.11: *Relationship between platinum dispersion and temperature required to remove oxygen from the catalyst during the preparation:* ●– $[Pt^{II}(NH_3)_4](NO_3)_2$, ▲ – $[Pt^{II}(NH_3)_4](OH)_2$, ■ – $H_2Pt(OH)_6$

The possible chlorine species that can be present during the treatment in oxidizing ambient are $PtCl_x$ (such as $PtCl_2$ and $PtCl_4$) [13], $[PtCl_{(6-x)}(H_2O)_x]^{(2-x)-}$ (x = 0, 1, 2) [11] and $Pt(OH)_xCl_y$ (x = 1, 2; y = 4, 5) and PtO_xCl_y [16, 17]. Dorling et al. [13] reported lower dispersions for supported platinum catalysts calcined prior to reduction, and attributed this to the presence of $PtCl_x$ species, which enabled platinum particle growth through vapor-phase transport. As our TG results show, in the cases where the chlorine containing species are removed at very low temperatures (< 100 °C) (Figures 2.1,2.2) the catalyst gives higher platinum dispersion as expected. Unlike chloride species, formation of oxichloride PtO_xCl_y, is reported [16] to assist in the redispersion of platinum crystallites when alumina was used as support. In our case both chlorine and oxygen are present during thermal treatment in air, however, the resulting catalysts have poor platinum dispersions. It maybe possible that PtO_xCl_y type species are not easily formed on silica, and only $PtCl_x$ species are present. Lietz et al. [16] showed that the lower acidity of silica in comparison to alumina makes it less suited for the formation of such oxychloro complexes. Another explanation would be that alumina is well wetted by PtO_xCl_y, whereas silica is not, since silica surfaces are hydrophobic.

Figure 2.11 shows that a similar correlation is found in the case of catalysts prepared with oxygen containing, chlorine-free, precursors. For example, in the case of $H_2Pt(OH)_6$ a direct reduction at 130 °C is sufficient for complete removal of precursor oxygen and obtained catalyst is reasonably well dispersed (85 %, Table 2.2). In air, the catalyst had to be treated at much higher temperatures (550 °C) and obtained platinum dispersion is poor (5 %). Same trend is also observed for $[Pt^{II}(NH_3)_4](NO_3)_2$ and $[Pt^{II}(NH_3)_4](OH)_2$, i.e., when oxygen is removed at lower temperatures (< 320 °C) the platinum dispersions are high (around 100 %) and calcination at higher temperatures (500 °C) leads to deterioration of platinum dispersion (55 %). These observations indicate that the loss in platinum dispersion is caused by a combination of oxygen and elevated temperatures. It is well established that PtO_x species are present during thermal treatment in oxygen [6, 14, 18, 19]. Our own TGA results clearly support this. Goguet et al. [6] showed indeed that presence of PtO_x species at 350 °C can cause decrease in dispersion while preparing catalysts from $[Pt^{II}(NH_3)_4](OH)_2$. Our own results show conclusively (Figs. 2.10 and 2.11, Table 2.2) that presence of oxygen species at higher temperatures is detrimental. However, sintering is less severe in the presence of oxygen than in the presence of chloride species. Thus, not only the choice of impregnation conditions, but also the thermal treatment variables have a significant influence on the platinum dispersions.

The dispersion of the catalyst prepared from $Pt(C_5H_7O_2)_2$ could be increased from 7 % to 28 % by additional calcinations at 270 °C. Although TGA analysis of the pure precursor in hydrogen, showed full decomposition to platinum, it is possible that remainders of carbon are responsible for this effect. Traces of carbon at the surface of platinum would be sufficient to cause this effect, which would be below the sensitivity of the TGA. The obtained dispersions are low, despite the relatively low temperatures used for the thermal treatments. This is probably caused by weak interaction of the $Pt(C_5H_7O_2)_2$ with the silica [20].

2.5 Conclusions

In order to prepare well-dispersed silica supported platinum catalysts, factors such as choice of platinum precursor, preparation method, thermal treatment temperatures and the gas ambients (oxidizing vs. reducing) need to be taken into consideration. It is shown that well dispersed Pt/SiO_2 catalysts can be prepared using mild thermal treatments. Chlorine containing platinum species, if present at temperatures higher than 250 °C, results in agglomeration and thus results in poorly dispersed catalysts. In the case of oxygen containing, chloride-free platinum species, this problem is less severe and temperatures up to 350 °C give high dispersions. In both cases, direct reduction of the silica supported platinum precursor removes chlorine and oxygen containing species efficiently at very low temperatures and results in well dispersed catalysts.

$PtCl_4$, $H_2PtCl_6 \cdot 6\,H_2O$ and $H_2Pt(OH)_6$ are suitable precursors to make well dispersed platinum catalyst based on structured silica in polymer reactors for carrying out studies in liquid phases reactions. Direct reduction in hydrogen at temperatures lower than 150 °C is enough to result in metallic platinum particles that are well dispersed.

Acknowledgements

The authors thank, Ing. L. Vrielink for XRF and BET analysis, Ing. M. Smithers for TEM measurements, Drs. S. S. Guilera for preparation of catalysts, Ing. J. Spies and Ing. B. Geerdink for technical assistance. Financial support for the project by STW (The Netherlands) is kindly acknowledged.

References

[1] C. H. Bartholomew and R. J. Farrauto. *Fundamentals of industrial catalytic processes.* John Wiley & Sons, Inc., Publication (2006).

[2] `http://www.chromolith.com`

[3] G. C. Bond and P. B. Wells. Characterization of the Standard Platinum/Silica Catalyst Europt-1; 1. Philosophy and Achievement. *Applied Catalysis*, 18(2), 221–224 (1985).

[4] G. C. Bond and P. B. Wells. Characterization of the Standard Platinum/Silica Catalyst Europt-1; 2. Preparation, Physical Properties, and Chemical Composition. *Applied Catalysis*, 18(2), 225–230 (1985).

[5] G. C. Bond and Z. Paál. Recently published work on EUROPT-1, a 6 % Pt/SiO_2 reference catalyst. *Applied Catalysis A*, 86, 1–35 (1992).

[6] A. Goguet, D. Schweich and J. P. Candy. Preparation of a Pt/SiO_2 catalyst: II. Temperature-programmed decomposition of the adsorbed platinum tetrammine hydroxide complex under flowing hydrogen, oxygen, and argon. *Journal of Catalysis*, 220, 280–290 (2003).

[7] A. Frennet and P. Wells. Characterization of the Standard Platinum/Silica Catalyst Europt-1; 4. Chemisorption of Hydrogen. *Applied Catalysis*, 18, 243–257 (1985).

[8] A. Goguet, D. Schweich and J. P. Candy. Preparation of a Pt/SiO_2 Catalyst: I. Interaction between Platinum Tetrammine Hydroxide and the Silica Surface. *Journal of Catalysis*, 209, 135–144 (2002).

[9] J. R. Iller. *The Chemistry of Silica.* John Willey & Sons (1979).

[10] J. Park and J. R. Regalbuto. A Simple, Accurate Determination of Oxide PZC and the Strong Buffering Effect of Oxide Surfaces at Incipient Wetness. *Journal of Colloid and Interface Science*, 175, 239–252 (1995).

[11] S. Boujday, J. Lehman, J. F. Lambert and M. Che. Evolution of Transition Metal Speciation in the Preparation of Supported Catalysts: Halogenoplatinate(IV) on Silica. *Catalysis Letters*, 88, 23–30 (2003).

[12] H. A. Benesi, R. M. Curtis and H. P. Studer. Preparation of highly dispersed catalytic metals: Platinum supported on silica gel. *Journal of Catalysis*, 10(4), 328–335 (1968).

[13] T. A. Dorling, B. W. J. Lynch and R. L. Moss. The structure and activity of supported metal catalysts; V. Variables in the preparation of platinum/silica catalysts. *Journal of Catalysis*, 20, 190–201 (1971).

[14] M. Chen and L. D. Schmidt. Morphology and sintering of Pt crystallites on amorphous SiO_2. *Journal of Catalysis*, 55, 348–360 (1978).

[15] G. R. Wilson and W. K. Hall. Studies of the hydrogen held by solids; XIX. H_2 and O_2 chemisorption on silica-supported platinum. *Journal of Catalysis*, 24, 306–314 (1972).

[16] G. Lietz, H. Lieske, H. Spindler, W. Hanke and J. Völter. Reactions of platinum in oxygen- and hydrogen-treated $Pt/\gamma\text{-}Al_2O_3$ catalysts; II. Ultraviolet-visible studies, sintering of platinum, and soluble platinum. *Journal of Catalysis*, 81, 17–25 (1983).

[17] H. Lieske, G. Lietz, H. Spindler, W. Hanke and J. Völter. Reactions of platinum in oxygen- and hydrogen-treated $Pt/\gamma\text{-}Al_2O_3$ catalysts; I. Temperature-programmed reduction, adsorption, and redispersion of platinum. *Journal of Catalysis*, 81, 8–16 (1983).

[18] C. P. Hwang and C. T. Yeh. Platinum-Oxide Species Formed on Progressive Oxidation of Platinum Crystallites Supported on Silica and Silica-Alumina. *Journal of Catalysis*, 182, 48–55 (1999).

[19] C. P. Hwang and C. T. Yeh. Platinum-oxide species formed by oxidation of platinum crystallites supported on alumina. *Journal of Molecular Catalysis A*, 112, 295–302 (1996).

[20] J. G. van Ommen, H. Bosch, P. J. Gellings and J. R. H. Ross. *Preparation of Catalysts*. Elsevier Science Publishers B. V., Amsterdam (1987).

3

Development of a transient response technique for heterogeneous catalysis in liquid phase: Electron Spray Ionization Mass Spectrometry (ESI-MS) as detector

In Chapter 3, a novel transient response technique for liquid phase heterogeneous catalytic studies, equipped with Electron Spray Ionization Mass Spectrometry (ESI-MS) detector is described. The technique was successfully applied as an on-line method for real-time detection of species dissolved in aqueous product streams at the exit of a catalytic reactor. Two test reactions, nitrite reduction with Pt/ SiO_2 *and glucose oxidation with Pt/CNF/Ni were used to demonstrate semi-quantitative monitoring of reactants, intermediates and products. The capability of the novel technique is demonstrated by the fact that the ESI-MS detector is sufficiently sensitive to determine quantitatively extreme small amounts of physisorbing nitrite, down to 0.5 % of a monolayer on the Pt surface. Nitrite also reacts with pre-adsorbed hydrogen and the quantitative experimental result agrees with the fact that both nitrogen and ammonia are formed. The ESI-MS detector is able to distinguish between different components simultaneously, as was used in the case of glucose oxidation, demonstrating the most significant advantage over existing transient techniques.*

Accepted for publication in *Journal of Catalysis*

3.1 Introduction

HETEROGENEOUS CATALYTIC REACTIONS in liquid phase are very important in areas such as production of bulk chemicals, fine chemicals and pharmaceuticals [1, 2]. It is well known that production of fine-chemicals and pharmaceuticals is in most cases less efficient compared to bulk chemicals, which is caused by multi-step synthesis procedures and by the use of stoicheometric reduction- and oxidation-reactions. Therefore, efficient and selective catalysts are required to improve these processes. Many of the targeted molecules are relatively complex and have limited thermal stability, implying that most of the reactions require solvents.

Development of highly efficient catalysts for gas phase reactions has always been assisted by powerful characterization techniques as well as methods that allow characterization *in-situ* or *operando* [3]. Transient experiments, including pulse and step change modes have been extensively used to obtain kinetic and mechanistic information [4–6]. These methods were significantly optimized by Gleaves et al. [7] when developing the Temporary Analysis of Products method (TAP), which has been recently used by many researchers, e.g. by Yablonsky et al. [8] and Nijhuis et al. [9].

A similar approach is appropriate to develop and improve catalysts for application in liquid phase. However, many of the experimental techniques that were developed for gas phase experiments require vacuum or low pressure and cannot be applied in liquid phase. An example of successful modification of a characterization technique to enable experiments in liquid phase is Infra-red (IR) spectroscopy in Attenuated Total Reflection (ATR) mode, pioneered by Bürgi and Baiker [10] and further developed by Ebbesen et al. [11].

In the case of transient experiments, including chemisorption experiments in pulse mode or step change mode, there is no principal problem to operate in liquid phase. The challenge is mostly technical in character, because fast analysis of species at the exit of the reactor is required for transient studies. In gas phase transient experiments this is normally achieved using an on-line mass spectrometer (MS) which allows real-time multi-component analysis at least semi-quantitatively. The goal of the present study is to develop and demonstrate a similar technique that can be used for heterogeneous catalytic experiments in liquid phase.

There have been attempts to perform transient type experiments in liquid phase. A Refractive Index (RI) detector was used in a few studies [12, 13]. Denayer et al. [12] performed pulse type transient experiments to determine the influence of polarity, pore size and topology on the adsorption of n-alkanes, isoalkanes, aromatics and other organic components on FAU and MFI zeolites. These authors have been using a High Performance Liquid Chromatography (HPLC) cartridge filled with FAU or MFI zeolites, combined with an in-line differential RI detector. Jonker [13] used tracer pulse experiments in order to determine effective diffusion coefficient (D_e) of edible oils and their fatty acid methyl esters over Ni/SiO_2 catalyst. These authors also used an HPLC cartridge filled with catalyst (5–40 μm) as reactor, combined with an in-line differential RI detector. Continuous flow Ultraviolet-Visible spectroscopy (UV-Vis) detectors were also used [14–16]. Hejtmánek and Schneider [14] performed step type transient experiments to determine axial dispersion coefficients for tracer/carrier-liquid systems such as acetone-water, toluene-methanol or acetone-ethylene glycol, using HPLC cartridges filled with 4.5 μm mono-dispersed spherical glass particles. Lin and Ma [15] performed tracer studies using liquid chromatography to determine effective intraparticle diffusion coefficients and adsorption equilibrium constants, on silicalite and alumina, of various alcohols in water and of toluene, acetone and ethyl acetate dissolved in cyclohexane. Kiraly et al. [16] used an HPLC cartridge filled with a Pt/Al_2O_3 catalyst in transient pulse experiments, in order to determine Pd dispersion at the solid-liquid interface. Gao et al. [17] used a flow-through liquid cell for Fourier Transform Infrared Spectroscopy (FTIR) analysis, connected to an HPLC cartridge filled with 55 μm Pt/Al_2O_3 catalyst particles for studying hydrogenation of acetophenone.

All these examples have in common that the equipment consists of

1. a liquid feed section equipped with a device to generate pulses or steps,
2. a catalytic reactor mostly based on HPLC cartridges filled with catalyst and
3. a detector.

The most significant difference is the choice of detector. Commonly used detectors (e.g., RI or UV-Vis [18] have the disadvantage that these cannot distinguish between different compounds. This is a serious limitation when more then one component is present in the mixture leaving the reactor. Therefore, we have developed alternative methods to detect different species leaving the reactor simultaneously, based on Electron Spray Ionization Mass Spectrometry (ESI-MS). Mass spectrometry is a fast technique and in principle able to detect multiple components simultaneously [19], although this is not trivial. Mass spectrometers with electro-spray ionization are available commercially as part of HPLC-MS systems, equipped with a liquid phase-MS interface [20]. To the best of our knowledge, a transient response technique for liquid phase heterogeneous catalytic studies equipped with an ESI-MS as detector has not been described before.

The pressure drop in the catalytic reactor has been minimized in this study in order to generate sufficient flexibility to optimize liquid flow rates. The first approach was to use a catalyst based on mono-disperse silica support particles (Microsorb silica)[21]. The second approach was to use carbon-nano-fibers (CNFs) supported on Ni (CNF/Ni) [22] foam as catalyst support with extreme high porosity.

Two catalytic reaction systems in aqueous phase have been selected to develop and demonstrate this technique:

1. catalytic reduction of nitrite (NO_2^-) over a Pt/SiO_2 catalyst and
2. catalytic oxidation of glucose over Pt supported on carbon.

Nitrite hydrogenation [23] is a relevant reaction for both nitrate to nitrogen de-nitrification of drinking water [24], as well as nitrate hydrogenation to hydroxyl-amine, an intermediate in the production of caprolactam [1]. Oxidative conversion of glucose is important in view of the anticipated shift towards renewable feedstocks for the chemical industry. Glucose can be upgraded to more valuable compounds e.g. gluconic acid, a building block for production of chelating agents [25–27].

3.2 Experimental

3.2.1 Materials

HPLC silica (Microsorb from Varian, BET surface area 198 m^2/gr; mean particle size 5 μm) was used as support for Pt/SiO_2. The fixed bed reactor was made by filling an HPLC cartridge (internal diameter $4.6 \cdot 10^{-3}$ m, 0.1 m long) with Pt/SiO_2 catalyst. The catalyst bed was fixed in the cartridge with two metallic 2 μm frits at the inlet and the outlet. CNF/Ni foam was prepared as described elsewhere [22, 28]. The CNF loading was 30 wt% and the total surface area was 50 m^2/gr (BET, Micromeritics). Pt/CNF supported on Ni foam was obtained in cylindrical pieces ($4.55 \cdot 10^{-3}$ m wide and $5 \cdot 10^{-3}$ m long). Tetra ammonium-platinum hydroxide $(NH_3)_4Pt(OH)_2$ (99.9 %, Aldrich) was used as platinum precursor for the SiO_2 supported catalyst while as platinum precursor for CNF a $Pt(C_5H_7O_2)_2$ (99 %, Aldrich) was used. Ultra pure LC-MS grade water (Biosolve) was used to prepare $(NH_3)_4Pt(OH)_2$ solutions as well as to prepare $NaNO_2$ (99 %, Aldrich) solutions, glucose (99 %, Aldrich) solution and gluconic-acid (50 % aqueous solution, Aldrich) solutions. Toluene (99 %, Merck) was used to prepare solutions of $Pt(C_5H_7O_2)$. Argon (Air Products BIP, 99.9999 %) was further purified by using an oxygen trap (OxyTrap, Alltech), to decrease the oxygen content to 10 ppb or lower. Hydrogen (99.999 %) and oxygen (99.999 %) were purchased from Indugas.

3.2.2 Catalyst preparation and characterization

The Pt/SiO_2 catalyst was prepared by ion-exchange as described in Chapter 2 [21]. The platinum loadings of fresh and spent catalysts were determined with X-ray fluorescence spectroscopy (XRF; Phillips PW 1480 spectrometer). The Pt/CNF/Ni catalyst was made by wet impregnation in the following sequence: first, 0.9 grams CNF/Ni was contacted overnight with 60 mL $Pt(C_5H_2O_7)_2$ in toluene. Then, the CNF/Ni pieces were dried for 3 h at 60 °C in a rotary evaporator, followed by calcination at 270 °C for 2 h in 20 % O_2 in N_2 and reduction in 20 % H_2 in N_2 for 1 h. Flow rates of gases during treatments were 100 $ml \cdot min^{-1}$. The Pt concentration of the Pt/CNF/Ni catalyst could not be determined with XRF because the foam does not fit in the XRF spectrometer. However, the amount of platinum introduced should result in 3 % by weight.

Platinum dispersions of the Pt/SiO_2 and Pt/CNF/Ni catalysts were measured with pulse flow chemisorption apparatus (ChemiSorb 2750, Micromeritics). The platinum metal dispersion was calculated, assuming $H : Pt_s$ ratio of unity [29]. Particle sizes of fresh Pt/SiO_2 and Pt/CNF/Ni catalysts were cross checked with transmission electron microscopy (TEM; Phillips CM 30 microscope, 300 kV); the sizes of typically one hundred platinum particles were determined in each sample.

3.2.3 Transient response experimental set-up

A schematic representation of the equipment is presented in Figure 3.1. The set-up consists of

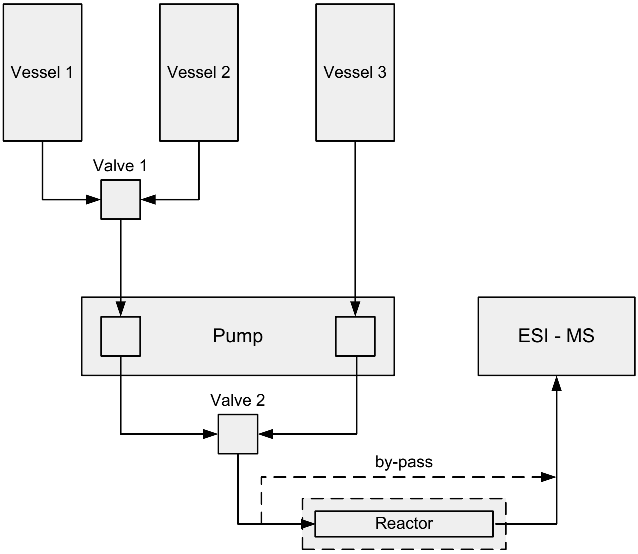

Figure 3.1: *Scheme of the experimental set-up*

1. a feed section (containers, selection valve and pump) with a switching valve to introduce a well-shaped step/pulse function in the reactant concentration,

2. a catalytic reactor, i.e. packed bed or filled with foam and

3. an ESI-MS detector directly connected to the reactor outlet.

Feed section with pulse/step introducing device

Gas tight liquid containers (three homemade 1.8 L vessels made of Pyrex glass) were connected to a pulse free HPLC binary pump (G1312A, Agilent) with 1/8” tubings (Swagelock), either directly (container 3 containing pure water) or via an HPLC valve 1 (G1160A, Agilent) (containers 1 and 2 containing dissolved gases and/or with reacting species). The containers were stirred electromagnetically. Gas was supplied to the liquid containers through glass frits positioned close to the stirrer. The HPLC pump yielded flow rates in the range 0.2–0.5 ml·min^{-1} (±1 %). Pulse or step-type changes in the reactant concentrations were introduced by switching HPLC valve 2 (G1158A, Agilent). The system was automated and controlled with Chemstation software (Version b 02.01, Agilent) [20].

Reactors

Two types of catalytic reactors were used, i.e. Pt/SiO$_2$ fixed bed and Pt/CNF/Ni supported on Ni-foam. To prevent channeling of liquid, filling of the cartridge with the Pt/SiO$_2$ catalyst was carefully done, following standard procedures for making HPLC columns [30]. The CNF foam was tightly fitted in the cartridge and the distance to the wall was in the same range as the pore diameter in the foam ($1–5 \cdot 10^{-4}$ m). The volume of the voids within the reactors was estimated by weighing the reactors before and after filling with water. The estimated volume was used to calculate residence time and was always within 5 % error. The dynamic behavior of the reactors (filled with silica support or with CNF/Ni support, without Pt) was determined by pulsing nitrite solution (concentration $2.2 \cdot 10^{-4}$ mol·dm^{-3}, 50 ml during 100 minutes) or glucose solution (concentration $5.6 \cdot 10^{-5}$ mol·dm^{-3}, 12.5 ml during 25 minutes). It was observed that silica leached when flowing alkaline glucose solution [30] and therefore Pt supported on CNF/Ni was used for experiments with glucose.

The catalytic reactor was placed in an oven, made of aluminium blocks with two integrated heating fingers (G4A78, Watlow/Kurval). The temperature of 60 °C in the oven was uniform (±0.5 °C) and controlled by a temperature controller (Eurotherm 2132).

Analyzer

Qualitative and quantitative analysis of ionic species present in the effluent from the reactor was performed with an on-line mass spectrometry detector (MSD) (Agilent, SL/G1956B) equipped with an electro-spray ionization (ESI) liquid phase interface (Agilent, G1948A). The liquid chromatography part of the equipment was removed and the effluent from the reactor was directly injected into the electron-spray ionization chamber.

The ESI process involves three main steps [31]:

1. production of charged droplets at the ES capillary tip,
2. shrinkage of the charged droplets by solvent evaporation leading to very small charged droplets capable of producing gas-phase ions and
3. formation of gas-phase ions from charged droplets. Parameters that can affect the ESI process are solvent composition, temperature, spray voltage, solvent flow rate and nebulizing gas flow rate [32].

ESI is usually applied to analyze high-molecular-weight and polar molecules, like organic acids, which easily form ions. Unfortunately, compounds that are difficult to ionize, e.g. nitrogen and other dissolved gases, cannot be detected with ESI-MS. In the present study, analysis was performed in the mass range between m/z 10 and 500. The signal to noise ratio for relevant compounds was optimized via the choice of parameters shown in Table 3.1.

Table 3.1: *Instrumental parameters for ESI-MS analysis*

Capillary voltage (kV)	4.0 / 3.8[1]
Desolvation gas temperature (°C)	350
Nebulising gas flow rate (L·min^{-1})	12
Water with analyte flow rate (mL·min^{-1})	0.5
Water flow rate (mL·min^{-1})	0.5

[1] Capillary voltage used in experiments with glucose

3.2.4 Catalytic experiments

Prior to experiments, vessels 1 and 3 were filled with approximately 1 liter of pure water and vessel 2 with 1 liter of aqueous solution containing the reacting species (glucose or nitrite ions). An aqueous solution of NaOH ($1 \cdot 10^{-3}$ mol) was used to adjust pH of the glucose solution to pH = 9 ± 0.3 in order to prevent inhibition of the catalysts with carboxylic acids [33]. The liquids in vessels 2 and 3 were flushed with argon in order to remove any dissolved gases (60 minutes, 200 ml·min^{-1}), while in vessel 1 water was saturated with oxygen or hydrogen (30 minutes, 200 ml·min^{-1}, 22 °C). Experiments were performed with 0.5 ml·min^{-1} flow rate at 60 °C.

Pulse titration experiments with aqueous nitrite solution over Pt/SiO$_2$ were performed in the following sequence. First, water saturated with hydrogen (from vessel 1) was flowed for 60 minutes through the reactor in order to pre-adsorb hydrogen. Then, pure water (from vessel 3) was flowed through the reactor for 30 minutes in order to remove dissolved hydrogen from the solution and physisorbed hydrogen from Pt/SiO$_2$. Finally, the pre-adsorbed hydrogen was contacted with pulses of nitrite solution (concentration $2.2 \cdot 10^{-4}$ mol·dm^{-3}, 5 ml during 10 minutes); pulses were repeated every 20 minutes, flowing pure water between pulses.

Another sequence was applied to study the interaction of Pt/CNF/Ni with aqueous glucose solution. First, water saturated with oxygen (from vessel 1) was flowed for 30 minutes (flow 0.5 ml·min^{-1}) at 60 °C through the reactor in order to pre-adsorb oxygen. Then, pure water (from vessel 1) was flowed through reactor for 60 minutes in order to remove dissolved oxygen from the solution and physisorbed oxygen from Pt/CNF/Ni. Finally, pre-adsorbed oxygen was contacted with pulses of glucose solution (concentration $5.6 \cdot 10^{-5}$ mol·dm^{-3}, 30 ml during 60 minutes). Pulses were repeated after 20 minutes, flowing pure water between pulses. Calibrations for quantitative interpretation will be described in the result and discussion section.

3.3 Results and discussion

First, the results of catalyst preparation and characterization will be presented and discussed. Then, pressure drop, response time of the detector and the hydrodynamic behavior of the reactors will be commented. Subsequently, detection and calibration of species with ESI-MSD will be described and commented. Finally, the results of transient catalytic experiments, probing the reactivity of pre-adsorbed hydrogen with nitrite and pre-adsorbed oxygen with glucose, will be reported and discussed.

3.3.1 Catalyst preparation and characterization

The platinum loading of Pt/SiO$_2$ (1 ± 0.05 wt%) is agreeing well with the expectation based on the preparation procedure (Table 3.2). Pt/CNF/Ni could not be analyzed with XRF, therefore, the platinum loading according the preparation procedure (3 wt%) is assumed.

No contamination could be detected with XRF on all catalysts, before or after experiments. Table 3.2 also reports the platinum dispersion measured with hydrogen chemisorption (65 % for Pt/SiO$_2$ and 25 % for Pt/CNF/Ni). The platinum dispersions estimated from the average metal-particle size obtained from TEM analysis agree well with hydrogen chemisorption data, indicating that the assumption on the Pt loading of Pt/CNF/Ni is reasonable. In the case of Pt/SiO$_2$, the calculated dispersion based on TEM is slightly lower than according chemisorption, indicating that possibly this catalyst contains some very small particles (< 2 nm) which can not be clearly observed with TEM.

Table 3.2: *Catalyst loadings and dispersions determined in gas phase*

Catalyst	Loading, (wt%)	H/Pt	Amount of Pt		H/Pt – TEM[1]
			Bulk (μmoles/g)	Surface (μmoles)[3]	
Pt/SiO$_2$	1.0±0.05	0.65	51	10.0	0.55
Pt/CNF	3.0[2]	0.25	154	11.0	0.29

[1] calculated based on D(TEM) = $\frac{1.08}{d(nm)}$ [29]

[2] the Pt loading calculated based on a preparation procedure

[3] amount of surface platinum atoms available in the reactor

3.3.2 Pressure drop, response time of detector and hydrodynamic behavior of the reactors

Flowing 0.5 ml·min^{-1} over the Pt/SiO$_2$ packed bed results in a typical pressure drop of 40 bars; 2–3 bars is typically due to the two metal frits. After one week of operation, the pressure drop slightly increased (from 40 to 43 bars) remaining constant afterwards. This effect may be due to further compaction of the bed. For the same flow rate, the pressure drop over the foam increased from 2 bars initially to 12 bars after 2 weeks of use. During the following 2 weeks of use, pressure drop remained constant. Inspection of the used reactor showed black CNF fines deposited on the frit at the outlet. After cleaning the frit, the pressure drop recovered completely and no new fines and rise of pressure drop was observed. Thus, a small part of the CNFs on Ni foam is not well attached and could be removed by flowing compressed air. This observation agrees well with the results of Jarrah et al. [28, 34], describing the preparation of CNFs on Ni foam; it was reported that a small fraction of the CNFs is loosely attached whereas the remaining CNFs is strongly bonded to the Ni-foam support.

The response time of the detector (time required for the signal to reach a level of 95 % of the stable value) is in the order of 20 seconds, as observed in the blank experiment by-passing the reactor for both nitrite ions (Figures 3.2–A, 3.3–A) and glucose (Figures 3.2-C, 3.3-C). Figure 3.2 presents the complete response to the pulse whereas Figure 3.3 shows details of the response to the step up part of the pulse.

Figures 3.2-B and 3.3-B show the response to a nitrite pulse with the SiO_2 fixed bed. A delay of 1.45 minutes is observed, in good agreement with the residence time in the reactor (1.40 minutes) based on the free volume in the reactor. The breakthrough curve from the reactor with silica is sharp and the signal stabilizes within 20 seconds (Figure 3.3-B). The same experiment with glucose and SiO_2 is shown in Figures 3.2-D and 3.3-D. Surprisingly, a delay of 6.10 minutes is observed, both at the front and the back end of the pulse, whereas the residence time is still 1.4 minutes. The step response indicates that about 0.1 μmole glucose adsorbs reversibly. Figure 3.2-E shows

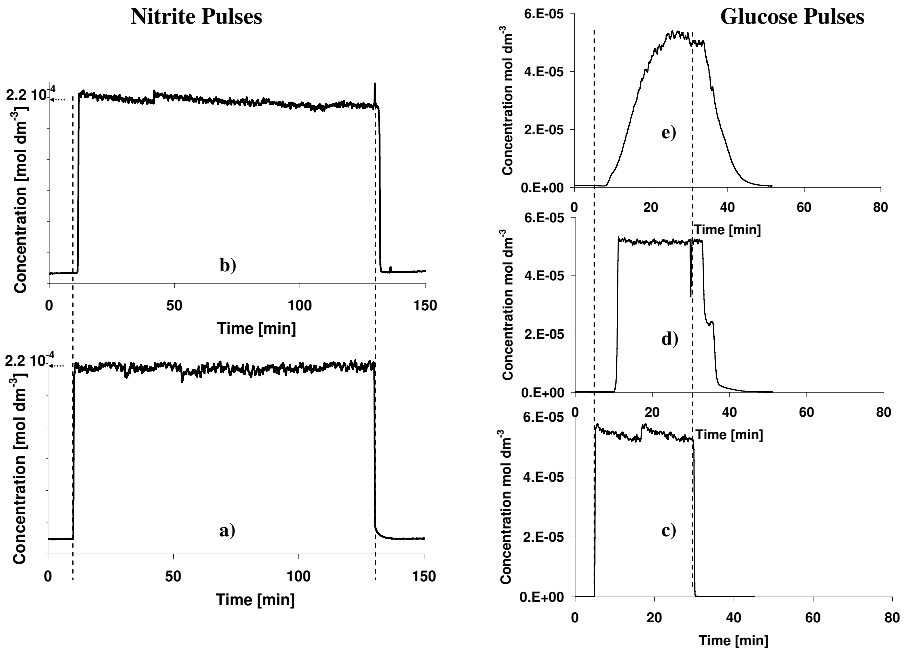

Figure 3.2: *Response of A) by-pass and B) reactor with silica to the pulse of nitrite (*50 ml *during 100 minutes with flow rate* 0.5 ml·min^{-1}, $c_M(NO_2^-) = 2.2 \cdot 10^{-4}$ mol·dm^{-3}, $T = 60$ °C*); Response of C) by-pass, D) column with silica and E) column with CNF to a pulse of glucose (*12.5 ml *during 25 minutes with flow rate* 0.5 ml·min^{-1}, $c_M(C_6H_{12}O_6) = 5.6 \cdot 10^{-5}$ mol·dm^{-3}, $T = 60$ °C*)*

the response of a reactor with CNF/Ni to a glucose pulse. Stabilization of the signal was attained after 20 minutes (Figures 3.2-E and 3.3-E), much longer than the residence time in the free volume of the CNF/Ni reactor which is 3 minutes. Furthermore,

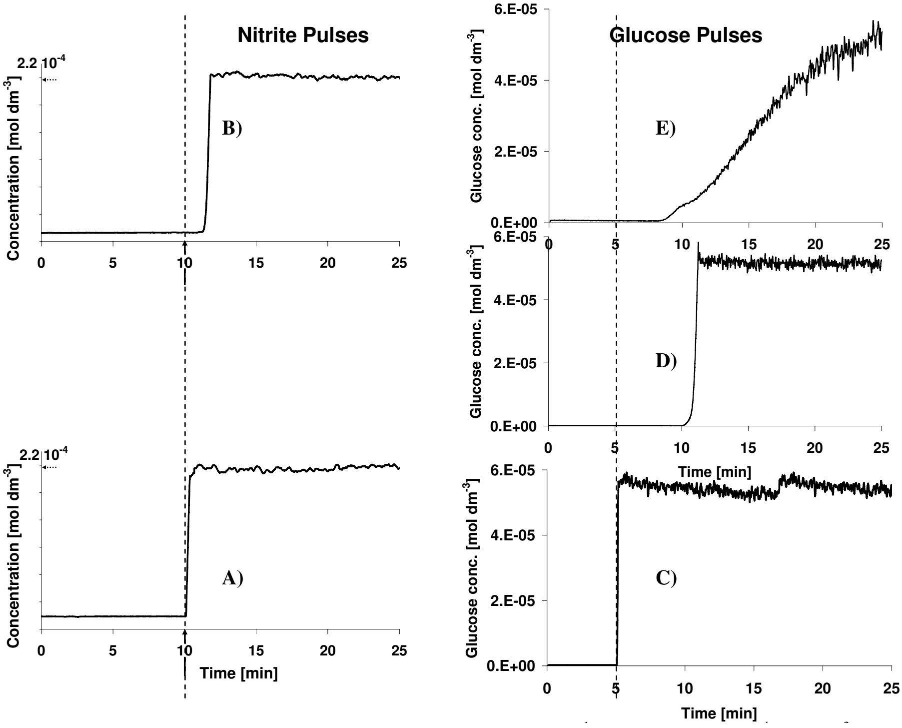

Figure 3.3: *Pulse of nitrite (*50 ml *during 100 minutes with flow rate* 0.5 ml·min^{-1}, $c_M(\mathrm{NO_2^-})$ = 2.2·10^{-4} mol·dm^{-3}*) A) by-pass and B) reactor with silica at T* = 60 °C*) and pulse of glucose (*12.5 ml *during 25 minutes with flow rate* 0.5 ml·min^{-1}, $c_M(\mathrm{C_6H_{12}O_6})$ = 5.6·10^{-5} mol·dm^{-3}, *T* = 60 °C*) C) by-pass, D) column with silica and E) column with CNF*

3.3.3 Calibration

Figure 3.4 shows a typical MS spectrum for a sodium-nitrite solution revealing significant peaks at m/z 46, 115 and 184. Mass m/z 46 corresponds to the $\mathrm{NO_2^-}$ anion while m/z 115 and 184 are agglomerates of nitrite and sodium ions [35] (i.e. $([2\,\mathrm{NO_2^-}]\mathrm{Na^+})^-$ and $([3\,\mathrm{NO_2^-}]2\,\mathrm{Na^+})^-$ respectively).

The most intense peak (i.e. m/z 115) can be used for quantitative determination, because intensity increases regularly with concentration (Figure 3.5); surprisingly the intensities of m/z 46 and m/z 184 decrease with increasing concentration. This indicates that the m/z values to be used need generally careful selection based on calibration experiments. The concentration of nitrite can be accurately determined in the concentration window between 2·10^{-5} mol·dm^{-3} (detection limit with signal/noise

>5) up to about $5\cdot10^{-4}$ mol·dm^{-3}; at higher concentrations the MS signal hardly increases anymore (Figure 3.5). This is a saturation effect [36] caused by a decrease of the ionization efficiency. Ammonia is, next to nitrogen, a product when hydrogenating nitrite. Unfortunately, ammonia could not be detected, due to the low molecular mass. On the other hand, it was checked that the presence of ammonia does not affect the calibration of nitrite.

Figure 3.6 shows a typical spectrum of glucose; the most significant peaks are observed at m/z 215 and 179. The peak at m/z 215 corresponds to the de-protonated glucose ion with two associated molecules of water ($2\,H_2O\cdot[C_6H_{11}O_6]^-$) and is the most suitable for quantitative determinations because the calibration curve for this peak increases linearly with increasing glucose concentration (Figure 3.7).

The peak at m/z 179 corresponds to $[C_6H_{11}O_6]^-$ (i.e. de-protonated glucose molecule without water); also here the signal cannot be used because it does not increase regularly with increasing glucose concentrations. Less significant peaks, i.e. m/z 59, 61, 89, 119 and 149 belong to fragments of glucose, $[C_2H_3O_2]^-$, $[C_2H_5O_2]^-$, $[C_3H_5O_3]^-$, $[C_4H_7O_4]^-$ and $[C_2H_5O_2]^-$, respectively. The limit of detection for glucose was $6\cdot10^{-6}$ mol·dm^{-3} and the concentration of glucose can be accurately determined up to $1.5\cdot10^{-4}$ mol·dm^{-3}, before the saturation effect occurs (Figure 3.7).

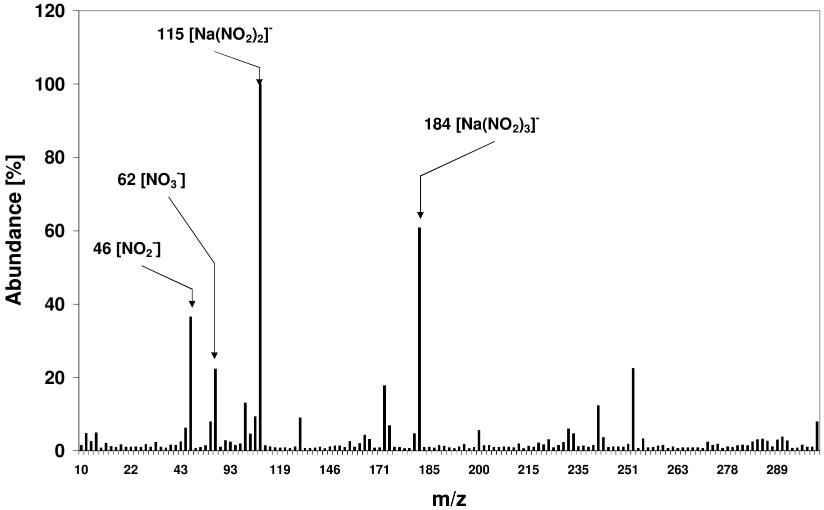

Figure 3.4: *Spectrum obtained during analysis of* $2\cdot10^{-4}$ mol·dm^{-3} *nitrite* (NO_2^-) *aqueous solution at* 60 °C *and liquid flow rate of* 0.5 ml/min^{-1}

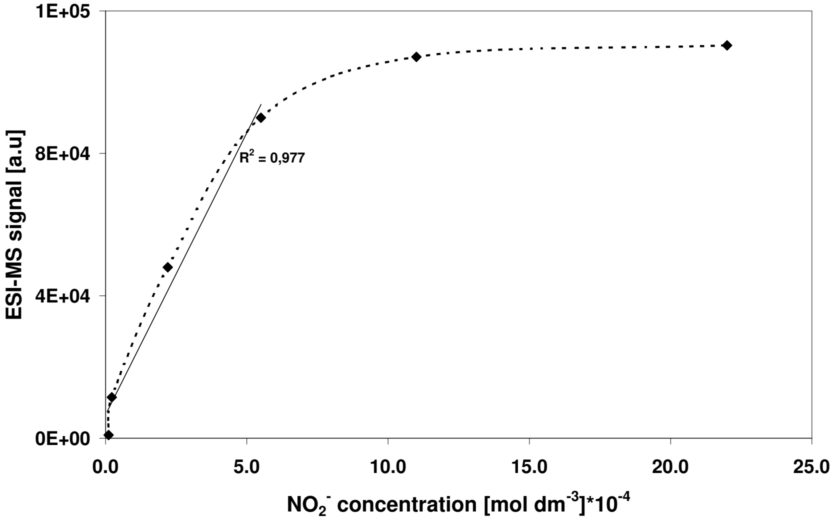

Figure 3.5: *Calibration curve for nitrite (m/z 115 — $[Na(NO_2)_2]^-$) obtained at* 60 °C *and liquid flow rate of* $0.5\,\mathrm{ml/min^{-1}}$

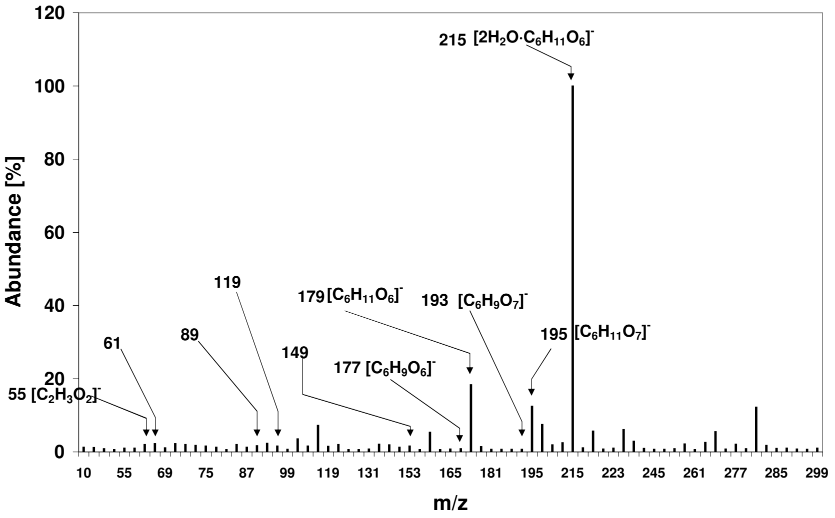

Figure 3.6: *Glucose spectrum for* $5.6\cdot10^{-5}\,\mathrm{mol{\cdot}dm^{-3}}$ *at* 60 °C *and liquid flow rate of* $0.5\,\mathrm{ml/min^{-1}}$

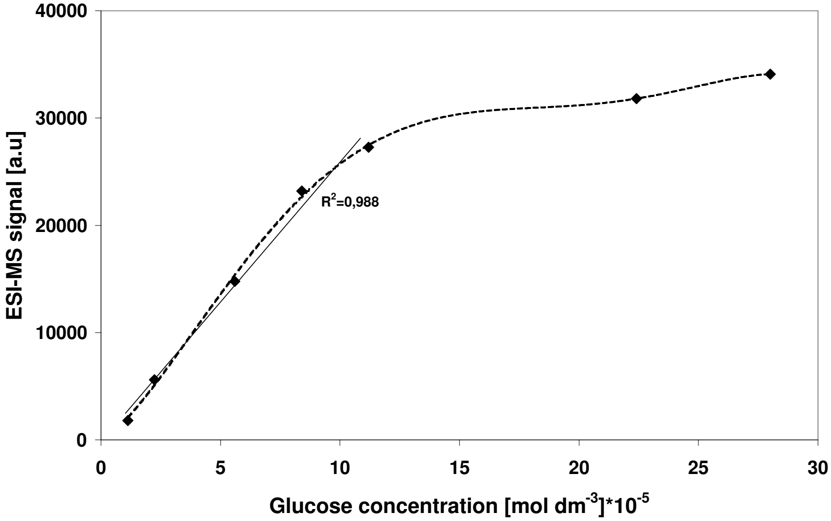

Figure 3.7: *Calibration curve for glucose (m/z 215 — $2\,H_2O \cdot [C_6H_{11}O_6]^-$) obtained at* 60 °C *and liquid flow rate of* 0.5 ml/min^{-1}

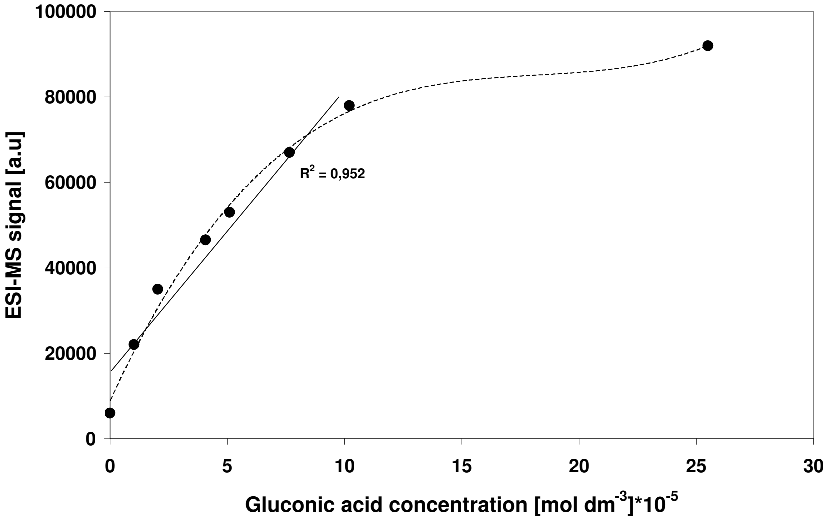

Figure 3.8: *Calibration curve for gluconic acid (m/z 195 — $[C_6H_{11}O_7]^-$) obtained at* 60 °C *and liquid flow rate of* 0.5 ml/min^{-1}

Calibration was also done for gluconic acid (Figure 3.8); the most significant signal observed was at m/z 195 (corresponding to de-protonated gluconic acid $[C_6H_{11}O_7]^-$ anion). Gluconic acid can be accurately determined between $1\cdot10^{-6}$ mol·dm^{-3} up to $1\cdot10^{-4}$ mol·dm^{-3}. Experiments with mixtures of glucose ($5.6\cdot10^{-5}$ mol·dm^{-3}) and gluconic acid ($5.1\cdot10^{-5}$ mol·dm^{-3}) revealed some charge competition, i.e. the glucose concentration is underestimated whereas gluconic acid is overestimated. The error in both cases is at maximum 20 %, which we currently accept as experimental inaccuracy at this stage of development.

Calibrations were repeated every two weeks resulting in reproducible results within 10 % error. Application of the ESI-MS detector in continuous flow mode caused frequent blockages of the nebulizing needle due to deposition of dissolved species on the wall of the needle (especially during the analysis nitrite). This was manifested by the pressure rise in the ESI (2–3 bars after one month of operation). This effect was prevented by daily cleaning and replacement of the nebulizing needle when pressure started to rise.

3.3.4 Catalytic reduction of nitrite species over Pt/SiO_2

Figure 3.9 shows the experimental result of pulsing nitrite for both the pre-reduced Pt/SiO_2 catalyst as well as for silica support only, serving as a blank experiment. Complete consumption of nitrite is observed during the first pulse on the reduced Pt/SiO_2. A breakthrough occurs during the next three pulses. Finally, the surface area of the peaks becomes identical to the blank experiment, indicating that hydrogen is not consumed anymore. The total amount of nitrite converted was 2.4 μmoles.

Selective hydrogenation of nitrite with hydrogen pre-adsorbed on platinum under the present experimental conditions results in formation of nitrogen and ammonia, according the following equations [37]:

$$2NO_2^- + 6H_a \longleftrightarrow N_2 + 2OH^- + 2H_2O \tag{3.1}$$

$$NO_2^- + 6H_a \longleftrightarrow NH_4^+ + 2OH^- \tag{3.2}$$

The total amount of hydrogen available, adsorbed on the Pt catalyst, is 10 μmoles, assuming one hydrogen atom on every surface Pt atom (Table 3.2). Accordingly, the amount of nitrite that could be converted if ammonia would be the only product (Eq. 3.2) is 1.7 μmoles (maximal consumption of H_a). If nitrogen would be the only product (Eq. 3.1), the amount of converted nitrite would be 3.3 μmoles (minimal consumption of H_a). The observed conversion in our experiment (i.e. 2.4 μmoles) is between these boundary values, indicating that both ammonia and nitrogen are formed. Unfortunately, the MS is not able to detect these species because of their low molecular weight and stability against the relatively soft ESI ionization method. Nevertheless,

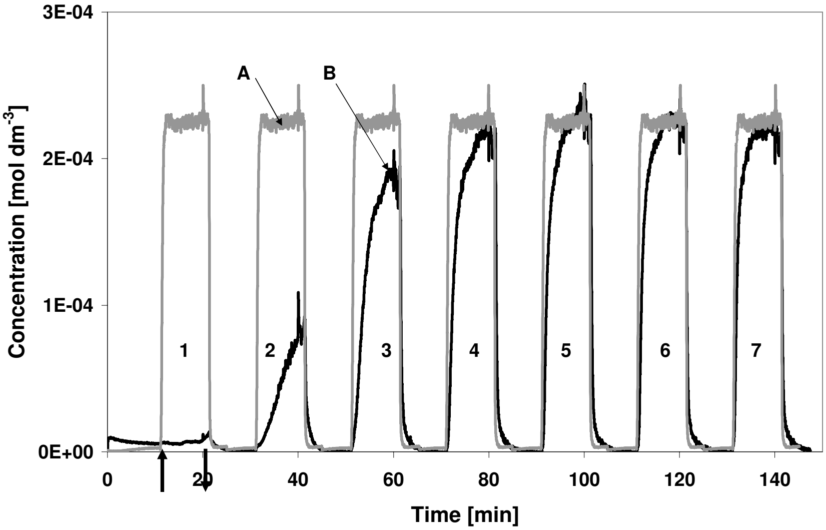

Figure 3.9: *Titration of pre-adsorbed hydrogen on Pt/ SiO_2 using pulses with nitrite aqueous solution (10 minutes long,* 0.5 ml/min, $c_M = 2 \cdot 10^{-4}$ mol/dm^3 NO_2^-, $T = 60\,°C$*) over: A) Reactor filled with silica and B) Reactor filled with Pt/ SiO_2 catalyst with pre-adsorbed hydrogen*

the sensitivity of the MS detector allows quantitative determination of nitrite conversion caused by hydrogen coverage as low as 3 %.

Figure 3.10 shows the details of the responses to the nitrite pulse after all hydrogen has been consumed. The striking difference in shape of the responses for Pt/SiO_2 and support only, clearly indicates a reversible and significant interaction of dissolved nitrite with the platinum surface. The step response indicates that about 0.05 μmole of nitrite adsorbs. This must take place on the Pt surface because the result in Figure 3.10 presents the difference between catalyst and support only.

The step-down response is less clear in the sense that the amount of nitrite desorbing seems smaller than the amount that was adsorbed; probably desorption prolongs for a long time and the resulting nitrite signal cannot be distinguished anymore from the base-line. Strong interaction of nitrite with Pt was reported by Ebbesen et al. [38] in an ATR-IR study on adsorption of NO_2^- on Pd/Al_2O_3 and Pt/SiO_2. However, beside strong adsorption, we can conclude based on our data that reversible adsorption also takes place. The amount is equivalent to 0.5 % of a monolayer on platinum and we speculate that NO_2^- interacts exclusively with a small fraction of specific sites at the surface of the Pt particles, e.g. corner-sites. The remarkable sensitivity of the detector should be recognized at this point, allowing quantitative determination of nitrite adsorption of less then 0.01 monolayer (ML).

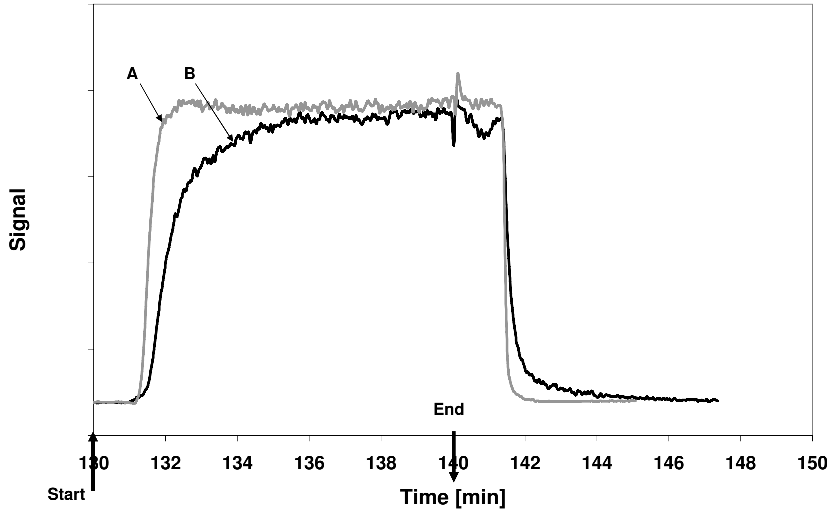

Figure 3.10: *Titration of pre-adsorbed hydrogen on Pt/ SiO_2 using pulses with nitrite aqueous solution (10 minutes long,* 0.5 ml/min, c_M =2 · 10^{-4} mol/ dm^3 NO_2^-, *T* = 60 °C*) over: A) Reactor filled with silica and B) Reactor filled with Pt/ SiO_2 catalyst with pre-adsorbed hydrogen*

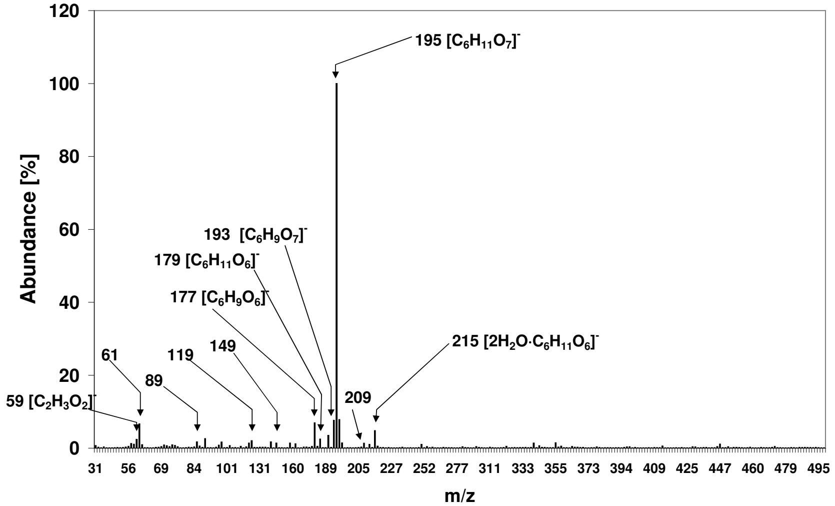

Figure 3.11: *Spectrum from the first pulse during titration of pre-adsorbed oxygen on Pt/ CNF catalyst with glucose from aqueous solution (pulse of* 30 ml, 0.5 ml/min, c_M =5.6 · 10^{-5} mol/ dm^3, *T* = 60 °C*)*

We observed a lower conversion of nitrite (i.e. 1.8 μmoles) in subsequent NO_2^- titration experiments, which implies a loss of platinum surface area. Furthermore, XRF analysis of the Pt/SiO_2 catalyst after three titration experiments showed a decrease in Pt loading (from 1.0 to 0.87 wt%). Hydrogen chemisorption of the Pt/SiO_2 catalyst after the titration experiments revealed a decrease in Pt dispersion from 0.65 to 0.58. These effects are possibly due to leaching of the smallest metal particles during the titration experiments, as this would account for both the loss of Pt as well as the decrease in dispersion. Similar effects were also reported by Douidah et al. [39] for small silica-supported platinum particles in aqueous media under hydrogen atmosphere.

The second part of this article describes the development and application of a detector similar to Membrane Inlet Mass Spectrometry (MIMS) for on-line and real-time analysis of dissolved gasses like N_2, in order to compensate for the inability of the ESI-MS detector in this respect.

3.3.5 Catalytic oxidation of glucose over a Pt/CNF/Ni supported on Ni-foam

Figure 3.11 shows the MS spectrum of the reactor effluent when a glucose solution in pulsed over Pt/CNF/Ni-foam containing pre-adsorbed oxygen.

A major part of the glucose is clearly converted because peaks at m/z 215 and m/z 179 are much lower as compared the blank experiment in Figure 3.6. The most significant peak in Figure 3.11 at m/z 195 is due to gluconic acid. Furthermore, peaks are observed at m/z 177, 193 and 209 in contrast to the blank experiment, corresponding to fragments of side- or intermediate-products during glucose oxidation. These peaks are assigned to respectively glucose dialdehyde ($[C_6H_9O_6]^-$ at m/z 177) glucuronic acid ($[C_6H_9O_7]^-$ at m/z 193) and glucaric acid ($[C_6H_9O_8]^-$ at m/z 209).

Figure 3.12 shows the result of repetitive pulsing with glucose on the pre-oxidized Pt/CNF/Ni catalyst. The left-hand plane compares the amount of remaining glucose (B) with the amount of glucose in the blank experiment in the absence of Pt (CNF-only, curve A), whereas curve C shows the amount of gluconic acid formed. Clearly, glucose is converted to gluconic acid and both conversion and yield of gluconic acid decreases when pulsing repetitively, approaching zero in the fifth pulse.

The total amount of glucose converted was 8.2 μmoles, whereas 5.6 μmoles gluconic acid was formed. The right-hand plane of Figure 3.12 shows the response signal for the species with m/z 177, 193 and 209. Glucose dialdehyde and glucuronic acid are clearly formed but it should be noted that intensities of these signals are much smaller as compared to gluconic acid. Intensities decrease during repetitive pulsing. The peculiar differences in the shape of the first peak indicate that glucuronic acid is

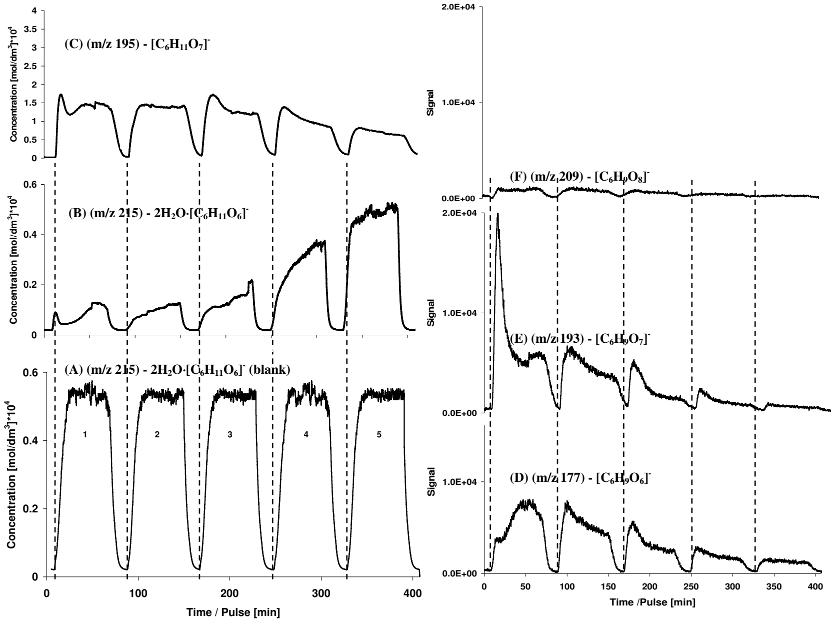

Figure 3.12: *Titration of oxygen pre-adsorbed on Pt/CNF supported on Ni-foam catalyst with the pulses of glucose aqueous solution (pulse of* 30 ml, 0.5 ml/min, $c_M = 5.6 \cdot 10^{-5}$ mol/dm^3, $T = 60\,°C$*)— reactor with CNF/Ni A) Glucose; - reactor with Pt/CNF/Ni B) Glucose; C) Gluconic acid; D) Glucose dialdehyde; E) Guluronic acid; F) Glucuronic acid*

especially formed at very high oxygen coverage. The mechanistic relevance of this observation is beyond the scope of this paper. The intensity of the signal due to glucaric acid is even smaller, but the intensity is significant at least in the first few pulses.

The main reaction during selective oxidation of glucose is described with the following equation (Eq. 3.3.5):

$$\underset{\text{glucose}}{C_6H_{12}O_6} + \frac{1}{2}O_2 \longrightarrow \underset{\text{gluconic acid}}{C_6H_{12}O_7} \qquad (3.3)$$

The amount of oxygen available in the reactor is 10 μmoles O_a ($O_a : Pt_s = 1$) and therefore maximal 10 μmoles glucose can be converted to gluconic acid. The amount of glucose converted in our experiment (i.e. 8.2 μmoles) is slightly less and the amount of gluconic acid formed (5.6 μmoles) is even lower. The discrepancy between glucose converted and gluconic acid formed (i.e. 8.2 *versus* 5.6 μmoles) is at least partly due to ionization suppression and charge competition effects between glucose and gluconic acid during ionization in ESI. In other words, calibration is influenced by the presence of the other species. Also, conversion to other products may contribute somewhat, given the fact that traces of other compounds are detected as discussed above.

Figure 3.13 shows the relation between the relative averaged reaction rate of glucose oxidation in each pulse (calculated based on the conversion level in each pulse) and the oxygen surface coverage. It is assumed that O_a : Pt_s is equal to unity initially and that each glucose molecule reacts with one pre-adsorbed oxygen atom. The highest reaction rate is observed for the first pulse at high oxygen coverage, resulting in about 70 % conversion. Figure 3.13 shows decreasing reaction rates with decreasing oxygen coverage. This result demonstrates that in principle the effect of O-surface coverage on the reaction rate can be determined; however, a higher flow-rate is needed to decrease the level of conversion in order to obtain the reaction order in adsorbed oxygen.

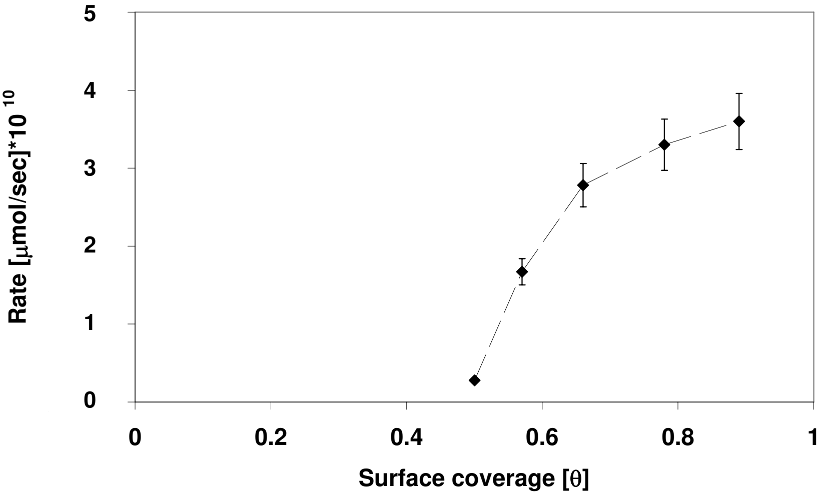

Figure 3.13: *Glucose oxidation reaction rate as function of the maximum estimate of the oxygen surface coverage (θ)*

The novel technique introduced here performs better as compared to existing transient techniques. The most significant advantage is the ability of the ESI-MS detector to distinguish between different components as clearly demonstrated in the case of glucose oxidation. In contrast, RI and UV-Vis detectors can follow only single compounds. ATR-IR can, in principle, also distinguish between different compounds; however, IR absorption peaks need to be well separated which is not generally the case and sensitivity is significantly lower. The response time of the detector allows detection in the range of 20 seconds which is significantly faster then typical responses of the RI (range of 40 seconds for flows between 0.2–3 ml/min) or FTIR (range of 5 minutes for flows between 3–7 ml/min), emphasizing the advantages of ESI-MS. Typical concentrations detected in our transient experiments ($1 \cdot 10^{-6}$–$1 \cdot 10^{-4}$ mol/dm^3) are significantly lower in comparison to the concentrations that can be detected by RI ($1 \cdot 10^{-4}$–$1 \cdot 10^{-2}$ mol/dm^3) or by FTIR ($1 \cdot 10^{-2}$ mol/dm^3). The experiment with nitrite, detecting of nitrite that reversibly interacts with 0.01 ML Pt, demonstrates the advantages of the ESI-MS detector. Clearly, application of the ESI-MS detection improves the sensitivity of the pulse-experiment significantly.

3.4 Conclusions

A novel, transient response technique for liquid phase heterogeneous catalytic studies was developed and successfully applied for the first time, based on an on-line method for real-time detection of species dissolved in an aqueous stream at the exit of a catalytic reactor. Electron Spray Ionization Mass Spectrometry (ESI-MS) is used for detection of dissolved molecules that easily ionize as well as dissolved ions. Two test reactions, nitrite reduction with Pt/SiO_2 and glucose oxidation with Pt/CNF/Ni were used to demonstrate semi-quantitative monitoring of reactants, intermediates and products. The capability of the novel technique is demonstrated by the fact that the ESI-MS detector is sufficiently sensitive to determine, quantitatively, extremely small amounts of physisorbing nitrite, down to 0.5 % of a monolayer on the Pt surface. Nitrite also reacts with pre-adsorbed hydrogen and the quantitative experimental result agrees with the fact that both nitrogen and ammonia are formed. The ESI-MS detector is able to distinguish between different components simultaneously, as was shown in the case of glucose oxidation, hence demonstrating the most significant advantage over existing transient techniques.

Acknowledgements

The authors thank, Ing. L. Vrielink for XRF and BET analysis, Ing. M. Smithers for TEM measurements, Ing. A. Hovestad for assistance with reactors preparation, Ing. J. Spies and Ing. B. Geerdink for technical assistance. Financial support for the project (TPC 5694) by STW (The Netherlands) is kindly acknowledged. This work was performed under the auspices of NIOK.

References

[1] C. G. M. van de Moesdijk. *The catalytic reduction of nitrate and nitric oxide to hydroxylamine: kinetics and mechanism.* Ph.D. thesis, University of Eindhoven (1979).

[2] J. H. Clark. Catalysis for green chemistry. *Pure and Applied Chemistry*, 73(1), 103–111 (2001).

[3] J. W. Niemantsverdriet. *Spectroscopy in Catalysis: An Introduction.* Wiley-VCH, 2 edition (2000).

[4] H. Kobayashi and M. Kobayashi. Transient Response Method in Heterogeneous Catalysis. *Catalysis Review: Science and Engineering*, 10, 139–176 (1974).

[5] C. O. Bennett, M. B. Cutlip and C. C. Yang. Grandientless reactors and transient methods in heterogeneous catalysis. *Chemical Engineering Science*, 27, 2255–2264 (1972).

[6] A. T. Bell and L. L. Hegedus, editors. *Catalysis Under Transient Conditions, ACS, Symposium Series*, volume 178. American Chemical Society, Washington, DC (1982).

[7] J. T. Gleaves, J. B. Ebner and T. C. Kueschler. Temporal analysis of products (TAP) — a unique catalyst evaluation system with submillisecond time resolution. *Catalysis Review — Science and Engineering*, 30, 49–116 (1988).

[8] G. S. Yablonsky, M. Olea and G. B. Marin. Temporal analysis of products: basic principles, applications, and theory. *Journal of Catalysis*, 216(1–2), 120–134 (2003).

[9] T. A. Nijhuis, L. J. P. van den Broeke, M. J. G. Linders, J. M. van de Graaf, F. Kapteijn, M. Makkee and J. A. Moulijn. Measurement and modeling of the transient adsorption, desorption and diffusion processes in microporous materials. *Chemical Engineering Science*, 54(20), 4423–4436 (1999).

[10] T. Bürgi and A. Baiker. In Situ Infrared Spectroscopy of Catalytic Solid-Liquid Interfaces Using Phase-Sensitive Detection: Enantioselective Hydrogenation of a Pyrone over Pd/TiO_2. *Journal of Physical Chemistry B*, 106, 10649–10658 (2002).

[11] S. D. Ebbesen, B. L. Mojet and L. Lefferts. In situ ATR-IR study of CO adsorption and oxidation over Pt/Al_2O_3 in gas and aqueous phase: Promotion effects by water and pH. *Journal of Catalysis*, 246, 66–73 (2007).

[12] J. F. Denayer, A. Bouyermaouen and G. V. Baron. Adsorption of Alkanes and Other Organic Molecules in Liquid Phase and in the Dense Vapor Phase: Influence of Polarity, Zeolite Topology, and External Fluid Density and Pressure. *Industrial & Engineering Chemical Research*, 37, 3691–3698 (1998).

[13] G. H. Jonker. *Hydrogenation of edible oils and fats.* Ph.D. thesis, University of Groningen (1999).

[14] V. Hejtmánek and P. Schneider. Diffusion of large molecules in porous glass. *Chemical Engineering Science*, 49(16), 2575–2584 (1994).

[15] Y. Lin and Y. H. Ma. A comparative chromatographic study of liquid adsorption and diffusion in microporous and macroporous adsorbents. *Industrial & Engineering Chemical Research*, 28, 622–630 (1989).

[16] Z. Kiraly, A. Mastalir, A. Csaszar, H. Demir, D. Uner and G. H. Findenegg. Liquid chromatography as a novel method for determination of the dispersion of supported Pd particles. *Journal of Catalysis*, 245, 267–271 (2007).

[17] F. Gao, K. P. Ng, C. Z. Li, K. I. Krummel, A. D. Allian and M. Garland. A versatile and compact experimental apparatus for the on-line spectroscopic study of liquid-phase heterogeneous catalytic systems. *Journal of Catalysis*, 237(1), 49–57 (2006).

[18] W. J. Lough and I. W. Wainer, editors. *High Performance Liquid Chromatography: Fundamental principles and practice.* Blackie Academic & Professional (1996).

[19] D. C. Harris. *Quantitative Chemical Analysis.* W. H. Freeman & Co., 6 edition (2003).

[20] `http://www.agilent.com`

[21] D. Radivojević, K. Seshan and L. Lefferts. Preparation of well-dispersed Pt/SiO_2 catalysts using low-temperature treatments. *Applied Catalysis A: General*, 301(1), 51–58 (2006).

[22] N. A. Jarrah, J. G. van Ommen and L. Lefferts. Mechanistic aspects of the formation of carbon-nanofibers on the surface of Ni foam: A new microstructured catalyst support. *Journal of Catalysis*, 239(2), 460–469 (2006).

[23] S. Ebbesen. *Spectroscopy under the Surface — In-Situ ATR-IR Studies of Heterogeneous Catalysis in Water.* Ph.D. thesis, University of Twente, Enschede, The Netherlands (2007).

[24] A. Pintar. Catalytic processes for the purification of drinking water and industrial effluents. *Catalysis Today*, 77(4), 451–465 (2003).

[25] M. Besson and P. Gallezot. Selective oxidation of alcohols and aldehydes on metal catalysts. *Catalysis Today*, 57, 127–141 (2000).

[26] H. Saito, O. Shinji and F. Shigeo. US Patent 4 843 173. *Kawaken Fine Chemical Corp. Ltd and Kao Corp.* (1989).

[27] K. Deller, H. Krause, E. Peldszus and B. Despeyroux. US Patent 5 132 452. *Degussa* (1992).

[28] N. A. Jarrah, F. H. Li, J. G. van Ommen and L. Lefferts. Immobilization of a layer of carbon nanofibres (CNFs) on Ni foam: A new structured catalyst support. *Journal of Materials Chemistry*, 15(19), 1946–1953 (2005).

[29] C. H. Bartholomew and R. J. Farrauto. *Fundamentals of industrial catalytic processes.* John Wiley & Sons, Inc., Publication (2006).

[30] K. K. Unger. *Porous silica — its properties and use as support in column liquid chromatography,* volume 16. Elsevier — Journal of Chromatography Library (1994).

[31] P. Kebarle and Y. Ho. *Electrospray Ionization Mass Spectrometry — Fundamentals, Instrumentation and Applications (On the Mechanism of Electrospray Mass Spectrometry).* John Wiley & Sons, Inc. (1997).

[32] Y. Cai, M. C. Concha, J. S. Murray and R. B. Cole. Evaluation of the role of multiple hydrogen bonding in offering stability to negative ion adducts in electrospray mass spectrometry. *Journal of the American Society for Mass Spectrometry,* 13(12), 1360–1369 (2002).

[33] T. Mallat and A. Baiker. Heterogeneously catalyzed selective oxidations in the liquid phase. Oxidation of alcohols with molecular oxygen on platinum metal catalysts in aqueous solutions. *Catalysis Today,* 19, 247–283 (1994).

[34] N. A. Jarrah. *Microstructured Catalyst Support Based on Carbon Nano-Fibers (CNFs).* Ph.D. thesis, University of Twente, Enschede, The Netherlands (2004).

[35] M. J. van Stipdonk, D. R. Justes, C. M. Force and E. A. Schweikert. Speciation of sodium nitrate and sodium nitrite using kiloelectronvolt energy atomic and polyatomic and megaelectronvolt energy atomic projectiles with secondary ion mass spectrometry. *Analytical Chemistry,* 72(11), 2468–2474 (2000).

[36] C. G. Enke. A predictive model for matrix and analyte effects in electrospray ionization of singly-charged ionic analytes. *Analytical Chemistry,* 69(23), 4885–4893 (1997).

[37] M. D'Arino, F. Pinna and G. Strukul. Nitrate and nitrite hydrogenation with Pd and Pt/SnO_2 catalysts: the effect of the support porosity and the role of carbon dioxide in the control of selectivity. *Applied Catalysis B: Environmental,* 53, 161–168 (2004).

[38] S. D. Ebbesen, B. L. Mojet and L. Lefferts. In situ attenuated total reflection infrared (ATR-IR) study of the adsorption of NO_2^-, NH_2OH, and NH_4^+ on Pd/Al_2O_3 and Pt/Al_2O_3. *Langmuir,* 24(3), 869–879 (2008).

[39] A. Douidah, P. Marécot and J. Barbier. Toward a better understanding of the stability of supported platinum catalysts in aqueous phase under hydrogen atmosphere at room temperature. *Applied Catalysis A,* 225(1–2), 11–19 (2002).

4

Development of a transient response technique for heterogeneous catalysis in liquid phase: Membrane Inlet Mass Spectrometry (MIMS) as detector for dissolved gasses

In Chapter 4, development of a home-made analyzer for dissolved gasses in water, based on membrane inlet mass spectrometry (MIMS), is described. The technique was applied for measuring the metal dispersion of three different catalysts (EuroPt-1, Pt/SiO_2 and Pt/CNF) in liquid phase via H_2–O_2 titration. The titration stoichiometry obtained (i.e. ratio of H_2 and O_2 consumption) is in agreement with the stoichiometry obtained in gas phase titration experiments in literature. The platinum dispersions obtained in liquid phase are in excellent agreement with dispersions based on hydrogen chemisorption in gas phase for all three catalysts. In addition, the detector is universal and allows calibration of H_2, O_2, N_2 and Ar dissolved in water with insignificant cross contamination. Despite the relatively slow dynamic response of the detector, it was proven possible to perform quantitative experiments in pulse mode, with a detection limit in the order of 0.5 m^2 Pt. The capability of this method is further demonstrated by the surprising observation that dissolved hydrogen physisorbs significantly on a reduced Pt catalyst whereas dissolved oxygen does not interact with an oxidized catalyst.

Accepted for publication in *Journal of Catalysis*

4.1 Introduction

IN CHAPTER 3 OF THE THESIS [1], we reported on the development of a transient reactor with real-time analysis of the effluent using on-line ESI-MS (electrospray ionization mass spectrometry). With this technique it is possible to follow semi-quantitatively species formed during transient catalytic oxidation of glucose and catalytic reduction of nitrite in liquid phase. Unfortunately, the limitation of this technique is the inability to detect gases dissolved in liquids, due to the relatively mild ionization process *via* electrospray. We therefore searched for alternative detectors for dissolved gasses.

Commercially available analyzers like Orbisphere [2] and Fugatron HYD 400 [3] are usually applied to analyze gases dissolved in liquids. Detection based on electrochemical reactions (Orbisphere analyzer) is usually lacking long term stability of the sensor. The Fugatron HYD 400 analyzer uses a coated probe permeable for dissolved gases, which improves the reliability of detection. These analyzers are able to detect single gasses present in liquids in industrial applications such as beverage production and nuclear power plants.

Home made analyzers such as Differential Electrochemical Mass Spectormetry (DEMS) [4, 5] or Membrane Inlet Mass Spectrometry (MIMS) [6] are usually described for scientific applications. The principle of operation of DEMS and MIMS is similar, i.e. removal of gases from the solution via permeation through a hydrophobic membrane, such as a porous Teflon membrane in the case of DEMS and a dense polymeric rubber membrane in the case of MIMS. The permeated gas is analyzed with a mass spectrometer in both cases. For example, Kana et al. [6] used a technique based on the MIMS principle for determination of nitrogen and oxygen dissolved in sea water. Kostiainen et al. [7] used a concept similar to MIMS to analyze volatile organic compounds like toluene, o-xylene, MTBE and phenol in water. In order to test the suitability of such an analyzer for transient experiments, we have chosen H_2–O_2 titration experiments on supported platinum catalysts in water as a case study.

Supported platinum catalysts have been used in this study in view of its wide application [8] and Pt on carbon has been included because of its frequent application in liquid phase oxidation and hydrogenation reactions [9, 10]. EuroPt-1 reference catalyst (platinum supported on silica) was used because it is well characterized in many labs [11, 12].

Hydrogen chemisorption is the standard technique to determine the dispersion of supported platinum catalysts [13, 14]. This technique is however not directly applicable in liquid phase because desorption of chemisorbed hydrogen by heating is an essential step, which cannot be done in liquid phase. Hydrogen titration of pre-adsorbed oxygen on platinum is an even more sensitive method and especially suitable for the catalysts with a low metal loading. It was applied for the first time by Benson and Boudart [15] who observed a titration stochiometry of H_2-chemisorption:O_2-chemisorption:H_2-titration = 1:1:3. This implies that hydrogen is consumed by both reaction with chemisorbed oxygen as well as by chemisorption on the metal. Consequently, if one assumes a Pt:O = 1:1 ratio, three atoms of hydrogen are consumed for every exposed platinum atom.

There are only two studies, to the best of our knowledge, addressing the question whether the presence of a liquid would influence the dispersion of supported precious-metal catalysts. Another issue is the question whether solvents would affect the dispersion measurement via influencing the chemisorption stoicheometry of oxygen and hydrogen. CS_2 was recently used as a probe molecule to determine Pd dispersion at the solid-liquid interface with transient pulse experiments [16]. It was claimed that the Pd dispersion obtained was approximately three times less then the dispersion obtained using gas phase (H_2 and CO) chemisorption (i.e. $(D_L) = 11\,\%$ vs. $(D_G) = 36\,\%$). Bradley and Busser [17] determined platinum dispersions with hydrogen chemisorption and compared the results with H_2–O_2 titrations, both in the liquid phase using a volumetric method. They found good agreement for dispersion measurements of colloidal polymer-supported platinum nanoclusters. Unfortunately, it is not clear how in this work an uncovered surface was obtained, which is necessary for the chemisorption experiment.

The volumetric method, as applied by Bradley and Busser [17], is very sensitive for temperature deviations. The pulse flow technique, which has been successfully applied for dispersion determination of supported platinum in the gas phase, does not suffer from that problem. In principle, the same approach can be applied using gases dissolved in a liquid phase. However, the key challenge is to find a sensitive detector which allows on-line analysis of all dissolved gases present in the liquid phase.

We here report on the development and application of a detector similar to MIMS to perform H_2–O_2 titrations over a series of platinum catalysts (EuroPt-1, Pt/SiO_2 and Pt/CNF) in water. When successful, this detector can be coupled to the ESI-MS detection system in order to arrive at an universal transient technique for liquid phase experiments allowing detection of both organic compounds and ions (ESI-MS) as well as dissolved gases. To the best of our knowledge, application of pulse experiments with gases dissolved in water to determine platinum dispersions was not described before and we are reporting here on the influence of water on the interaction of hydrogen and oxygen with Pt.

4.2 Experimental

4.2.1 Materials

EuroPt-1 catalyst (6.3±0.05 wt% Pt), obtained from Johnson-Matthey, was crushed and sieved and the fraction of 30–50 μm was used. Pt/SiO_2 and Pt/CNF supported on Ni-foam catalysts, as well as chemicals and gasses used, are described in detail in Chapters 2 and 3 of this thesis.

4.2.2 Methods

The Pt loading of the catalysts was determined with X-ray fluorescence spectroscopy (Phillips PW 1480 spectrometer). Platinum dispersions of catalysts EuroPt-1, Pt/SiO_2 and Pt/CNF were measured with hydrogen chemisorption (ChemiSorb 2750, Micromeritics). Platinum metal dispersion was calculated assuming $H:Pt_s$ ratio equal to one [18]. Metal particle sizes in fresh Pt/SiO_2 and Pt/CNF catalyst were also estimated with transmission electron microscopy (TEM) by averaging sizes of typically 100 platinum particles, using a Philips CM 30 microscope (300 kV).

Experimental set-up

The experimental set-up was described in the Chapter 3, except for the detector.

Analyzer for gases dissolved in liquid

The analyzer consisted of a probe (Figure 4.1) and the MS detector (Figure 4.2). The probe was made of perforated stainless steel tubing (1/16”, 40 holes with ø0.25 mm, Figure 4.1) and covered with silicon rubber (1.0 × 1.4 mm, Vitton). Then, the probe was inserted into a Swagelock T joint adjusted to minimize dead volume (Figure 4.1). Gases can permeate from the liquid phase through silicon rubber to vacuum.

The permeating gas enters the low-vacuum part of the equipment (Figure 4.2) that typically operates at $5 \cdot 10^{-4}$ mbar. The permeating gas is then allowed to flow into the high vacuum part via a 1 μm orifice (O_1).

Gases were analyzed in the MS chamber with a quadropole mass spectrometer detector (QMG422, Pfeiffer Vacuum, with secondary electron multiplier), operated in “selected ion mode”. The MS chamber is connected to a turbo-molecular pump (TSH 521, Pfeifer Vacuum) capable of creating vacuum in the range of 10^{-8} mbar. Valve V_1 closes automatically in case the pressure in the MS chamber exceeds a value of 10^{-5} mbar, in order to protect the mass spectrometer.

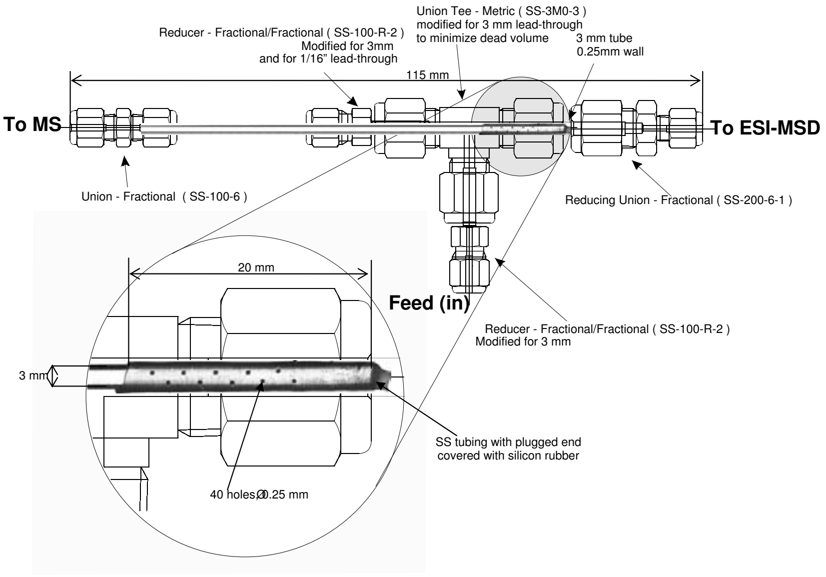

Figure 4.1: *Schematic representation of the probe*

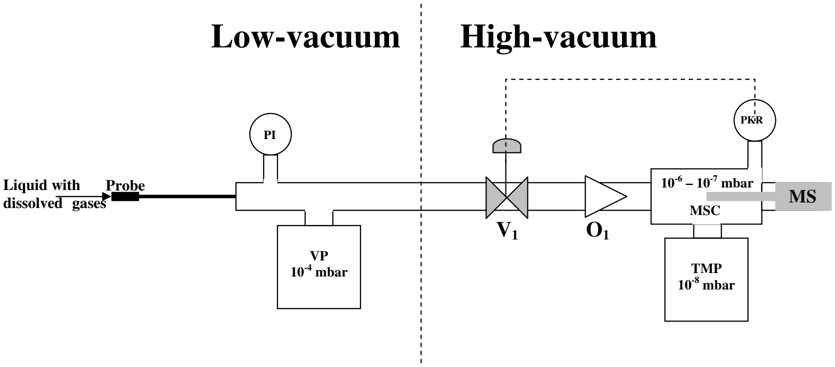

Figure 4.2: *Schematic representation of the set-up based on MIMS principle for determination of gases dissolved in liquids. PI-pressure indicator, VP-vacuum pump, (V_1)-closing valve, (O_1)-orifice, PKR-pressure controller and regulator, MSC-mass spectrometer chamber, MS-mass spectrometer, TMP-turbo-molecular pump*

Response time of detector

The response time of detector was determined by-passing the reactor with pulses of water (10 ml during 20 minutes with flow rate of 0.5 ml·min^{-1}, Figures 4.3–4.5) saturated with various gases (argon, hydrogen or oxygen). The response time was defined as the time required for the signal to reach a level of 95 % of the final (stable) value. A delay of about 0.7 minutes was observed with all gases. The detector responds relatively fast to hydrogen (4 minutes, Figure 4.4) and somewhat slower to argon (8 minutes, Figure 4.3).

Hydrodynamic behavior of reactors with different catalyst

The hydrodynamic behavior of the reactors loaded with the different catalyst supports (HPLC silica as well as CNFs without Pt) was checked with pulses saturated with inert Ar (10 ml during 20 minutes with flow rate 0.5 ml·min^{-1}). Similar experiments with the by-pass and the empty reactor were performed for comparison.

Calibration of gas analyzer in pulse-mode

The calibration of the detector was done with pulses (2.5 ml, during 5 minutes at flow rate 0.5 ml·min^{-1}) of dissolved gases (H_2, O_2, Ar and N_2) in the absence of catalyst (blanks). The amount of the gases present in the pulses was varied by changing the partial pressure of gases in the saturator (partial pressure was adjusted with argon as a second gas) and the resulting concentrations of dissolved gases were calculated using Henry's constants [19]. Calibration curves were obtained using the surface areas of peaks observed.

H_2–O_2 and O_2–H_2 titration experiments in liquid phase

Water in vessels 1 and 2 (see Figure 3.1 in Chapter 3 for details) was saturated with oxygen and hydrogen, respectively (30 minutes, 200 ml·min^{-1}). Water in vessel 3 was flushed with argon (30 minutes, 200 ml·min^{-1}), in order to remove any dissolved oxygen. Then, water saturated with oxygen (from vessel 1) was flown through the reactor during 30 minutes in order to pre-adsorb oxygen on the catalyst. Subsequently, pure water (from vessel 3) was flown through reactor during 30 minutes in order to remove any physisorbed oxygen from the catalyst and dissolved oxygen from the water present in the reactor. All experiments were performed with a flow rate of 0.5 ml·min^{-1}.

Next, the oxygen-covered catalyst was contacted with pulses of hydrogen solution from vessel 2 (concentration $7.8 \cdot 10^{-4}$ mol/l, 2.5 ml during 5 minutes); pulses were repeated every 20 minutes, flowing water saturated with Ar between pulses.

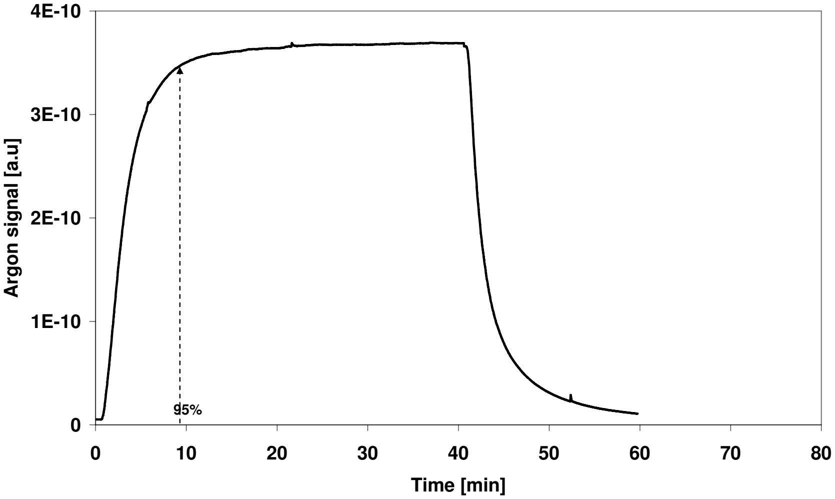

Figure 4.3: *Response of the analyzer to a pulse of argon (*20 ml *during 40 minutes,* F = 0.5 ml·min^{-1}, $c_M(\mathrm{Ar}) = 1.4 \cdot 10^{-3}$ mol·dm^{-3}, $T = 22$ °C*)*

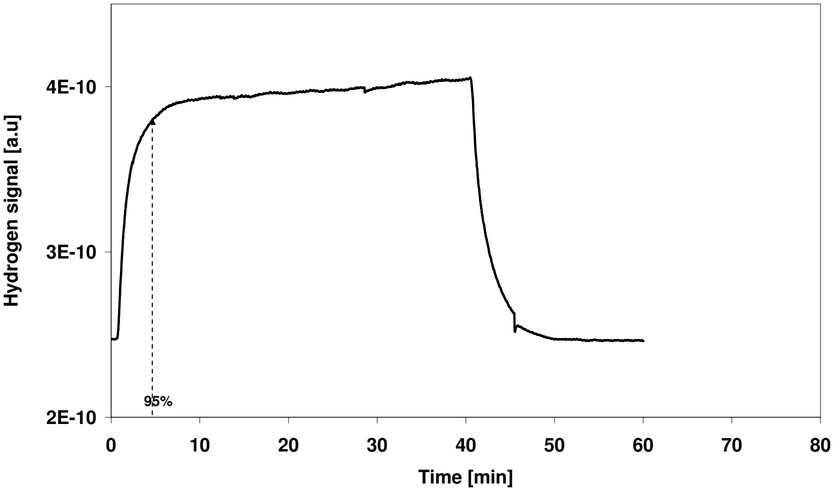

Figure 4.4: *Response of the analyzer to a pulse of hydrogen (*20 ml *during 40 minutes,* F = 0.5 ml·min^{-1}, $c_M(\mathrm{H_2}) = 0.8 \cdot 10^{-3}$ mol·dm^{-3}, $T = 22$ °C*)*

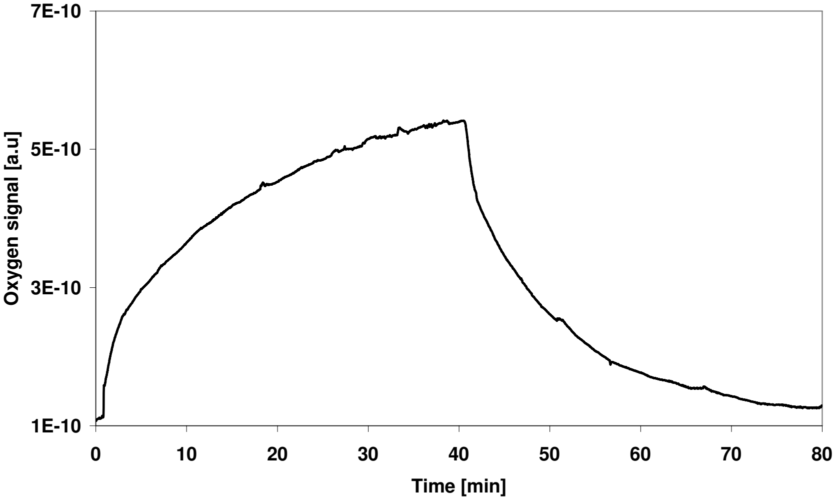

Figure 4.5: *Response of the analyzer to the pulse of oxygen (*20 ml *during 40 minutes, F =* 0.5 ml·min^{-1}, $c_M(O_2)$ = 1.3 · 10^{-3} mol·dm^{-3}, T = 22 °C*)*

Also after the final pulse with hydrogen in water, Ar saturated water (from vessel 3) was flown through the reactor for 30 minutes, before pre-adsorbed hydrogen was titrated with pulses of oxygen solution (concentration 1.3 · 10^{-3} mol/l, 2.5 ml during 5 minutes); again, pulses were repeated every 20 minutes. These sequences were subsequently repeated 3 times.

4.3 Results and discussion

First, the results of catalyst characterization will be presented and the hydrodynamic behavior of the reactors will be shortly discussed. Most importantly, results of H_2–O_2 titration experiments as well as the interaction between dissolved hydrogen and oxygen with the catalyst will be discussed.

4.3.1 Catalyst preparation and characterization

The platinum loading of the three catalysts was determined with XRF (Table 4.1). The platinum loading of the EuroPt-1 (6.3±0.05 wt%) agrees well with literature data [11, 12]. The platinum loadings of fresh Pt/SiO_2 and Pt/CNF (3 wt%) were reported before (see Table 3.2 in Chapter 3).

Table 4.1 also gives platinum dispersions measured with gas phase hydrogen chemisorption, resulting in 65 % for EuroPt-1 and 61 % for Pt/SiO_2. The Pt dispersion of Pt/CNF was 25 % , as reported in detail in Chapter 3 (see Table 3.2 in Chapter 3).

4.3.2 Response time of the detector

The delay time observed in Figures 4.3, 4.4 and 4.5 was 0.7 min, independent of the gas dissolved, well in agreement with the residence time in the dead volume of the bypass (0.35 ml). The response time (the moment at which 95 % of final signal was reached) differed significantly for three gases (Figures 4.3, 4.4 and 4.5) and increased in the order $H_2 < Ar < O_2$. Probably, this is at least partly caused by differences in the diffusivity of the gases in the membrane; D_{eff} for hydrogen, argon and oxygen are $1.0 \cdot 10^{-9}$ m^2/s, $2.0 \cdot 10^{-9}$ m^2/s and $3.0 \cdot 10^{-9}$ m^2/s, respectively [20, 21].

One important cause of the long response time could be the thickness of our membrane (200 μm). Much faster response (typically 0.3 min) was reported by Kostiainen et al. [7] for organic compounds (VOC's) dissolved in water, applying a similar configuration using a much thinner membrane (25 μm). Unfortunately, thinner membranes cannot be used in our set-up because of mechanical instability, inducing leakage of water into the vacuum system.

Anyhow, the relative slow response of the detector implies that real time concentrations cannot be monitored reliably in transient experiments. We will show later that calibration of integral pulses is possible and reliable though.

4.3.3 Reactor behavior and spreading of the response to the pulse

The responses to an argon pulse with different configurations are represented in Figure 4.6. The most obvious difference is the change in delay time, which can be fully accounted for based on the differences in the dead volumes of the bypass, empty reactor, silica fixed-bed reactor and CNF/Ni foam reactor, respectively. Furthermore, the differences in the shapes of the break-through curves are modest, indicating that hydrodynamics are quite similar for all cases, despite significant differences in pressure drop, varying between 2 bars and 40 bars for the CNF support and the fixed bed of HPLC silica, respectively.

The response to a glucose pulse of CNF/Ni foam reactor presented in Chapter 3 showed even more distortion of the pulse-shape, which was explained with significant reversible adsorption of glucose on the CNF support. The experimental result with Ar supports this interpretation by demonstrating less peak distortion using a species that certainly does not adsorb (Ar).

Table 4.1: *Catalyst loadings and dispersions determined in gas phase and in liquid phase*

Catalyst	Loading (wt%)	D_{Gas} (H/Pt) Gas phase chemisorption	Amount of Pt in reactor		H/Pt - TEM[1]	$(H_2)_{\text{Liquid}}$ (μmoles)	$(O_2)_{\text{Liquid}}$ (μmoles)	D_{Liquid} (H/Pt)[3]
			Bulk (μmoles/g)	Surface (μmoles)				
EuroPt-1	6.3±0.05	0.65	323	10.5	-	16	8.5	0.66
Pt/CNF	3.0[2]	0.25	154	11.2	0.29	17	9.2	0.25
Pt/SiO_2	1.0±0.05	0.61	51	8.8	0.54	12	7	0.56

[1] Calculated based on: $D(TEM) = \frac{1.08}{d(nm)}$ [18]

[2] The Pt loading assumed based on preparation procedure

[3] Dispersion in liquid phase (D_L) $D_{liquid} = \frac{2(H_2)L}{3(BulkPt)W_{(cat)}}$

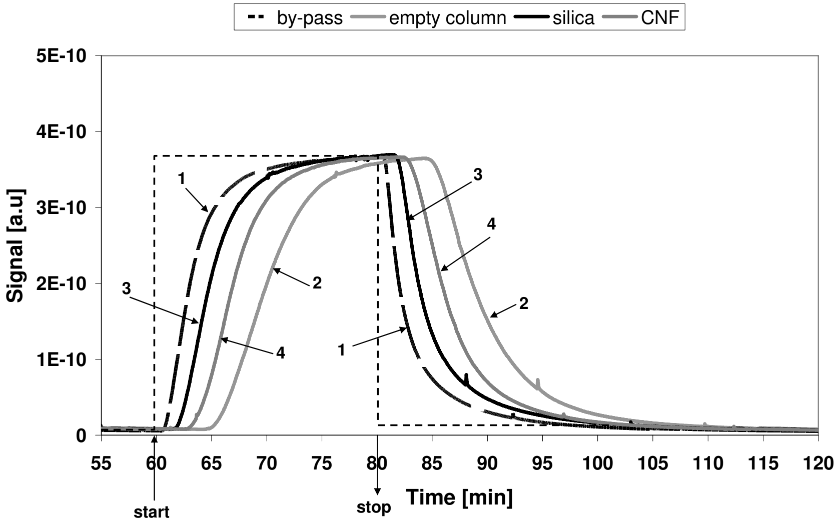

Figure 4.6: *Response of 1) by-pass, 2) empty column, 3) column with silica and 4) column with CNF to a pulse of argon (*10 ml *during 20 minutes with flow rate* 0.5 ml·min^{-1}, c_M(Ar) = $1.4 \cdot 10^{-3}$ mol·dm^{-3}, $T = 22$ °C*)*

4.3.4 Calibration of the analyzer in pulse-mode

The calibration curves presented in Figures 4.7 and 4.8 show a linear relationship between the amount of hydrogen and oxygen present in a single pulse with the surface area of the peak obtained in a blank experiment.

The amount of dissolved gas present was varied via the concentration. This result is not trivial when taking in consideration that the response of the analyzer is relatively slow, especially for oxygen, as discussed before. Apparently, the delays in the rising part and the declining part of the peak compensate each other. Comparable results were obtained for Ar and N_2 (not shown), demonstrating that the method can be generally applied for dissolved gasses. Also, the presence of a second dissolved component does not significantly influence the calibration (< 2 %).

The smallest amount of hydrogen and oxygen that can be quantitatively determined is in the order of 0.1 μmoles and 0.3 μmoles respectively. Calibrations were done before and after titration experiments, resulting in reproducible data within 10 % experimental error.

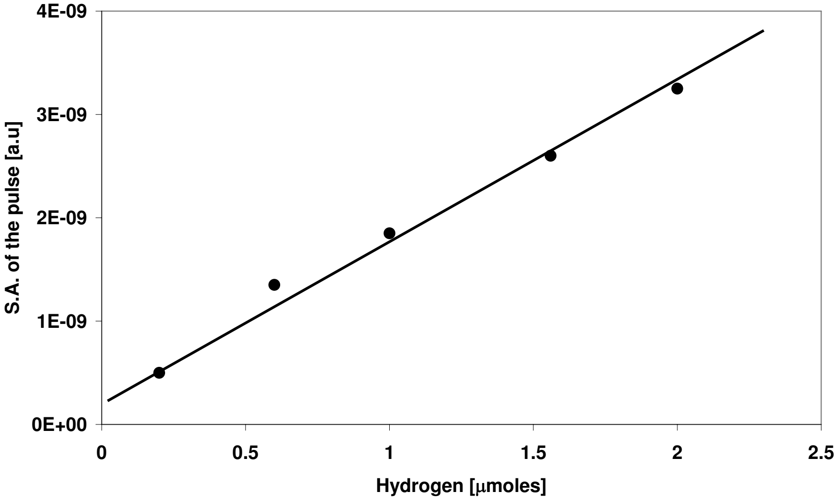

Figure 4.7: *Hydrogen (m/z 2) calibration curve based on a surface area of the pulse (*5 minutes *pulse,* $F = 0.5\,\mathrm{ml{\cdot}min^{-1}}$, $c_M(\mathrm{H_2}) = 0.08 - 0.8 \cdot 10^{-3}\,\mathrm{mol{\cdot}dm^{-3}}$, $T = 22\,°\mathrm{C}$, $R^2 = 0.99$)

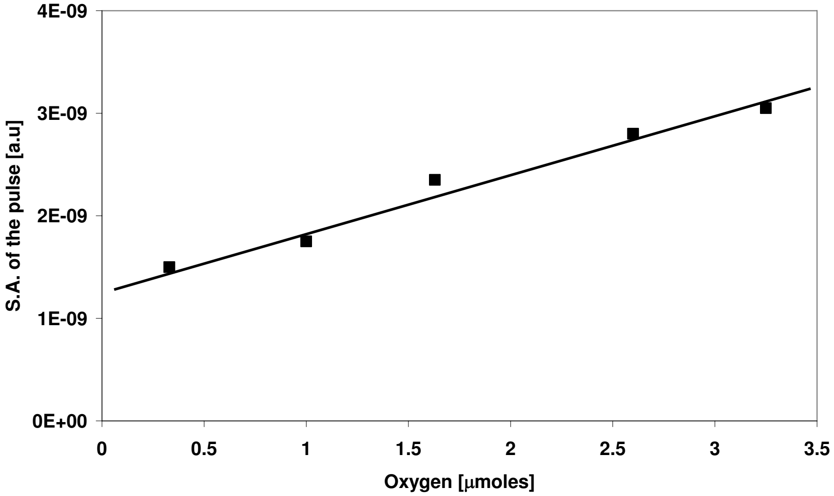

Figure 4.8: *Oxygen (m/z 32) calibration curve based on a surface area of the pulse (*5 minutes *pulse,* $F = 0.5\,\mathrm{ml{\cdot}min^{-1}}$, $c_M(\mathrm{O_2}) = 0.13 - 1.3 \cdot 10^{-3}\,\mathrm{mol{\cdot}dm^{-3}}$, $T = 22\,°\mathrm{C}$, $R^2 = 0.98$)

4.3.5 O_2 and H_2 titration in aqueous solution

Figure 4.9 shows the result of pulsing hydrogen on pre-oxidized EuroPt-1 as well as on silica only (blank). Consumption of hydrogen on silica was not observed. However, complete consumption of hydrogen is observed during the first seven pulses on the oxidized EuroPt-1. A gradual breakthrough occurs during the next four pulses. Finally, the surface areas of the peaks become identical to the blank experiment, despite the difference in peak shape, which will be discussed later, indicating that hydrogen is not consumed anymore. The total amount of hydrogen consumed was 16 μmoles, applying the calibration curve in Figure 4.7.

Two subsequent oxygen pulses Figure 4.10 are completely consumed, followed by a gradual breakthrough during the 3rd and 4th pulse. Next, the response stabilized and became equal to the response in the blank experiment. The total amount of oxygen consumed is 8.5 μmoles, using the calibration curve in Figure 4.8. The same experiments were performed with Pt/CNF and Pt/SiO_2 (not shown) and the total amounts of hydrogen and oxygen consumed with Pt/CNF and Pt/SiO_2 catalyst were 17 μmoles H_2/9.2 μmoles O_2 and 12 μmoles H_2/7 μmoles O_2 respectively (Table 4.1).

The amount of hydrogen consumed in the titration experiment using EuroPt-1 (16 μmoles) is almost 3 times the amount of pre-adsorbed oxygen (5.3 μmoles), in agreement with the following assumptions:

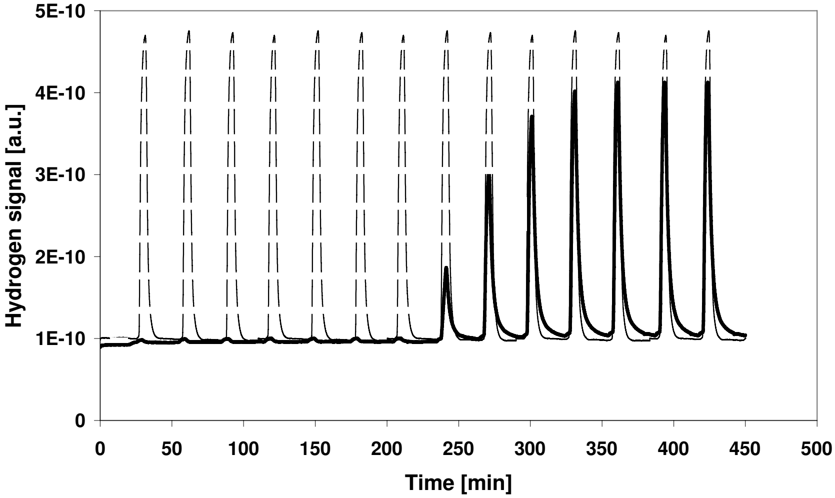

Figure 4.9: *Titration of pre-adsorbed oxygen on EuroPt-1 using water saturated with hydrogen (*2.5 ml *pulse,* $F = 0.5$ ml·min^{-1}*,* $c_M(H_2) = 0.8 \cdot 10^{-3}$ mol·dm^{-3}*,* $T = 22$ °C*), [—] H_2-O_2 titration; [- - -] Blank experiment*

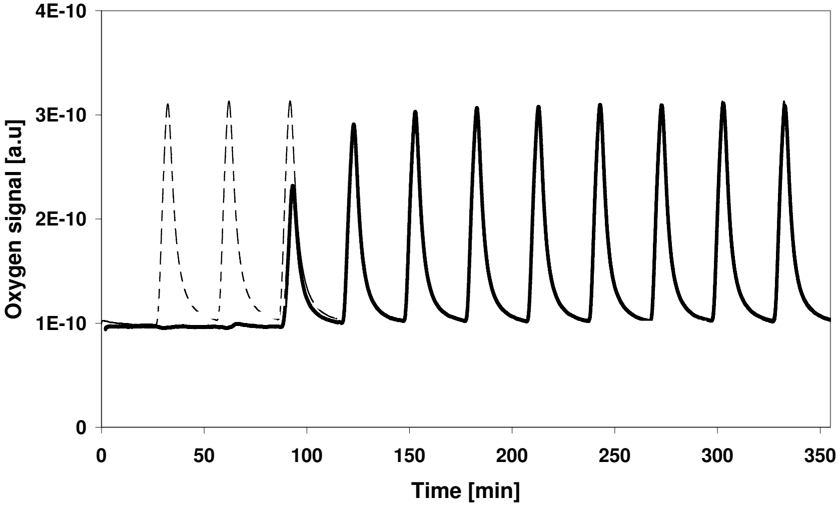

Figure 4.10: *Titration of pre-adsorbed hydrogen on EuroPt-1 catalyst using water saturated with oxygen* (2.5 ml *pulse,* $F = 0.5\,\text{ml}\cdot\text{min}^{-1}$, $c_M(\text{O}_2) = 1.3\cdot 10^{-3}\,\text{mol}\cdot\text{dm}^{-3}$, $T = 22\,°\text{C}$). *The experiment was done immediately after the titration with hydrogen; [——] O_2-H_2 titration; [- - -] Blank experiment*

1. two hydrogen atoms react with one pre-adsorbed oxygen atom (O_a) to form water and one hydrogen atom would subsequently adsorb on platinum (Eq. 4.1),

$$\text{H}_2 + 2\,\text{Pt}_\text{s}{-}\text{O}_\text{a} \longrightarrow 2\,\text{H}_2\text{O} + 2\,\text{Pt}_\text{s}{-}\text{H}_\text{a} \tag{4.1}$$

2. adsorption stoichiometry of O on Pt is one
3. adsorption stoichiometry of H on Pt is one

In the following experimental sequence, the amount of oxygen consumed in the titration experiment (8.5 μmoles) agrees well with the amount of oxygen that would be consumed (8.0 μmoles) if one oxygen atom would react with two pre-adsorbed hydrogen atoms (H_a) to form water and one oxygen atom would subsequently adsorb on platinum like (Eq. 4.2).

$$1.5\text{O}_2 + 2\,\text{Pt}_\text{s}{-}\text{H}_\text{a} \longrightarrow \text{H}_2\text{O} + 2\,\text{Pt}_\text{s}{-}\text{O}_\text{a} \tag{4.2}$$

Thus, hydrogen-oxygen titration results in liquid phase for the EuroPt-1 catalyst agree well with the gas phase titration stochiometry reported by Benson and Boudart [15] in Eq. 4.1. Ratios between the amounts of oxygen and hydrogen consumed in titration experiments for all three catalysts are, within experimental error, close to 2, as would be expected from equations 4.1 and 4.2. More importantly, the platinum dispersions obtained in liquid phase are in excellent agreement with dispersions based on hydrogen chemisorption in gas phase, for all three catalysts as shown in Table 4.1.

The minimal amount of hydrogen detectable in a single pulse is 0.1 μmoles H_2. This amount is equivalent to approximately 0.7 % of a pre-adsorbed oxygen monolayer on EuroPt-1 catalyst, which is equivalent to about 0.5 m^2 Pt surface. The sensitivity thus obtained is similar to the method of Kiraly et al. [16], titrating with CS_2. An obvious advantage of the H_2–O_2 titration method is that it is in principal not destructive because no irreversible adsorption is taking place, in contrast to the CS_2 method. The advantage of our method as compared to the H_2–O_2 titration results of Bradley and Busser [17] is robustness by avoiding volumetric methods, needing extremely accurate temperature control. Anyhow, our data support the result of Bradley and Busser [17] and disagree with the observations of Kiraly et al. [16], in the sense that no significant influence of solvent (i.e. water) on chemisorption of hydrogen and oxygen on precious metals was found, and consequently no effect exists on the dispersion. Therefore, we conclude that the difference in dispersion of Pd-Al_2O_3 measured in gas-phase versus measured in methanol, as reported by Kiraly et al. [16], is due to the uncertainty in the adsorption stoicheometry of CS_2 and is not caused by a real difference in the number of accessible sites. The underlying assumption is that methanol, used by Kiraly et al. [16], and water, used in our study, would induce comparable effect seems reasonable.

The striking difference between Figure 4.11 and 4.12 clearly indicates that a weak but significant interaction is taking place between dissolved H_2 and a hydrogen covered platinum surface. A reversible interaction can well explain the broadening of the peaks as observed in Figure 4.11. This must take place on the Pt surface because no such effect is observed with silica only. In contrast, Figure 4.12 shows no significant influence of the platinum on the peak shape of oxygen. Similar results were obtained with Pt/SiO_2 and Pt/CNF.

This result shows that the technique developed here can provide unique information on the influence of solvent (water in this case) on reversible interactions of dissolved species with catalyst surfaces. It is well known that charge separation on an oxidized Pt surface is much larger then on a H-covered Pt surface, because of the significant larger difference in electron affinity between O and Pt versus H and Pt. As a result, more charge separation on the oxidized surface renders a more hydrophilic platinum surface and a-polar O_2 molecules are not likely to interact. The charge separation on the H-covered surface is much less, the surface will be less hydrophilic and H_2 molecules could well interact, as observed in Figure 4.11. In fact, H_2 molecules will prefer the relatively a-polar H-covered Pt surface over solvatation with highly polar water molecules. This interpretation is schematically presented in Figure 4.13. An alternative explanation would be that H_2 dissociative chemisorption is reversible under the conditions applied in this study, whereas O_2 chemisorption is apparently irreversible. Anyhow, unique information on reversible versus irreversible adsorption is obtained.

We also observed ageing phenomena during subsequent experiments. When repeating H_2–O_2 titrations with Pt/SiO_2 catalyst three times, a decrease of the hydrogen and oxygen uptake in subsequent titrations was observed. In addition, XRF analysis of the Pt/SiO_2 catalyst after the titration experiments showed a decrease of the Pt loading (from 1.0 to 0.87 wt%); apparently some platinum is lost during the experiments. Hydrogen chemisorption of the Pt/SiO_2 catalyst after the titration experiments showed a decrease of the Pt dispersion (from 0.61 to 0.53).

It can be speculated that these effects are due to dissolution of the smallest metal particles during the titration sequence, as this would account for both the loss of Pt as well as the decrease in dispersion. However, we cannot rule out H_2 induced ageing, as reported by Douidah et al. [22] for silica-supported platinum particles in aqueous media under hydrogen atmosphere. The relevant point here, however, is the fact that this result demonstrates the ability of the methods described, to observe changes in the characteristics of catalyst in liquid phase without the necessity to remove the aqueous phase. Another advantage is non-destructive testing, i.e. catalyst does not need to be removed from the reactor, which is especially an advantage in case of (micro-) struc-

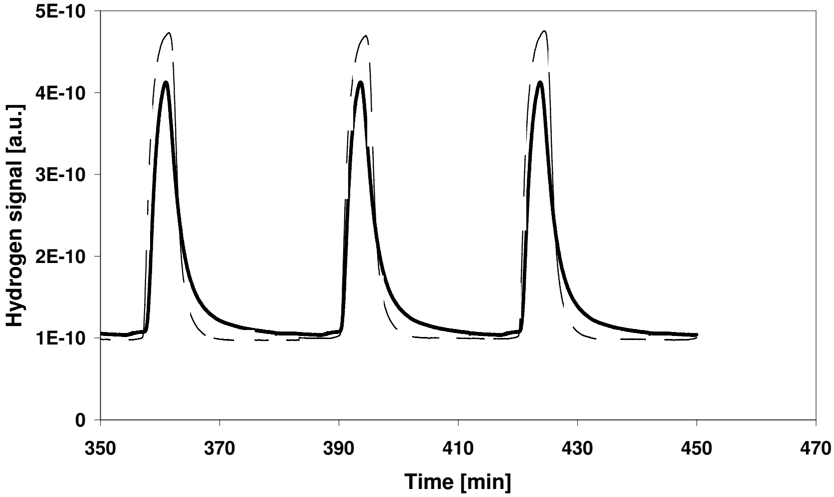

Figure 4.11: *Details of the last three pulses using water saturated with hydrogen on EuroPt-1 catalyst after the titration of pre-adsobed oxygen has been completed (*2.5 ml *pulse,* F = 0.5 ml·min^{-1}, $c_M(H_2)$ = 0.8 · 10^{-3} mol·dm^{-3}, T = 22 °C*), [——] H_2-O_2 titration; [- - -] Blank experiment*

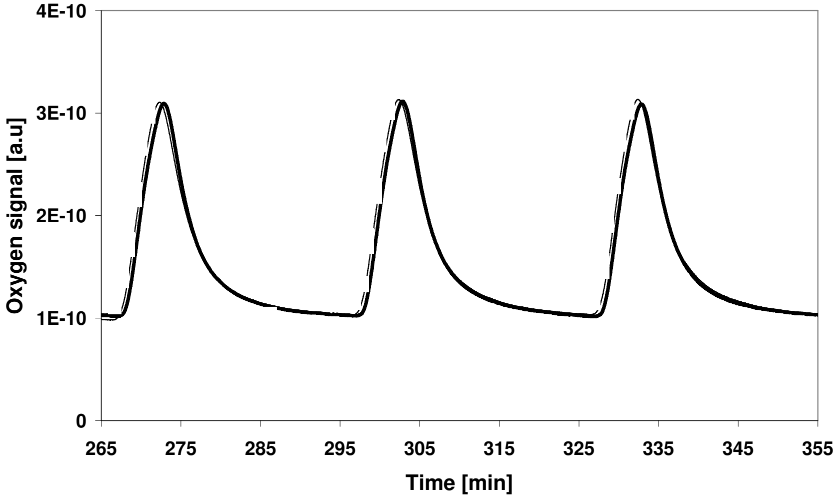

Figure 4.12: *Details of the last three pulses using water saturated with oxygen on EuroPt-1 catalyst, titration of pre-adsobed hydrogen has been completed (*2.5 ml *pulse,* F = 0.5 ml·min^{-1}, $c_M(O_2)$ = 1.3 · 10^{-3} mol·dm^{-3}, T = 22 °C*). The experiment was done immediately after the titration with hydrogen; [——] O_2-H_2 titration; [- - -] Blank experiment*

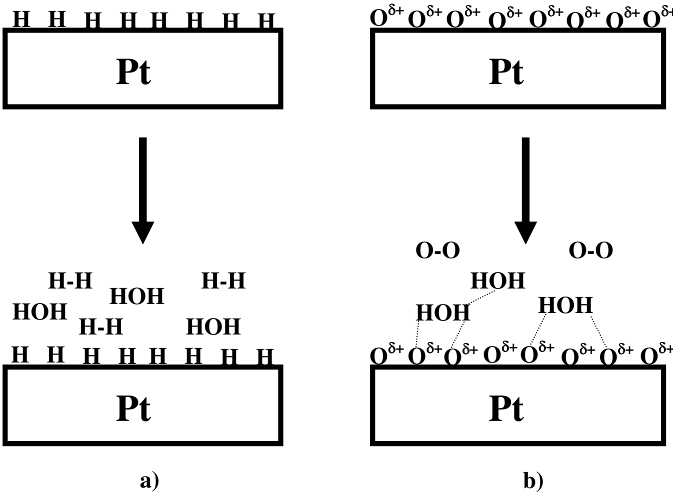

Figure 4.13: *Influence of solvent (water) on reversible interactions of dissolved a) hydrogen and b) oxygen with Pt catalyst surface*

tured reactors and micro-reactors because catalysts are not easily removable. Also, the sensitivity of detection is useful for characterization of micro-fluidic catalytic devices and future work will be in this direction.

Finally, it is demonstrated that quantitative evaluation of pulse experiments in the range of minutes is possible. Thus, transient experiments consuming or producing dissolved gasses can be monitored quantitatively as long as the typical width of the signals is comparable. However, the ESI-MS detector is responding within a few seconds; when using both detectors, experimental design needs to consider the response times of both detectors. Thus, application of the detector discussed here will limit the window of operation of the complete set-up. On the other hand, it is obvious that the most relevant gasses for liquid phase catalysis, i.e. hydrogen and oxygen for hydrogenation reactions and oxidation reaction respectively, can be detected, as well as N_2 which would be important for studying hydrogenation of nitrite and nitrate.

4.4 Conclusions

We have, for the first time, successfully applied an analyzer for gasses dissolved in water, based on membrane inlet mass spectrometry (MIMS), for on-line detection in the exit of a catalytic reactor in a transient experiment. The technique was applied for determination of the dispersion of platinum supported catalyst in the liquid phase via H_2–O_2 titration. The titration stoichiometries obtained in liquid phase for the 3 different catalysts (EuroPt-1, Pt/SiO_2 and Pt/CNF) agree well with the gas phase titration stoichiometry reported in literature. The platinum dispersions obtained in liquid phase are in excellent agreement with dispersions based on hydrogen chemisorption in gas phase for all three catalysts and we conclude that water has no influence on the actual dispersion of Pt and on the stoichiometry of adsorption. Despite the relatively slow dynamic response of the detector, it was proven possible to perform quantitative experiments in pulse mode. The capability of this method is further demonstrated by the surprising observation that dissolved hydrogen physisorbs significantly on a reduced Pt catalyst whereas dissolved oxygen does not interact with an oxidized catalyst.

Acknowledgements

The authors thank, Ing. L. Vrielink for XRF and BET analysis, Ing. M. Smithers for TEM measurements, Ing. A. Hovestad for assistance with reactors preparation, Ing. A. Wonders (University of Eindhoven), Ing. J. Spies and Ing. B. Geerdink for technical assistance, Dr. J. Kromkamp and J. Peene (NIOO-KNAW) for discussions on MIMS.

Financial support for the project (TPC 5694) by STW (The Netherlands) is kindly acknowledged. This work was performed under the auspices of NIOK.

References

[1] D. Radivojević, M. Ruitenbeek, K. Seshan and L. Lefferts. Development of a transient response technique for heterogeneous catalysis in liquid phase, Part 1: applying membrane inlet mass spectrometry (MIMS) for detection of dissolved gasses (2008). Accepted for publication in *Journal of Catalysis*.

[2] `http://www.orbisphere.com`

[3] M. Meyberg and F. Roessler. In Situ Measurement of Steady-State Hydrogen Concentrations during a Hydrogenation Reaction in a Gas-Inducing Stirred Slurry Reactor. *Industrial & Engineering Chemical Research*, 44, 9705–9711 (2005).

[4] O. Wolter, J. Heitbaum and B. Bunsenges. Differential electrochemical mass spectrometry (DEMS). *Physical Chemistry*, 88, 2–6 (1984).

[5] G. E. Dima, A. C. A. de Vooys and M. T. M. Koper. Electrocatalytic reduction of nitrate at low concentration on coinage and transition-metal electrodes in acid solutions. *Journal of Electroanalytical Chemistry*, 554, 15–23 (2003).

[6] T. M. Kana, C. Darkangelo, M. D. Hunt, J. B. Oldham, G. E. Bennett and J. C. Cornwell. Membrane Inlet Mass Spectrometer for Rapid High-Precision Determination of N_2, O_2, and Ar in Environmental Water Samples. *Analytical Chemistry*, 66, 4166–4170 (1994).

[7] R. Kostiainen, T. Kotiaho, I. Mattila, T. Mansikka, M. Ojala and R. A. Ketola. Analysis of Volatile Organic Compounds in Water and Soil Samples by Purge-and-Membrane Mass Spectrometry. *Analytical Chemistry*, 70, 3028–3032 (1998).

[8] U. K. Singh and M. A. Vannice. Kinetics of liquid-phase hydrogenation reactions over supported metal catalysts — a review. *Applied Catalysis A*, 213, 1–24 (2001).

[9] T. Mallat and A. Baiker. Heterogeneously catalyzed selective oxidations in the liquid phase. Oxidation of alcohols with molecular oxygen on platinum metal catalysts in aqueous solutions. *Catalysis Today*, 19, 247–283 (1994).

[10] J. M. H. Dirkx and H. S. van der Baan. The oxidation of glucose with platinum on carbon as catalyst. *Journal of Catalysis*, 67, 1–13 (1981).

[11] G. C. Bond and P. B. Wells. Characterization of the Standard Platinum/Silica Catalyst Europt-1; 1. Philosophy and Achievement. *Applied Catalysis*, 18(2), 221–224 (1985).

[12] G. C. Bond and P. B. Wells. Characterization of the Standard Platinum/Silica Catalyst Europt-1; 2. Preparation, Physical Properties, and Chemical Composition. *Applied Catalysis*, 18(2), 225–230 (1985).

[13] C. R. Adams, H. A. Benesi, R. M. Curtis and R. G. Meisenheimer. Particle size determination of supported catalytic metals: Platinum on silica gel. *Journal of Catalysis*, 1, 336–344 (1962).

[14] T. E. Whyte Jr. Metal Particle Size Determination of Supported Metal Catalysts. *Catalysis Reviews*, 8, 117–134 (1974).

[15] J. E. Benson and M. Boudart. Hydrogen-oxygen titration method for the measurement of supported platinum surface areas. *Journal of Catalysis*, 4, 704–710 (1965).

[16] Z. Kiraly, A. Mastalir, A. Csaszar, H. Demir, D. Uner and G. H. Findenegg. Liquid chromatography as a novel method for determination of the dispersion of supported Pd particles. *Journal of Catalysis*, 245, 267–271 (2007).

[17] J. S. Bradley and W. Busser. Chemisorption measurements on polymer-stabilized colloidal platinum and rhodium nanoclusters in liquid dispersion. *Catalysis Letters*, 63(3–4), 127–130 (1999).

[18] C. H. Bartholomew and R. J. Farrauto. *Fundamentals of industrial catalytic processes*. John Wiley & Sons, Inc., Publication (2006).

[19] D. R. Lide, editor. *CRC Handbook of Chemistry and Physics*. CRC-Press, 79th edition (1998).

[20] M. B. Hägg. Membrane purification of Cl_2 gas I. Permeabilities as a function of temperature for Cl_2, O_2, N_2, H_2 in two types of PDMS membranes. *Journal of Membrane Science*, 170(2), 173–190 (2000).

[21] L. Brandão, L. M. Madeira and A. M. Mendes. Mass transport on composite dense PDMS membranes with palladium nanoclusters. *Journal of Membrane Science*, 288(1–2), 112–122 (2007).

[22] A. Douidah, P. Marécot and J. Barbier. Toward a better understanding of the stability of supported platinum catalysts in aqueous phase under hydrogen atmosphere at room temperature. *Applied Catalysis A*, 225(1–2), 11–19 (2002).

5

Frozen slurry catalytic reactor; a new structured catalyst for transient studies in liquid-phase

In Chapter 5 we present a method to prepare catalytic polymer membranes by incorporating mono-dispersed Pt/SiO$_2$ catalyst particles in an EVAL polymer porous matrix via immersion phase separation. Addition of a relatively high concentration (65 wt %) of catalyst particles is preventing the formation of macro voids, improving both mechanical stability of the membranes as well as improving homogeneity of the liquid flow distribution through the membrane. The catalyst particles remain intact during the preparation procedure. The catalyst particles are physically immobilized throughout the membrane, entrapped in the pores, preventing channeling that would occur when flowing through an equivalent shallow fixed bed. Furthermore, the novel frozen-slurry-like morphology results in significant lower pressure drop as compared to a fixed bed with identical diameter and containing the same amount of catalyst particles. The platinum particles are proven to be highly accessible in the swollen state, i.e. in liquid phase, as demonstrated both by the catalytic activity of the Pt/SiO$_2$ loaded membranes for glucose oxidation as well as by the observation that H$_2$–O$_2$ titrations confirms that close to all platinum surface atoms contribute.

Parts of this chapter are submitted to *Applied Catalysis A*

5.1 Introduction

Mass transfer limitation in heterogeneous catalyst is in many cases detrimental for selectivity in industrial catalytic multiphase processes [1]. As a consequence of the limited solubility of reacting gases, like O_2, H_2, and CO in many solvents, as well as relatively low diffusion coefficients in liquid phase, concentration gradients of reactants and products in a catalyst particle may easily occur. Use of highly porous support materials as well as small catalyst particles (resulting in short diffusion path) can minimize concentration gradients in catalyst particles. However, small catalyst particles are usually used in slurry reactors demanding filtration, which is expensive and sensitive for process disturbances. Unfortunately, application of small particles in a fixed bed causes unacceptable high pressure drop. Decreasing pressure drop by using shallow beds (pancake shape) is not a solution because of misdistribution (channeling) of the liquid flow. That is the driver for current developments of new, more accessible catalytic structures that have lower pressure drops and better mass transfer properties e.g. thin layers of catalyst on monoliths and foam materials [2]. Additional advantages can be obtained by using highly porous thin layers on monoliths and foams, e.g. based on carbon-nano-fibers. Particles and layers consisting of carbon nanofibers are promising catalyst supports because of the combination large pore volume (0.5–2 cm^3/g) and extremely open morphology, on one hand, and significant high surface area (100–200 m^2/g), on the other hand [3].

High Performance Liquid Chromatography (HPLC) is a mature experimental technique used for separation of compounds from liquid phase over variety of materials, i.e. resins and silica [4]. However, preparation of shallow fixed beds with conventional particles is a challenge for chromatographic columns also, due to inability to pack particles homogeneously [5].

Klein [6] recently described a new method to prepare membrane-like structures of any geometry and large variety of functionalities for HPLC applications. With this concept (Figure 5.1) one can establish various functions such as ion exchange, adsorption, catalysis and hybrids (such as reactive chromatography) by choosing the particles and the binder.

It was concluded that the polymer binder should have high porosity, high degree of pore interconnectivity as well as a low adsorption tendency towards the desired products. Avramescu [7] further demonstrated this method by developing adsorber membranes made of a random copolymer of ethylene and vinyl alcohol (EVAL) with incorporated ion exchange resin. Adsorber membranes were prepared in different shapes; they were used in stack of flat membranes or as a bundle of solid or hollow fiber membranes. Membranes were used to study adsorption of proteins and results were similar to results with usual adsorbent particles, implying that blocking of the adsorbing sites with polymer does not occur. Mild thermal and mechanical treatments during the

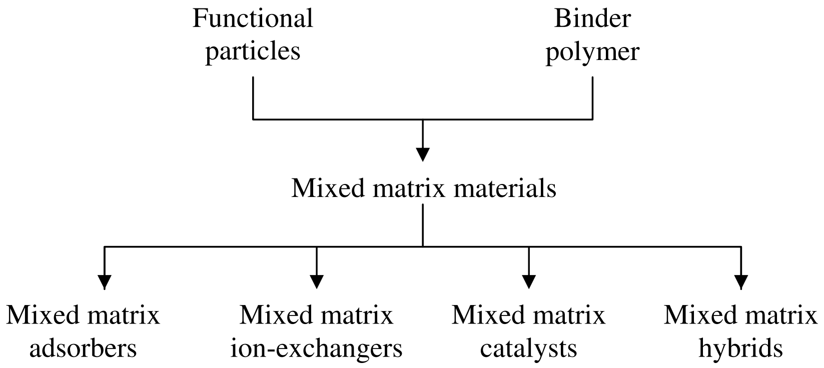

Figure 5.1: *Schematic representation of the functionalized polymeric matrix concept*

membrane preparation did not influence the integrity of the particulate material in membranes. A similar approach with catalyst particles will be explored here to obtain membrane-based structured catalysts.

In Chapter 3, we reported on development of a transient technique for liquid phase catalytic reactions [8]. Important part of the set-up is the catalytic reactor, prepared by filling an HPLC cartridge either with mono-dispersed Pt/SiO_2 or with the Pt/CNF catalyst on Ni foam modules. High pressure drop in a fixed bed (in the range of 40 bars) caused occasional leakages during the flow of liquid. Furthermore, attempts to make a shallow fixed bed (< 1 cm) were unsuccessful due to channeling.

The aim of the present work is to develop a novel membrane-based catalytic structure suitable for transient experiments in liquid phase, allowing more flexible operation i.e. lower pressure drop as compared to fixed bed reactors. This will be achieved by incorporating the Pt/SiO_2 catalyst particles in a polymeric porous matrix.

Two catalytic systems in aqueous phase have been selected to explore the properties of the novel catalytic structure:

1. H_2–O_2 titration in liquid phase and
2. catalytic oxidation of glucose.

H_2–O_2 titration is a relevant method for determination of the amount of surface platinum available for the reaction, routinely performed in gas phase [9], but recently it was also demonstrated in liquid phase (Chapter 4) [10, 11]. Hydrogen chemisorption requires high temperature treatment in inert (i.e. 300 °C [12]) to desorb hydrogen from the platinum surface after the reduction step. This is not possible with the Pt/SiO_2 particles embedded in polymer membranes because the polymers (i.e. EVAL or PES) are not stable at this temperature [13]. Furthermore, membranes are swelling in liquid phase [14], and therefore it is particular important to perform H_2–O_2 titration in liquid phase, mimicking the reaction conditions. Oxidative conversion of glucose is important in view of the anticipated shift towards renewable feedstocks for the chemical industry. Glucose can be upgraded to more valuable compounds e.g. gluconic acid, a building block for production of chelating agents [15–17].

5.2 Experimental

5.2.1 Materials

HPLC silica (Microsorb, BET surface area 198 m^2/g; mean particle size 5 μm obtained from Varian) was used as support for Pt/SiO_2. Catalysts were prepared using tetra ammonium-platinum hydroxide $(NH_3)_4Pt(OH)_2$ (99.9 %, Aldrich) as platinum precursor. Membranes were prepared from EVAL, a random copolymer of ethylene and vinyl alcohol (average ethylene content of 44 mol%, Aldrich) that was used without further modification. Dimethylsulfoxide (DMSO, Merck) was employed as solvent and 1-octanol (Fluka) as nonsolvent-additive in the casting solution. De-mineralized water was used as non-solvent in the coagulation bath. LC-MS water (Biosolve) was used to prepare solutions for catalyst preparation, glucose solution ($C_6H_{12}O_6$ 99 %, Aldrich) and gluconic acid solution ($C_6H_{12}O_7$ 50 %, Aldrich). Argon (Air Products BIP, 99.9999 %) was further purified by using an oxygen trap (OxyTrap, Alltech), to decrease the oxygen content to 10 ppb or lower. Hydrogen (99.999 %) and oxygen (99.999 %,) were purchased from Indugas.

5.2.2 Catalyst preparation and characterization

Pt/SiO_2 catalyst was prepared with wet impregnation as reported in detail in Chapter 2 [18]. The Pt loading of the Pt/SiO_2 catalysts was determined with X-ray fluorescence spectroscopy (Philips PW 1480 spectrometer) and platinum dispersion was measured with hydrogen chemisorption (ChemiSorb 2750, Micromeritics). Platinum metal dispersion was calculated assuming a H:Pt_s ratio of one [19]. Metal particle size in fresh Pt/SiO_2 catalyst was estimated with transmission electron microscopy (TEM) by averaging sizes of typically 100 platinum particles, using a Philips CM 30 microscope (300 kV).

5.2.3 Membrane preparation and characterization

All membranes were prepared by immersion precipitation [7]. Different amounts of catalytic particles were added to a solution containing 10 wt % EVAL in DMSO in order to obtain membranes with different catalyst loading; 1-octanol was added to the casting solution in order to improve the membrane morphology [20]. The mixture was stirred over night to break the clusters of particles. For the preparation of flat sheet catalytic membranes the polymeric solution was cast on a glass plate and immediately immersed into a water coagulation bath at 40 °C. All prepared membranes were washed to remove the additive and solvent and afterwards dried directly in air at 22 °C.

Morphology of membranes was studied with Scanning Electron Microscopy (SEM); cross sections were prepared using pieces of membranes first frozen in liquid nitrogen and then fractured. The fractured membranes were dried and platinum coated using a JFC-1300 Auto Fine Coater (JEOL). The coated samples were examined using a JSM-5600 LV Scanning Electron Microscope (JEOL). The membrane porosity was determined from the water uptake of a calibrated volume by a piece of dry polymer. Average values were obtained from three different samples. The pure water flux was determined under steady state conditions using a dead-end ultra-filtration cell [7].

5.2.4 Experimental set-up

The experimental set-up in the present study was described previously in Chapters 3 and 4[8, 11]. In short, it consisted of a feeding section (pulse free HPLC binary pump), flow cell with the catalytic polymer membranes and analyzers: Electro Spray Ionization Mass Spectrometry (ESI-MS) (chapter 3 [8]) for detection of dissolved ionic species and Membrane Inlet Mass Spectrometry (MIMS) (chapter 4 [11]) to detect dissolved gases. Design of the flow cell will be described in the following paragraph.

Flow cell and hydrodynamic behavior of the cell with the membranes

The flow cell was designed to provide uniform distribution of liquid flow through the membranes (Figure 5.2 and Figure 5.3). The dead volume in the reactor with and without membranes was estimated by weighting the reactors before and after filling with water. The estimated volume was within 5 % error and was used to calculate the residence time. Usually, a stack of three membranes was used. The cell was closed leak-tight using silicon-rubber O-rings.

The hydrodynamic behavior of the reactor was studied with pulses of water saturated with Ar (concentration $1.4 \cdot 10^{-3}$ mol·dm^{-3}, 10 ml during 20 minutes), as reported elsewhere in detail [11] using membranes containing silica only, without Pt. Similar blanc experiments were done with empty reactor as well as bypassing the reactor.

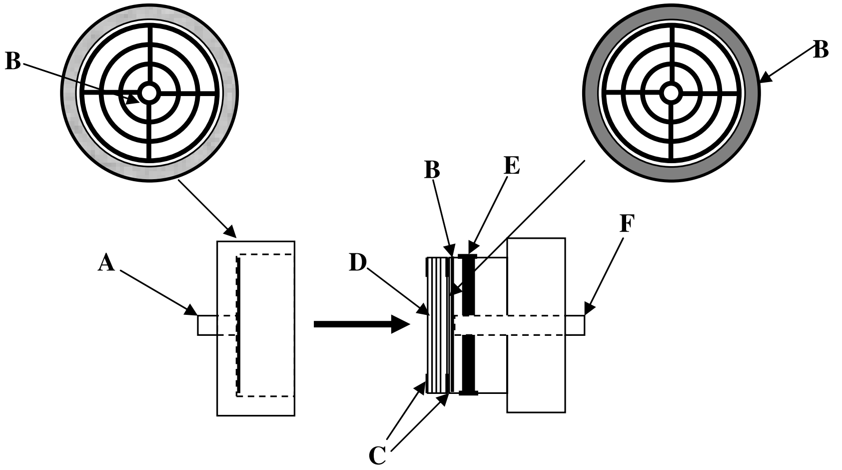

Figure 5.2: *Design of the flow cell: A- Liquid inlet; B-liquid flow distributor; C-small silicon rubber ring; D-membrane; E-large silicon rubber ring; F-Liquid outlet*

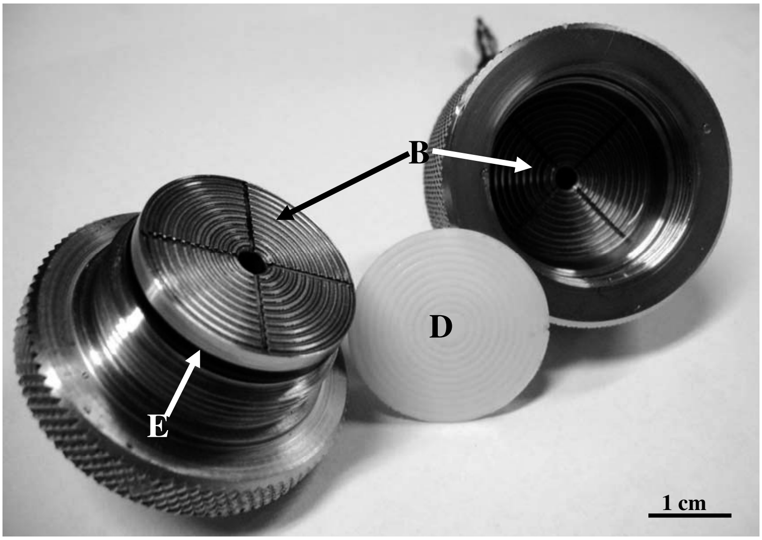

Figure 5.3: *Flow cell: B- Liquid flow distributor; D- membrane stack; E- large silicon rubber ring*

5.2.5 Catalytic experiments

A detailed description of the experimental procedure to perform H_2–O_2 titrations using liquid phase was described earlier [11]. In short, water saturated with oxygen was flown through the reactor in order to pre-adsorb oxygen on the catalyst. Subsequently, the reactor was flushed with water saturated with Ar in order to remove any physisorbed and dissolved oxygen from the reactor. All experiments were performed with a flow rate of 0.5 ml·min^{-1}. Next, the oxygen-covered catalyst was contacted with pulses of water saturated with hydrogen (concentration $0.8 \cdot 10^{-3}$ mol·dm^{-3}, 2.5 ml during 5 minutes); pulses were repeated every 10 minutes, flowing Ar-saturated-water in between. After the final pulse with hydrogen, water saturated with oxygen was flown through the reactor in order to remove pre-adsorbed hydrogen and to pre-adsorb oxygen on the catalyst. Titration experiments were repeated three times, with the oxygen treatment between cycles.

Steady state experiments with glucose were performed with aqueous solution of glucose ($5.6 \cdot 10^{-5}$ mol/dm^3). The pH of the glucose solution was adjusted to pH = 9 ± 0.3 in order to prevent inhibition of the catalysts by carboxylic acids [21]. Oxygen was introduced in the vessel with glucose after flowing Ar-saturated glucose solution 20 minutes,by changing the gas phase in the glucose vessel from pure Ar to 4 % O_2 in Ar, resulting in an O_2 concentration equal to $5.2 \cdot 10^{-5}$ mol/dm^3). Experiments were performed with 0.5 ml·min^{-1} flow rate at 60 °C.

Calibrations for quantitative interpretation will be described in the result and discussion section.

5.3 Results and discussion

First, the results of the preparation and characterization of the catalyst and catalytic membranes will be presented and discussed. Then, pressure drop and the hydrodynamic behavior of the reactor will be dealt with. After that, results of H_2–O_2 titration experiments as well as steady-state glucose oxidation experiments will be described and discussed.

5.3.1 Catalyst and membrane preparation and characterization

The platinum loading of Pt/SiO_2 (1 ± 0.05 wt%) is as expected based on the preparation procedure [18] (Table 5.1). Platinum dispersion based on hydrogen chemisorption (59 %, Table 5.1) is slightly higher than the dispersion estimated from TEM (52 %, Table 5.1), indicating possible presence of some very small particles (< 2 nm) which are difficult to observe with TEM. The catalyst in the membrane was also characterized, after removing the membrane via calcination in air at 300 °C for 3 hours; XRF confirmed 1 wt% Pt loading (Table 5.1) and also Pt dispersion remained essentially constant (55 %, Table 5.1). These results confirm that the membrane can be removed by calcination without affecting the catalyst.

The morphologies of the membranes prepared with different loading of catalyst particles are shown in (Figure 5.4 and Figure 5.5). Macro-voids are observed with catalyst particle loadings of 50 wt% (Figure 5.4) and less (not shown). Surprisingly, no macro-voids are observed when more catalyst is added to the membrane as shown in (Figure 5.5) for 65 wt% catalyst.

The presence of macro-voids in the membrane structure is undesirable, since the macro-voids can cause weak spots in the membrane leading to mechanical failure under pressure. Furthermore, the presence of macro-voids creates channels, decreasing the efficiency of the catalyst particles due to by-passing. Macro-voids are assumed to form by simultaneous inflow of solvent and non-solvent to nucleation sites underneath the skin layer. Macro-void growth takes place as long as the surrounding polymer solution remains stable against phase separation [7]. The presence of 1-octanol into our system EVAL-DMSO favors destabilization of the polymer solution in front of the first nuclei formed suppressing the macro-void formation. On the other hand the solid particles act as a nucleus in the casting solution limiting the grow size of the macro-voids. They also increase the viscosity of the polymer solution and therefore decrease the macro-void formation.

Figures 5.6(a) and 5.6(b) present more detailed structure of the membranes containing 65 wt% particles. Pores are interconnected without evident finger-like macro-voids across the entire cross-section (Figures 5.5 and 5.6(a)). Figure 5.6(b) shows that the catalyst particles are well embedded in a polymeric matrix because most of the pores are small enough to hold the particles physically immobilized in the pore system. Furthermore, Figure 5.6(a) indicates that the catalyst particles do not interact directly with the polymer.

Finally, pore interconnectivity and high porosity as indicated by the SEM micrographs in Figure 5.6(b) agrees with the high porosity of 75±10 % observed in swelling experiments, which is hardly influenced by the amount of particles incorporated into the polymeric structure.

5.3.2 Pressure drop and hydrodynamic behavior of the reactor

The pressure drop over a stack with ten membranes using the standard flow rate of 0.5 ml/min was less then 0.1 bar. Therefore, experiments with higher flowrates were performed, resulting in 1.2 bar pressure drop when flowing 10 ml/min.

Table 5.1: *Catalyst loadings and dispersions determined in gas phase and in liquid phase*

Catalyst	Loading (wt%)	D_{Gas} (H/Pt) Gas phase chemisorption	Amount of Pt in reactor		H/Pt - TEM[1]	$(O_2)_{\text{Liquid}}$ (μmoles)	$(H_2)_{\text{Liquid}}$ (μmoles)	D_{Liquid} (O/Pt)	D_{Liquid} (H/Pt)[2]
			Bulk (μmoles/g)	Surface (μmoles)					
Pt/SiO_2	1.0±0.05	0.59	51	3.3	0.52	-	-	-	-
Membrane	1.0[3]	0.55[4]	51	3.2	-	1.8	4.5	0.42	0.53

[1] Calculated based on: $D(TEM) = \frac{1.08}{d(nm)}$ [19]

[2] Dispersion in liquid phase (D_L) $D_{liquid} = \frac{2(H_2)L}{3(BulkPt)W_{(cat)}}$

[3] Loading of the matherial that remained after calcination of the membrane at 300 °C for 3 hours

[4] Platinum dispersion of the Pt/SiO_2 catalyst that remained after calcination of unused membranes

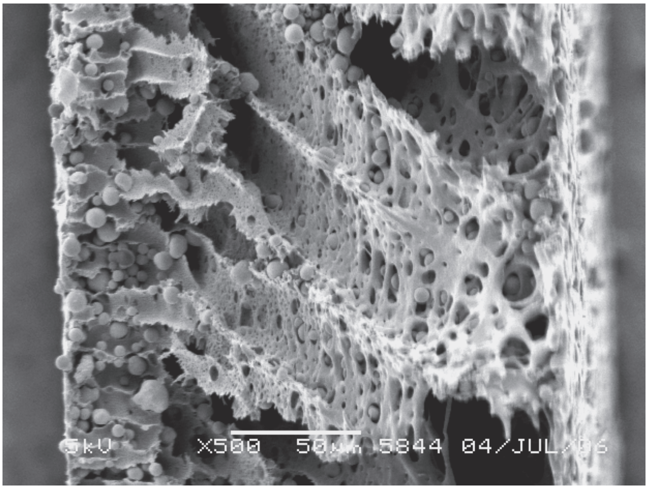

Figure 5.4: *SEM photomicrograph of the membrane prepared from* 10 % *EVAL in DMSO in the presence of* 10 % *1-octanol as additive by incorporation of* 50 % *of catalyst particles into the polymeric support (cross-section)*

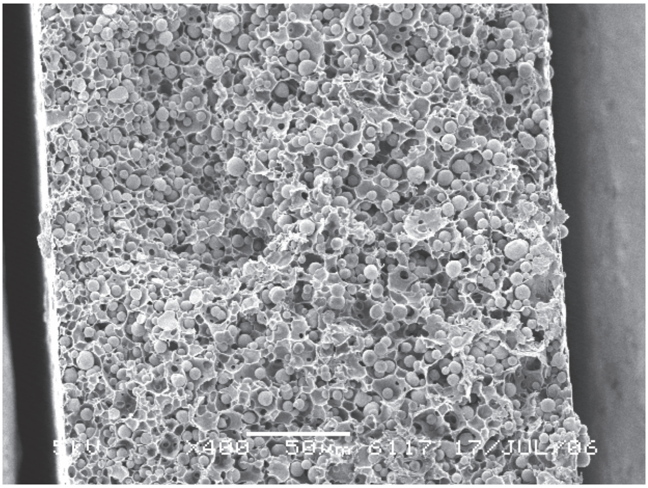

Figure 5.5: *SEM photomicrograph of the membrane prepared from* 10 % *EVAL in DMSO in the presence of* 10 % *1-octanol as additive by incorporation of* 65 % *of catalyst particles into the polymeric support (cross-section)*

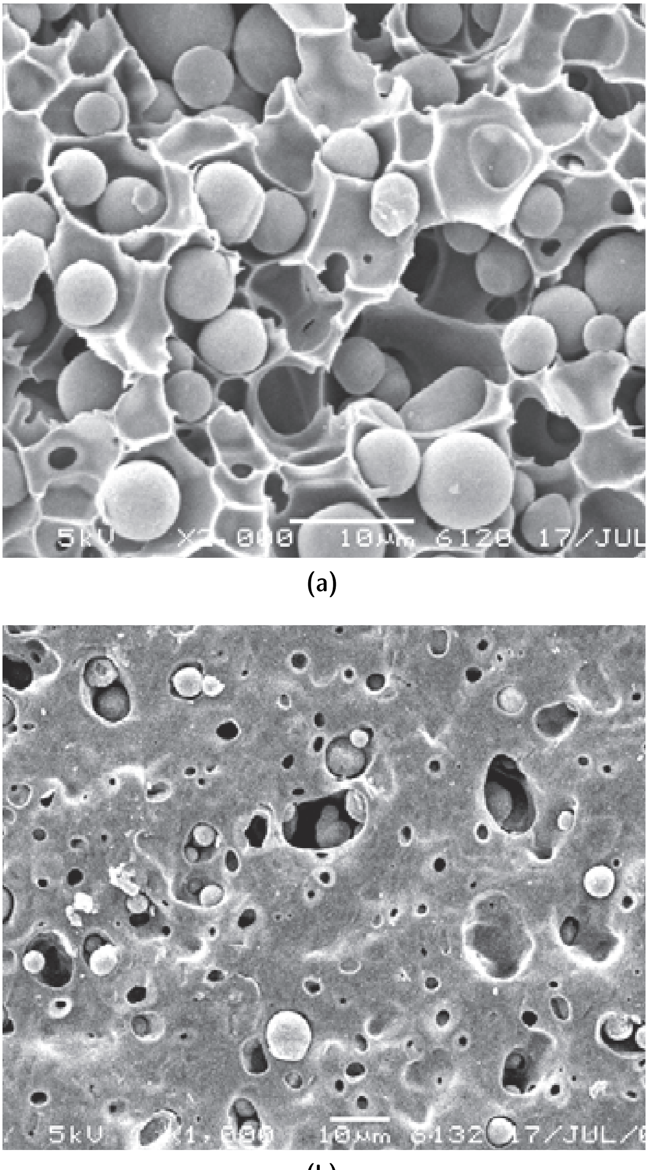

(a)

(b)

Figure 5.6: *SEM photomicrograph for the membranes prepared from* 10 wt% *EVAL in DMSO in the presence of* 10 wt% *1-octanol as additive by incorporation of* 65 wt% *catalytic particles into the polymeric support: (a) cross-section; (b) top-surface*

Pressure drop over conventional fixed beds can be estimated with the Ergun equation (eq. 5.1)[22]:

$$\frac{\Delta p}{L} = \frac{150\mu\,(1-\epsilon)^2\,u_0}{\epsilon^2 d_p^2} + \frac{1.75\,(1-\epsilon)\,\rho u_0^2}{\epsilon^3 d_p} \tag{5.1}$$

with L-the height of the bed, μ-the fluid viscosity, ϵ-the void fraction, u_0 = V/A– fluid superficial velocity, d_p– particle diameter and ρ- density. If we would form a packed bed with all catalyst particles embedded in the stack of ten membranes (1000 mg), keeping the diameter of the reactor constant ($2.4 \cdot 10^{-2}$ m), a bed height would result equal to $4 \cdot 10^{-4}$ m (five times less than the thickness of the stack of membranes). The Ergun equation then predicts a pressure drop equal to 3.2 bar, when flowing 10 ml/min. Obviously, such a bed can not be established without by-passing, demonstrating the first advantage of membrane embedded catalysts. In addition to that, the difference with the observed pressure drop for the stack of membranes (1.2 bar) convincingly demonstrates that distribution of the catalyst particles in the reactor space by immobilizing in a porous membrane indeed gives superior low pressure drop as compared to fixed beds. The distribution of the catalyst particles in the reactor volume resembles a frozen slurry reactor Figure 5.7.

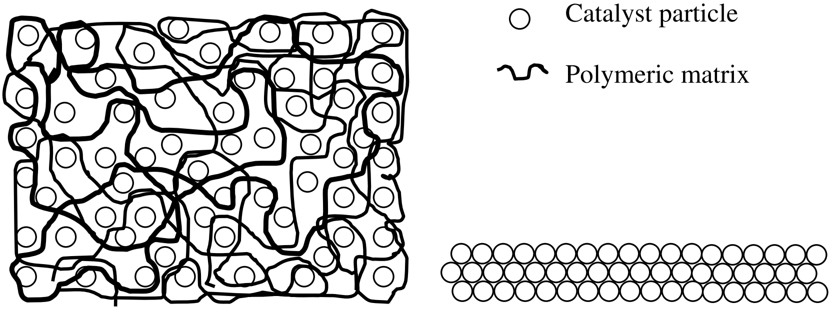

Figure 5.7: *Schematic representation of frozen slurry bed (left side) packed bed, prepared with the same amount of catalyst (right side)*

The advantage in pressure drop will be even larger when practical catalyst particles are used, having a less controlled particle size distribution. It is well known that broad particle size distributions increases the pressure-drop over a fixed bed dramatically because the small particle can be placed in the interstitial space between larger particles, efficiently blocking the liquid flow. The responses for different configurations to an argon pulse are presented in Figure 5.8.

The most obvious difference is the change in delay times of 0.6, 3 and 4 minutes, which correspond to the differences in the dead volumes of the bypass (Figure 5.8-1),

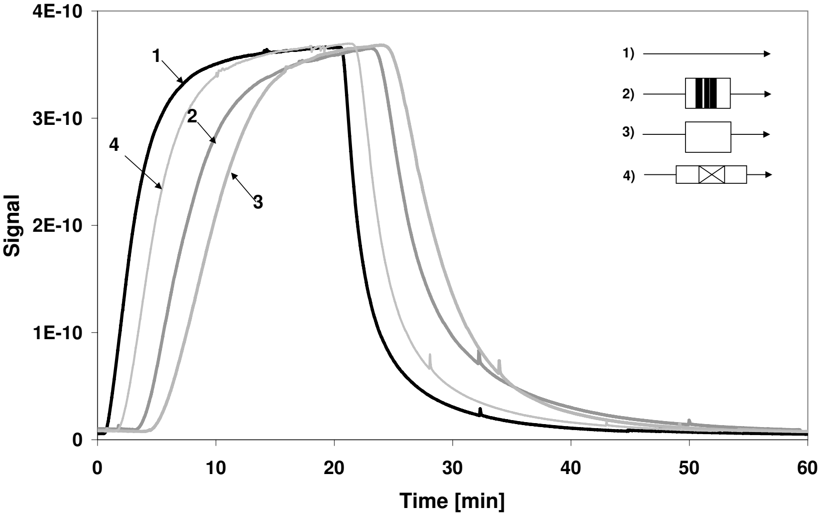

Figure 5.8: *Response to a pulse of argon (*10 ml *during 20 minutes with flow rate* 0.5 ml·min^{-1}*,* c_M(Ar) = 1.4 · 10^{-3} mol·dm^{-3}*,* T = 22 °C*) of 1) by-pass, 2) cell with three membranes containing silica and 3) empty cell, 4) reactor filled with silica [18]*

the cell with membranes containing silica particles (Figure 5.8-2) and the empty cell (Figure 5.8-3), respectively. In addition, the differences in the shapes of the break-through curves are modest, indicating that hydrodynamics are quite similar for all cases. There is no significant difference in the shape of break-through curves from present study with the curves obtained with a silica fixed bed in our previous study [11] (Figure 5.8-4), implying similar hydrodynamics despite significant difference in pressure drop, indicating that there is no misdistribution (channeling) of the flow through the membranes. A measure for the spreading of the residence time distribution (RTD) is the variance (σ^2) as defined according to Eq. 5.2 [23]:

$$\sigma^2 = \frac{\int_0^\infty t^2 C\,dt}{\int_0^\infty C\,dt} - \left(\bar{t}\right)^2 \tag{5.2}$$

The variances observed for the by-pass is obviously the lowest in this study (10.6 min^2), while for the silica packed bed (13.0 min^2), the cell including the stack of catalytic membranes (14.2 min^2) and the empty cell (15.5 min^2) show more back mixing. These data show that the extent of back mixing in the fixed bed reactor and the catalytic-membrane-stack is rather limited, despite the large difference in reactor diameters and thus linear liquid velocities.

5.3.3 Titration of pre-oxidized Pt/SiO_2 in membrane with H_2

Figure 5.9 shows the result of pulsing hydrogen on pre-oxidized Pt/SiO_2 in the membrane, as well as on membrane only (blank). The surface areas of the peaks are a measure for the amount of hydrogen present, as discussed in detail in our previous study [11]. No consumption of hydrogen was observed for the blank membrane. However, complete consumption of hydrogen is observed during the first pulse on the oxidized Pt/SiO_2 loaded membrane, followed with the breakthrough that occurs during the next four pulses. Finally, the surface areas of the peaks become identical to the blank experiment, indicating that hydrogen is not consumed anymore. The total amount of hydrogen consumed was 4.5±0.3 μmoles H_2. The amount of Pt in the reactor is 3.3 μmoles, as determined with H_2 chemisorption (Table 5.1).

The amount of hydrogen (H) consumed in titration experiment is almost 3 times the amount of pre-adsorbed oxygen (O_a), assuming O_a/Pt ratio to be one. This is in good agreement with the assumption that two hydrogen atoms react with one pre-adsorbed oxygen atom (O_a) to form water, followed by adsorption of one hydrogen atom per surface platinum atom.

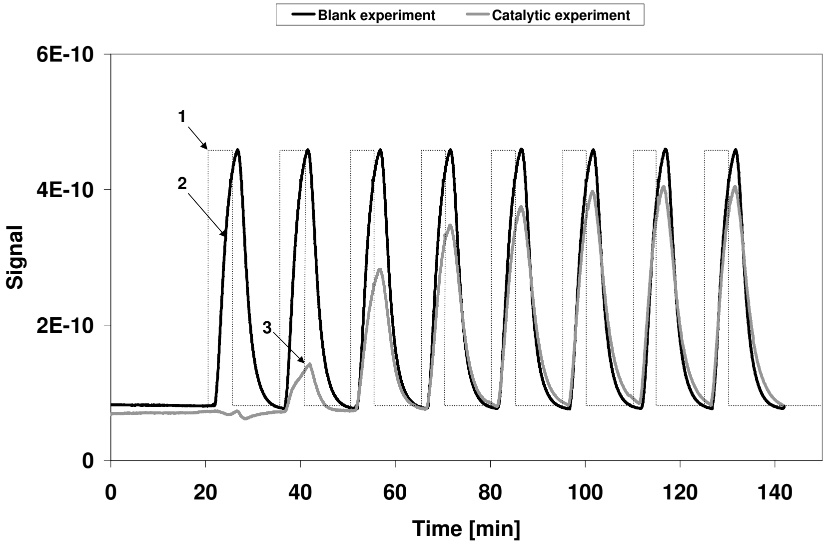

Figure 5.9: *Titration of pre-adsorbed oxygen on Pt/ SiO_2 incorporated in EVAL membrane using water saturated with hydrogen (2.5 ml pulse, $F = 0.5$ ml·min^{-1}, $c_M(H_2) = 0.8 \cdot 10^{-3}$ mol·dm^{-3}, $T = 22$ °C): 1) ideal pulse; 2) membrane with silica particles and 3) membrane with Pt/ SiO_2 particles with pre-adsorbed oxygen*

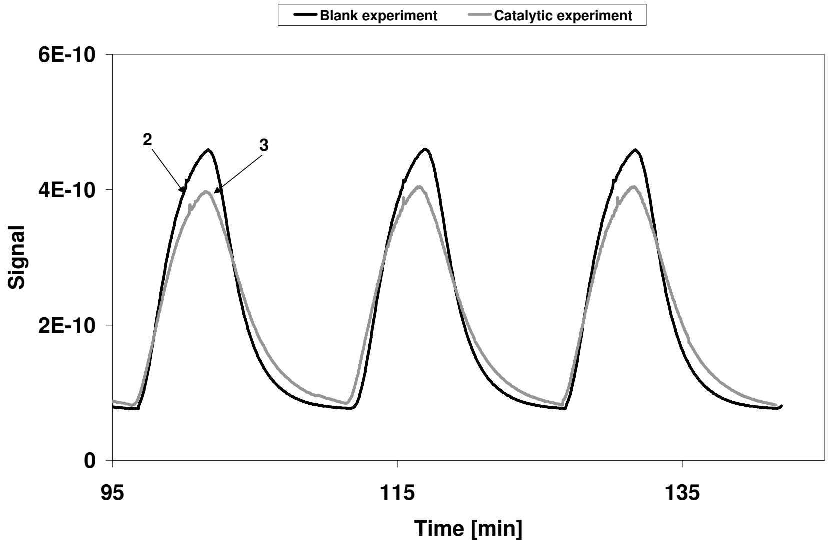

Figure 5.10: *Detail from Figure 5.9 - Detailed pulse shape for pulses after completion of the titration: 2) membrane with silica particles and 3) membrane with Pt/ SiO_2 particles with pre-adsorbed oxygen*

Thus, platinum dispersion obtained from H_2–O_2 titration in liquid phase for oxidized Pt/ SiO_2 catalyst in membrane (i.e. 53 %, Table 5.1) agrees reasonably well with dispersion obtained using hydrogen chemisorption in gas phase for the parent Pt/ SiO_2 catalyst (i.e. 59 %, Table 5.1). Therefore, we conclude that the polymer does not compromise the accessibility of the Pt particles, agreeing with the observation that the catalyst particles seem physically entrapped, as discussed earlier. Figure 5.10 indicates that a weak but significant interaction is taking place between dissolved H_2 and a hydrogen covered platinum surface; similar interaction between dissolved H_2 and Pt/ SiO_2 catalyst was already reported and explained, in terms of hydrophobic properties of a hydrogen covered Pt surface, in Chapter 4 [11].

The catalysts in the membranes were characterized after performing the hydrogen-oxygen pulse experiments, after removing the membrane via calcination (3 hours in air at 300 °C). It was discussed above that the catalyst is not affected, based on identical experiments with fresh catalytic membranes. The Pt content of the remaining catalyst appeared to decrease from 1.0 to 0.87 wt%. Apparently, some platinum is lost during three reduction-oxidation cycles. Removal of platinum under similar conditions from pt/sio2 catalyst in fixed bed operation was reported before [11, 24], and is probably due to dissolution of the smallest metal particles during the titration sequence.

5.3.4 Catalytic oxidation of glucose

Figure 5.11 shows the MS spectrum of the glucose solution; the most significant peaks are observed at m/z 215 and 179 in good agreement with previous work in Chapter 3 [8].

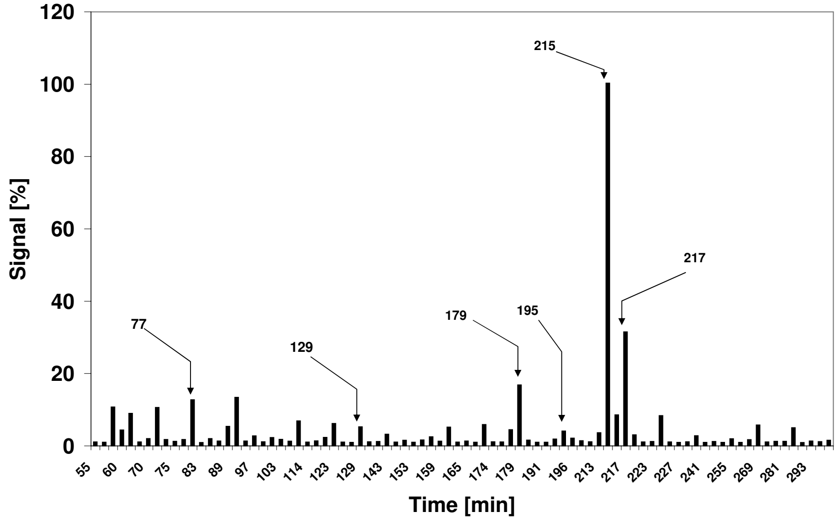

Figure 5.11: *Spectrum of the effluent from the flow cell containing membranes with silica particles; aqueous solution contained* $c_M = 5.2 \cdot 10^{-5}$ mol/dm^3 O_2 *and* $c_M = 5.6 \cdot 10^{-5}$ mol/dm^3 *glucose(flow of solution was* 0.5 ml/min *and* $T = 60$ °C*)*

In short, it was concluded that the peak at m/z 215 corresponds to the de-protonated glucose ion with two associated molecules of water ($2\,H_2O \cdot [C_6H_{11}O_6]^-$). In addition, the peak at m/z 179 corresponded to $[C_6H_{11}O_6]^-$ (i.e. de-protonated glucose molecule without water).

The most significant peak for gluconic acid was observed at m/z 195 (not shown), corresponding to a de-protonated gluconic acid $[C_6H_{11}O_7]^-$ anion. Peaks at m/z 129 and m/z 77 probably corresponds to traces of 1-octanol and DMSO, respectively, solvents used in the preparation and leaching from the catalytic membrane. Many remaining minor peaks between m/z 77 and m/z 129 can not be fully explained at this moment.

Figure 5.12 shows the MS spectrum of the reactor effluent when flowing a mixture containing $5.2 \cdot 10^{-5}$ mol/dm^3 O_2 and $5.6 \cdot 10^{-5}$ mol/dm^3 glucose through the membrane containing Pt/SiO_2. A part of the glucose is clearly converted because peaks at m/z 215 and m/z 179 are much lower as compared the blank experiment in Fig-

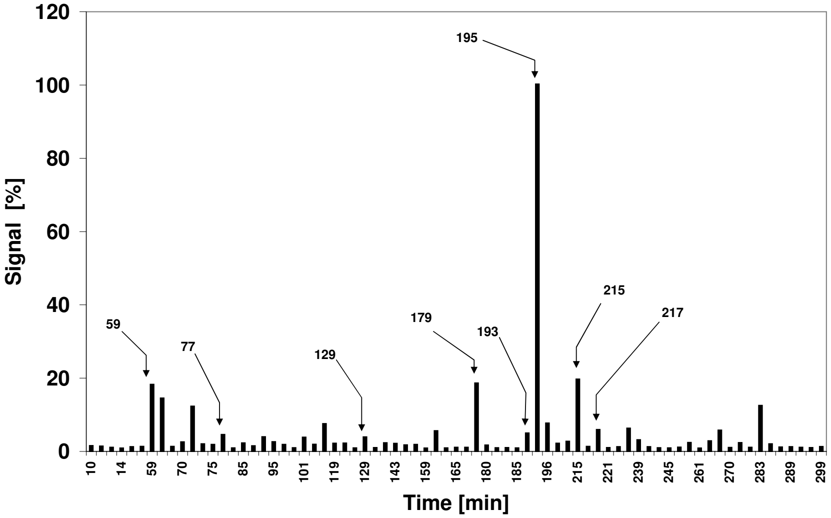

Figure 5.12: *Spectrum of the effluent from the flow cell containing membranes with* pt/sio2 *catalyst; aqueous solution contained* $c_M = 5.2 \cdot 10^{-5}\,\mathrm{mol/dm^3}$ O_2 *and* $c_M = 5.6 \cdot 10^{-5}\,\mathrm{mol/dm^3}$ *glucose(flow of solution was* 0.5 ml/min *and* $T = 60\,°\mathrm{C}$*)*

ure 5.11. The most significant peak in Figure 5.12 is at m/z 195 which belongs to gluconic acid; clearly, around 80 % of glucose is converted to gluconic acid, demonstrating catalytic activity of the novel structure.

In short, our results demonstrate not only that the Pt particles in the catalytic membrane are accessible and catalytically active, but also demonstrate the applicability of the titration method in liquid phase: characterization of the catalytic membrane in the swollen state, i.e. under reaction conditions.

5.4 Conclusions

We have successfully prepared catalytic polymeric membranes by incorporating Pt-loaded mono-disperse SiO_2 particles into an EVAL porous matrix by an immersion phase separation process. Addition of a relatively high concentration (65 wt%) of catalyst particles is preventing the formation of macro voids, improving both mechanical stability of the membranes as well as improving homogeneity of the liquid flow distribution through the membrane. The catalyst particles remain intact during the preparation procedure. The catalyst particles are physically immobilized throughout the membrane, entrapped in the pores, preventing channeling that would occur when flowing through an equivalent shallow fixed bed. Furthermore, the novel frozen-slurry-like morphology results in significant lower pressure drop as compared to a fixed bed with identical diameter and containing the same amount of catalyst particles. The platinum particles are proven to be highly accessible in the swollen state, i.e. in liquid phase, as demonstrated both by the catalytic activity of the Pt/SiO_2 loaded membranes for glucose oxidation as well as by the fact that H_2–O_2 titrations in liquid phase, i.e. the catalytic membrane in the swollen state, confirms that close to all platinum surface atoms contribute.

Acknowledgements

The authors thank, Ing. L. Vrielink for XRF and BET analysis, Ing. M. Smithers for TEM measurements, Ing. A. Hovestad for assistance with reactors preparation, Ing. A. Wonders (University of Eindhoven), Ing. J. Spies and Ing. B. Geerdink for technical assistance. Financial support for the project (TPC 5694) by STW (The Netherlands) is kindly acknowledged.

References

[1] N. A. Jarrah. *Microstructured Catalyst Support Based on Carbon Nano-Fibers (CNFs).* Ph.D. thesis, University of Twente, Enschede, The Netherlands (2004).

[2] C. P. Stemmet, J. N. Jongmans, J. van der Schaaf, B. F. M. Kuster and J. C. Schouten. Hydrodynamics of gas-liquid counter-current flow in solid foam packings. *Chemical Engineering Science*, 60, 6422–6429 (2005).

[3] J. K. Chinthaginjala, K. Seshan and L. Lefferts. Preparation and Application of Carbon-Nanofiber Based Microstructured Materials as Catalyst Supports. *Industrial & Engineering Chemical Research*, 46, 3968–3978 (2007).

[4] P. R. Brown and R. A. Hartwick, editors. *High Performance Liquid Chromatography.* Wiley, New York (1989).

[5] K. K. Unger. *Porous silica — its properties and use as support in column liquid chromatography*, volume 16. Elsevier — Journal of Chromatography Library (1994).

[6] E. Klein. Review; Affinity membranes: a 10-year review. *Journal of Membrane Science*, 179, 1–27 (2000).

[7] M.-E. Avramescu. *Membrane Adsorbers — Development and Applications.* Ph.D. thesis, University of Twente, Enschede, The Netherlands (2004).

[8] D. Radivojević, M. Ruitenbeek, K. Seshan and L. Lefferts. Development of a transient response technique for heterogeneous catalysis in liquid phase, Part 1:

applying membrane inlet mass spectrometry (MIMS) for detection of dissolved gasses (2008). Accepted for publication in *Journal of Catalysis*.

[9] J. E. Benson and M. Boudart. Hydrogen-oxygen titration method for the measurement of supported platinum surface areas. *Journal of Catalysis*, 4, 704–710 (1965).

[10] J. S. Bradley and W. Busser. Chemisorption measurements on polymer-stabilized colloidal platinum and rhodium nanoclusters in liquid dispersion. *Catalysis Letters*, 63(3–4), 127–130 (1999).

[11] D. Radivojević, M. Ruitenbeek, K. Seshan and L. Lefferts. Development of a transient response technique for heterogeneous catalysis in liquid phase, Part 2: applying membrane inlet mass spectrometry (MIMS) for detection of dissolved gasses (2008). Accepted for publication in *Journal of Catalysis*.

[12] G. C. Bond and P. B. Wells. Characterization of the Standard Platinum/Silica Catalyst Europt-1; 2. Preparation, Physical Properties, and Chemical Composition. *Applied Catalysis*, 18(2), 225–230 (1985).

[13] W. Marconi, R. Marcone and A. Piozzi. Sulfation and preliminary biological evaluation of ethylene-vinyl alcohol copolymers. *Macromolecular Chemistry and Physics*, 201, 715–721 (2000).

[14] W. Y. Chuang, T. H. Young, D. M. Wang, R. L. Luo and Y. M. Sun. Swelling behavior of hydrophobic polymers in water/ethanol mixtures. *Polymer*, 41, 8339–8347 (2000).

[15] M. Besson and P. Gallezot. Selective oxidation of alcohols and aldehydes on metal catalysts. *Catalysis Today*, 57, 127–141 (2000).

[16] H. Saito, O. Shinji and F. Shigeo. US Patent 4 843 173. *Kawaken Fine Chemical Corp. Ltd and Kao Corp.* (1989).

[17] K. Deller, H. Krause, E. Peldszus and B. Despeyroux. US Patent 5 132 452. *Degussa* (1992).

[18] D. Radivojević, K. Seshan and L. Lefferts. Preparation of well-dispersed Pt/SiO_2 catalysts using low-temperature treatments. *Applied Catalysis A: General*, 301(1), 51–58 (2006).

[19] C. H. Bartholomew and R. J. Farrauto. *Fundamentals of industrial catalytic processes.* John Wiley & Sons, Inc., Publication (2006).

[20] M. E. Avramescu, W. F. C. Sager, M. H. V. Mulder and M. Wessling. Preparation of ethylene vinylalcohol copolymer membranes suitable for ligand coupling in affinity separation. *Journal of Membrane Science*, 210, 155–173 (2002).

[21] T. Mallat and A. Baiker. Heterogeneously catalyzed selective oxidations in the liquid phase. Oxidation of alcohols with molecular oxygen on platinum metal catalysts in aqueous solutions. *Catalysis Today*, 19, 247–283 (1994).

[22] R. H. Perry, D. W. Green and J. O. Maloney, editors. *Chemical Engineer's Handbook*. McGraw-Hill, New York, 6. edition (1984).

[23] O. Levenspiel. *Chemical Reaction Engineering*. John Wiley & Sons, New York, USA, 3. edition (1998).

[24] A. Douidah, P. Marécot and J. Barbier. Toward a better understanding of the stability of supported platinum catalysts in aqueous phase under hydrogen atmosphere at room temperature. *Applied Catalysis A*, 225(1–2), 11–19 (2002).

6

Conclusions and recommendations

6.1 Introduction

Development of heterogeneous catalysts for liquid phase processes requires detailed knowledge about phenomena that occur on the catalyst surface during the catalytic reaction in liquid phase. Transient response techniques with detectors that can perform continuous, rapid, multi-component and simultaneous detection are ideal for such studies. However, there are hardly any transient techniques available that allow experimental investigation of adsorption of reactants, intermediates and probe-molecules from liquid phase on the surface of catalysts. The existing liquid phase detectors are not able to detect more than one specie simultaneously and rapidly, so that concentrations of reactants and products cannot be monitored simultaneously, limiting the application to pulse experiments without actual reactions occurring.

The work described in this thesis focuses on development and application of a transient response technique for studies of adsorption and catalytic reactions over heterogeneous catalysts in liquid phase using ESI-MS as detector. Two test reactions, i.e. reduction of nitrite over Pt/SiO_2 and oxidation of glucose over Pt/CNF/Ni catalysts, were used to demonstrate that it is possible to monitor reactants, intermediates and products during reaction (semi)quantitatively. The results clearly show potential for application of the transient response technique to study adsorption and catalytic reactions in liquid phase.

6.2 Preparation of well-dispersed Pt/SiO_2 catalysts using low-temperature treatments

Transient response technique requires reactors with sufficient catalyst available as well as sufficiently low pressure drop when flowing liquids through the reactor. One option to achieve this is to use a commercially available so-called “monolithic” HPLC column which are available in a polymer housing. Structured materials based on polymers are generally relevant in this perspective, implying limited thermal stability of the structured catalytic reactor. Therefore, a method to deposit active phase under mild conditions was explored, demonstrating that Pt/SiO_2 catalysts prepared using ion-exchange and direct reduction in hydrogen at moderate temperatures results in highly dispersed platinum particles on silica. Generally, chlorine containing platinum species ($PtCl_x$), result in agglomeration during calcination at temperatures above 250 °C and therefore result in poorly dispersed catalysts. In the case of oxygen containing, chloride-free platinum species (PtO_x), this problem is less severe and calcination at temperatures up to 350 °C results in high dispersions. In both cases, direct reduction of the silica supported platinum precursor with H_2 removes the chlorine and oxygen containing species efficiently at temperatures lower than 150 °C, resulting in well dispersed catalysts. $PtCl_4$, $H_2PtCl_6 \cdot 6\,H_2O$ and $H_2Pt(OH)_6$ are suitable precursors to make a well dispersed platinum catalyst in polymer reactors.

6.3 Transient response technique for heterogeneous catalysis in liquid phase

6.3.1 Electron Spray Ionization Mass Spectrometry (ESI-MS)

Transient response technique for liquid phase heterogeneous catalytic studies using ESI-MS as detector was developed and has been successfully applied for the first time.

Detector was calibrated with compounds using the most intense peaks (i.e. m/z 115 for nitrite, m/z 195 for gluconic acid and m/z 215 for glucose). The concentration of nitrite can be accurately determined in the concentration range between $2 \cdot 10^{-5}$ mol·dm^{-3} up to about $5 \cdot 10^{-4}$ mol·dm^{-3}. Furthermore, the limit of detection for glucose was $6 \cdot 10^{-6}$ mol·dm^{-3} and the concentration of glucose could be accurately determined up to $1.5 \cdot 10^{-4}$ mol·dm^{-3}. Gluconic acid can be accurately determined between $1 \cdot 10^{-6}$ mol·dm^{-3} up to $1 \cdot 10^{-4}$ mol·dm^{-3}. In all cases, the MS signal hardly increases further at higher concentrations due to the saturation effect caused by decreasing ionization efficiency of the ESI interface. This effect is limiting applicability of the novel technique for higher concentrations.

In the case of a packed bed with SiO_2 stable signals were obtained 20 seconds after introducing a step-change, while in the case of CNF/Ni foam, stabilization required typically 20 minutes due to back mixing. Consequently, longer pulses were used in experiments with Pt/CNF/Ni catalyst. Furthermore, due to the open structure of the foam, pressure drop over the foam was significantly lower as compared to the packed bed with Pt/SiO_2.

A quantitative experimental result for nitrite reduction requires detection of both products, i.e. nitrogen and ammonia. Unfortunately, detection of molecules with low mass (m/z < 20, like ammonia) is hardly possible. Another important limitation of the detector is the inability to detect gases dissolved in liquids, due to the relatively mild ionization process via electrospray and therefore a separate analyzer would be necessary to measure dissolved gasses, e.g. N_2 and H_2. The novelty and capability of the developed technique is nevertheless demonstrated with the fact that the ESI-MS detector is sufficiently sensitive to determine, quantitatively, extremely small amounts of physisorbed nitrite, down to 0.05 μmole.

It was possible to detect different compounds simultaneously with the ESI-MS detector, which is the most significant advantage over existing transient techniques reported in literature. This was demonstrated by simultaneously detecting glucose, gluconic acid, glucose dialdehyde, glucuronic acid and glucaric acid when exposing oxidized Pt catalyst to a glucose pulse. However, the technique shows cross contamination effects between glucose and gluconic acid, introducing an error in the range of 20 % in the quantitative measurements and further work is necessary to establish calibration matrices. Another problem that needs to be solved is frequent blockages of the nebulizing needle due to deposition of dissolved species on the wall of the needle (especially during the analysis nitrite).

6.3.2 Membrane Inlet Mass Spectroscopy (MIMS)

Detection of gases dissolved in an aqueous stream, at the exit of a catalytic reactor in a transient experiment was successfully done with the membrane inlet mass spectrometry (MIMS). Differences in the response times are caused by differences in the diffusivity of the gases in the membrane in the order $O_2 < Ar < H_2$. Important cause for the long response time could be the fact that relative thick membranes were used (200 μm). The relative slow response of the detector is responsible for the fact that concentrations cannot be reliably measured real time in transient experiments. On the other hand, it was shown that calibration of integral pulses is possible and reliable. In addition, the detector is universal and allows calibration of H_2, O_2, N_2 and/or Ar dissolved in water with insignificant cross contamination (< 2 %). The minimal amount of hydrogen that can be detected in a single pulse is 0.1 μmoles H_2, which is equivalent to about 0.5 m^2 Pt surface. Transient experiments consuming or producing dissolved gasses can be monitored quantitatively as long as the typical width of the signals is comparable. However, since the ESI-MS detector responds already within a few seconds, the detector for dissolved gases will limit the window of operation of the complete set-up i.e., when using both detectors. On the other hand, it is obvious that the most relevant gasses for liquid phase catalysis, i.e. hydrogen and oxygen for hydrogenation reactions and oxidation reaction respectively, can be detected, as well as N_2 which would be important for studying hydrogenation of nitrite and nitrate.

The technique was successfully applied for the measuring of a metal dispersion for three different catalysts (EuroPt-1, Pt/SiO_2 and Pt/CNF) in liquid phase via H_2–O_2 titration. The platinum dispersions obtained in liquid phase are in excellent agreement with dispersions based on conventional hydrogen chemisorption in gas phase for all three catalysts. Clearly, water does not influence the accessibility of the Pt atoms. The titration stoichiometry obtained agrees well with results of gas phase titration experiments in literature. An obvious advantage of the H_2–O_2 titration method is that it is in principal not destructive because no irreversible adsorption is taking place.

The capability of the transient method is further demonstrated by the surprising observation that dissolved hydrogen physisorbs significantly on a reduced Pt catalyst whereas dissolved oxygen does not interact with an oxidized catalyst. This result shows that the technique developed here can provide unique information on the influence of solvent (water in this case) on reversible interactions of dissolved species with catalyst surfaces.

6.4 Novel catalytic structures for transient technique

Catalytic polymer membrane is successfully prepared by incorporating mono-dispersed Pt/SiO_2 catalyst particles in an ethylene vinyl acetate copolymer (EVAL) porous matrix. Addition of a relatively high concentration (65 wt%) of catalyst particles even helps preventing the formation of macro voids, improving both mechanical stability of the membranes as well as improving homogeneity of the liquid flow distribution through the membrane. The catalyst particles remain intact during the preparation procedure. The catalyst particles are physically immobilized throughout the membrane, entrapped in the pores, preventing channeling that would occur when flowing through an equivalent shallow fixed bed. Furthermore, the novel frozen-slurry-like morphology results in significantly lower pressure drop as compared to a fixed bed with identical diameter and containing the same amount of catalyst particles. Thus, the frozen-slurry structured catalyst allows experiments in a broader window of operational conditions. Platinum dispersion for the membrane based system is in reasonable agreement with the dispersion of the parent catalyst implying that the accessibility of the Pt particles is not influenced by the polymer matrix. The results also demonstrate the applicability of the titration method in liquid phase, enabling characterization of the catalytic membrane in the swollen state, i.e. under reaction conditions.

6.5 Recommendations for future work

Although, it has been demonstrated in this thesis that transient experiments in liquid phase are possible, several key issues need further attention. These include optimization of the ESI process, decrease of the MIMS response time and integration to a transient system, preparation and implementation of the novel microreactors and exploration of the novel reactions.

The ESI interface is subject of a major debate because the fundamental ion-production mechanism is not well understood [1]. In the research presented in this thesis, capillary voltage, de-solvation gas temperature, nebulizing gas and liquid flow rate were optimized in order to obtain maximal signal to noise ratio. However, matrix effects in the range of 20 % were observed. In literature, sample dilution was reported to reduce matrix effect [2] and future work should focus on experiments with lower reactant concentrations or dilution of the effluent from the reactor. This will also help avoiding the frequent shut downs of the system, caused by the blocking of the nebulizing needle. Furthermore, pH of the solution and the polarity of solvent are important parameters that affect the ionization process in ESI and should be further investigated.

In this research it is proven that MIMS can be successfully used to detect gasses dissolved in liquids. However, due to the slow response caused by the slow diffusion through the thick membrane, real time concentrations cannot be monitored reliably in transient experiments. There are rubbery polyphosphazene polymeric materials described in literature with high gas permeabilities [3]. These are promising materials and future work should require their testing. Finally, in present research, MIMS was tested separately from the transient technique due to the pressure rise in the nebulizing needle of the ESI, which was causing undesirable leakages in the MIMS. Future work should focus on the integration of MIMS into the transient response set-up. Minimization of the dead volumes will improve response of the system.

In the present work we used three different reactors:

1. Pt/SiO_2 packed bed,

2. Pt/CNF on Ni foam modules and

3. Pt/SiO_2 catalyst incorporated in a porous polymer matrix.

In future work, transient response technique can be used to study the performance of catalytic micro-reactors. The benefits of micro-reactors include better process control and higher safety. The small diffusion distances lead to short diffusion times, which can speed up analyzes [4]. In such situation, minimization of the dead volume of the system would be a key issue, because the low flow rates would cause very long response times. Furthermore, development and adjustment of the reactor for high pressure reactions would broaden range of the applications of the transient technique.

The work described in this thesis clearly shows successful application of the transient response technique equipped with ESI-MS and MIMS to study adsorption and catalytic reactions in liquid phase. As such, ESI-MS and MIMS allow experimental investigation of adsorption of reactants and probe-molecules on heterogeneous catalysts in liquid phase, as well as formation of products in the case that adsorbing species not only adsorb but also convert on the catalyst surface, e.g. by interacting with a pre-adsorbed second reactant.

References

[1] Z. Liang, Q. Yang, W. B. Zhang, L. H. Zhang and Y. K. Zhang. Effects of experimental parameters on the signal intensity of capillary electrophoresis electrospray ionization mass spectrometry in protein analysis. *Chromatographia*, 57(9–10), 617–621 (2003).

[2] R. Dams, M. A. Huestis, W. E. Lambert and C. M. Murphy. Matrix effect in bio-analysis of illicit drugs with LC-MS/MS: Influence of ionization type, sample preparation, and biofluid. *Journal of the American Society for Mass Spectrometry*, 14(11), 1290–1294 (2003).

[3] C. J. Orme, J. R. Klaehn, M. K. Harrup, T. A. Luther, E. S. Peterson and F. F. Stewart. Gas permeability in rubbery polyphosphazene membranes. *Journal of Membrane Science*, 280(1–2), 175–184 (2006).

[4] W. Ehrfeld, V. Hessel and H. Löwe. *Microreactors: New Technology for Modern Chemistry*. Wiley-VCH, 1. edition (2000).

Acknowledgements

I have spent more than four years at the University of Twente and that was a great experience. During this period I managed to learn more not only about catalysis, but also about myself, other people and more about life. The fact that I write these lines imply that I managed to complete important part of my journey . It is my honor and my duty to mention people that helped me to make (at least part of) my journey successful.

Beste Leon, thank you for giving me the opportunity to learn a lot while contributing to the science. This journey was long and not easy. However, it is important that the mission is accomplished successfully. Your guidance was important part of my learning.

Dear Seshan, you were not only my daily supervisor but also a friend. I want to thank you for the warmness and hospitality in your and Jianti's home — I felt it very strongly.

Dear Igor and Jana, I was always considering you and your family close to my hart. Louise and Jan, it is my privilege to have two of you as friends. Lianne, thank you for helping me in different occasions and for being always with the smile. Bertolino, your help and broad knowledge were always available. Thank you for the nice moments during the borrels. Jeroen, your contribution to this project was very important. Your positive attitude helped me many times. Sonia, your experimental work was valuable contribution to this work.

Lady G. and Kumi, you were always there when I needed you. Thank you for being my paranimfs, it is my honor! Many thanks to former and current members of the group: Jan, Barbara, Cis, Jiang, Zhu, Sune, Valer, Sepp, Daryl, Cristiano, Davidenko, Nabeel, Kazu, Muji, Eva Jimenez, Marco Rep, Thomas, Sergio, Vijay, Berta, Marijana, Hans, Patrick, Special thanks to Jorrit de Jong and Magda Avramescu — cooperation with you was a nice experience.

Special thanks goes to the colleagues from SABIC. Dear Dieter I want to thank you for your kind support and for having trust in me. Matthijs, thanks for your help, discussions and contribution during the finalization of the Thesis. Special thanks goes to

Frans, Rick, Jos, Aurora, Koen, Jesusović — you made my stay in SABIC pleasant!

Током ових година, стекао сам много нових пријатељстава која сматрам немерљиво вредним.

Драги Каћа и Жељко, на муци се познају јунаци. Леп изглед ове тезе је првенствено ваших руку дело — пуно вам хвала. Пријатељу Жељко, циљ је близу, мораш да издржиш још мало — сигуран сам да ћеш успети. Малецка, судбина је хтела да се на истом месту боримо за кору хлеба. Твој долазак у САБИК ми много значи јер знам да имам пријатеља и савезника раме уз раме. Драги Љубо, Блажо и Драгана, част је имати вас за Кумове.

Моја захвалност је упућена и породицама Потић (Биља и Горан), Живковић (Тијана и Жика), Поповић (Игор и Светлана), Смиљанић (Марко и Весна), Кузмановић (Борис и Јелена), Живковић (Зоран и Тања), Војчи и Софки, цимерима Дулету и Бокију, даље Тањи Т., Наташи, Драгану, Младену, Милошу, Михајлу, Јелени М., Ивани и Вилију, Филипу, Ђолету. Посебну захвалност дугујем Проф.Др. Александру Орловићу, драгом колеги и пријатељу са Технолошко–металуршког факултета.

Моји вољени Радивојци, овога успеха не би било да није било ваше Љубави и подршке. Маро, твоја љубав ми је увек инспирација. Воли вас Деки!

Sittard,
May 2008

Dejan Radivojević

Summary

Processes in the chemical industry convert readily available starting materials to more valuable product molecules. Catalytic materials are used in these processes to accelerate chemical transformations so that reactions proceed in a highly efficient manner, achieving high yields of desirable products and avoiding unwanted by-products. Compared to classical stoichiometric procedures, catalysts often allow more economical and environment-friendly production.

Development of heterogeneous catalysts for liquid the phase processes requires detailed knowledge about phenomena that occur on the catalyst surface during the catalytic reaction in liquid phase. Transient response techniques with detectors that can perform continuous, rapid, multi-component and simultaneous detection are ideal for such studies. However, there are hardly any transient techniques available that allow experimental investigation of the adsorption of reactants, intermediates and probe-molecules from liquid phase on the surface of catalysts. The existing liquid phase detectors are not able to detect more than one specie simultaneously and rapidly, making the more detailed study of the catalytic reaction mechanisms impossible.

The work described in this thesis focuses on development and application of a transient response technique for studies of adsorption and catalytic reactions over heterogeneous catalysts in liquid phase with Electro-Spray Ionization (ESI-MS) and Membrane Inlet Mass Spectrometry (MIMS) as detectors. Two test reactions, i.e. reduction of nitrite over Pt/SiO_2 and oxidation of glucose over Pt/CNF/Ni catalysts, were used to demonstrate that it is possible to monitor reactants, intermediates and products during reaction in (semi)quantitative manner. Nitrite hydrogenation is a relevant reaction for both nitrate to nitrogen de-nitrification of drinking water, as well as nitrate hydrogenation to hydroxyl-amine, an intermediate in the production of caprolactam. Oxidative conversion of glucose is important in view of the anticipated shift towards renewable feedstocks for the chemical industry. Glucose can be upgraded to more valuable compounds e.g. gluconic acid, a building block for production of chelating agents.

Transient technique requires a reactor module which is in some cases temperature

sensitive (i.e. polymeric coating of microreactors). *Chapter 2* discusses the results of the attachment of active phase (i.e. platinum) to a silica support under the mild conditions. Therefore, thermal stability in both oxidizing and reducing atmosphere of eight different precursors was studied with thermo-gravimetric analyses (TGA-MS). Based on these data, the precursors were tested to prepare silica supported catalysts, resulting in relationship between the thermal stability of the precursors, the procedures of impregnation, reduction and calcination with the final dispersion on silica. Platinum precursors decomposed more easily in reducing than in oxidizing environment, due to thermochemistry. Catalysts prepared by using ion-exchange and direct reduction in hydrogen resulted in highly dispersed platinum particles on silica. ($PtCl_x$) and (PtO_x) species, when present during catalyst preparation, cause sintering of platinum at temperatures higher than 250 °C ($PtCl_x$) and 350 °C (PtO_x), respectively. These species can be converted more easily in hydrogen than in air. $PtCl_4$, $H_2PtCl_6 \cdot 6\,H_2O$ and $H_2Pt(OH)_6$ are suitable as precursors for achieving high platinum dispersion, keeping temperatures below 150 °C.

Development of a novel, transient response technique for liquid phase heterogeneous catalytic studies, equipped with an Electron Spray Ionization Mass Spectrometry (ESI-MS) detector was described and results discussed in *Chapter 3*. The technique was successfully applied as an on-line method for real-time detection of species dissolved in aqueous product streams at the exit of a catalytic reactor. Two test reactions, nitrite reduction with Pt/SiO_2 and glucose oxidation with Pt/CNF/Ni were used to demonstrate semi-quantitative monitoring of reactants, intermediates and products. The capability of the novel technique is demonstrated by the fact that the ESI-MS detector is sufficiently sensitive to determine quantitatively extreme small amounts of physisorbing nitrite, down to 0.5 % of a monolayer on the Pt surface. Nitrite also reacts with pre-adsorbed hydrogen and the quantitative experimental result agrees with the fact that both nitrogen and ammonia are formed. The ESI-MS detector is able to distinguish between different components simultaneously, as was used in the case of glucose oxidation, demonstrating the most significant advantage over existing transient techniques. The limitation of ESI-MS is the inability to detect gases dissolved in liquids, due to the relatively mild ionization process via electrospray.

Chapter 4 describes and discusses development and the results obtained with a home-made analyzer for dissolved gasses in water, based on membrane inlet mass spectrometry (MIMS). It was successfully applied for the first time as an on-line method for detection of gases dissolved in an aqueous stream, at the exit of a catalytic reactor in a transient experiment. The technique was applied for measuring the metal dispersion of three different catalysts (EuroPt-1, Pt/SiO_2 and Pt/CNF) in liquid phase via H_2–O_2 titration. The titration stoicheometry obtained (i.e. ratio of H_2 and O_2 consumption) is in agreement with the stoicheometry obtained in gas phase titration experiments in literature. The platinum dispersions obtained in liquid phase are in excellent agreement with dispersions based on hydrogen chemisorption in gas phase for all three catalysts. Clearly, water does not influence the accessibility of the Pt atoms, disagreeing with recent suggestions in literature. In addition, the detector is universal and allows calibration of H_2, O_2, N_2 and Ar dissolved in water with insignificant cross contamination. Despite the relatively slow dynamic response of the detector (between 4 minutes for hydrogen up to more than 40 minutes for oxygen), it was proven possible to perform quantitative experiments in pulse mode, with a detection limit in the order of $0.5\,m^2$ Pt. The capability of this method is further demonstrated by the surprising observation that dissolved hydrogen physisorbs significantly on a reduced Pt catalyst whereas dissolved oxygen does not interact with an oxidized catalyst.

Chapter 5 discusses preparation and performances of the catalytic polymer membrane that is successfully prepared by incorporating mono-dispersed Pt/SiO_2 catalyst particles in an ethylene vinyl acetate copolymer (EVAL) porous matrix. This structure is successfully demonstrated as a reactor for the transient response technique. Addition of a relatively high concentration (65 wt%) of catalyst particles is preventing the formation of macro voids, improving both mechanical stability of the membranes as well as improving homogeneity of the liquid flow distribution through the membrane. The catalyst particles remain intact during the preparation procedure. The catalyst particles are physically immobilized throughout the membrane, entrapped in the pores, preventing channeling that would occur when flowing through an equivalent shallow fixed bed. Furthermore, the novel frozen-slurry-like morphology results in significant lower pressure drop as compared to a fixed bed with identical diameter and containing the same amount of catalyst particles allowing experiments in a broader window of operational conditions. The platinum particles are proven to be highly accessible in the swollen state, i.e. in liquid phase, as demonstrated both by the catalytic activity of the Pt/SiO_2 locked membranes for glucose oxidation as well as by the observation that H_2–O_2 titrations confirms that close to all Pt surface atoms contribute. The results also demonstrate the applicability of the titration method in liquid phase, enabling characterization of the catalytic membrane in the swollen state, i.e. under reaction conditions.

Finally, *Chapter 6* summarizes the work described in this thesis which clearly shows successful application of the transient response technique equipped with ESI-MS and MIMS to study adsorption and catalytic reactions in liquid phase. As such, ESI-MS and MIMS allow experimental investigation of the adsorption of reactants, intermediates and probe-molecules from liquid phase on the surface of catalysts during adsorption and reactions step in heterogeneous catalytic reaction in liquid phase.

Samenvatting

In de chemische industrie worden makkelijk winbare uitgangsstoffen omgezet in meer waardevolle producten. Bij deze omzettingen worden katalytische materialen gebruikt om de chemische transformaties te versnellen, en op deze manier hogere opbrengsten van de gewenste eindproducten te behalen. Tevens wordt de vorming van ongewenste bijproducten zoveel mogelijk beperkt. Vergeleken met klassieke stoichiometrische procedures, kan er dankzij katalysatoren vaak op een meer economische en milieuvriendelijke manier geproduceerd worden.

Voor de ontwikkeling van heterogene katalysatoren voor toepassing in vloeistoffen is gedetailleerde kennis nodig van de fenomenen die plaatsvinden op het katalysatoroppervlak tijdens de reactie. Zogenaamde transient response technieken, waarbij met detectoren continu en snel meerdere componenten tegelijk gemeten worden, zijn ideaal voor het bestuderen van dergelijke fenomenen. Bij deze technieken wordt de reactie van systeem op een plotselinge verandering van omstandigheden getest. Helaas zijn er nauwelijks technieken beschikbaar die experimenteel onderzoek mogelijk maken van de adsorptie van reactanten, tussenproducten, en specifieke testmoleculen vanuit de vloeistoffase op het katalysatoroppervlak. Bestaande detectoren voor gebruik in vloeistoffen kunnen slechts een enkele component volgen, waarbij de meetfrequentie aan de lage kant is. Hierdoor is het onmogelijk om katalytische reactiemechanismen in detail te bestuderen.

Het werk wat in dit proefschrift beschreven staat, focust op de ontwikkeling en toepassing van een transient response techniek voor het bestuderen van adsorptie en katalytische reacties op heterogene katalysatoren in de vloeistoffase. Hierbij zijn Electro Spray Ionization (ESI-MS) en Membrane Inlet Mass Spectrometry (MIMS) als detectiemethoden gebruikt. Twee reacties zijn als testreacties gebruikt, te weten: i) reductie van nitriet over een Pt/SiO_2 katalysator en ii) oxidatie van glucose over een Pt/CNF/Ni katalysator. Aangetoond is dat het mogelijk is om op een (semi) kwantitatieve manier zowel reactanten als tussen- en eindproducten te volgen tijdens een reactie.

Reductie van nitriet door middel van hydrogenering is een relevante reactie voor zowel de denitrificatie van drinkwater als de omzetting van nitraat naar hydroxylamine, wat een tussenproduct is in de productie van caprolactam. De oxidatieve omzetting van glucose is een belangrijke reactie in het kader van het toenemend gebruik van hernieuwbare grondstoffen in de chemische industrie. Glucose kan omgezet worden naar meer waardevolle producten, zoals gluconzuur, wat een bouwblok is voor chelaten.

Transient response technieken vereisen een reactor module die in sommige gevallen temperatuurgevoelig is (bijvoorbeeld vanwege een polymere coating). In *Hoofdstuk 2* worden resultaten bediscussieerd van de experimenten waarin de hechting van een actieve fase, zoals platina, op een silica drager is getest onder milde omstandigheden. Hiervoor is met behulp van thermogravimetrische analyse (TGA-MS) de thermische stabiliteit van acht verschillende precursoren bestudeerd in zowel een oxiderende als reducerende atmosfeer. Op basis van deze data zijn de precursoren getest om katalysatoren op een silica drager te maken. Dit heeft geresulteerd in relaties tussen aan de ene kant thermische stabiliteit van de precursoren, de procedure van impregnering, reductie en calcinatie, en aan de andere kant de mate van uiteindelijke dispersie op silica. Platina precursoren ontleedden makkelijker in een reducerende dan in een oxiderende omgeving, wat veroorzaakt werd door thermochemische effecten. Het bereiden van katalysatoren met behulp van ionenuitwisseling en directe reductie in waterstof, leidde tot sterk gedispergeerde platinadeeltjes op silica. De aanwezigheid van ($PtCl_x$) en (PtO_x) verbindingen tijdens de katalysatorbereiding zorgde voor het sinteren van platina bij temperaturen respectievelijk boven de 250 °C ($PtCl_x$) of 350 °C (PtO_x). Deze verbindingen konden makkelijker in waterstof geconverteerd worden dan in lucht. $PtCl_4$, $H_2PtCl_6 \cdot 6\,H_2O$ and $H_2Pt(OH)_6$ zijn geschikt als uitgangsstoffen voor hoge platina dispersiteiten bij temperaturen onder de 150 °C.

In *Hoofdstuk 3* wordt de ontwikkeling beschreven van een nieuwe transient response techniek voor het bestuderen van heterogene katalytische processen in de vloeistoffase op basis van Electro Spray Ionization Mass Spectrometry (ESI-MS). De techniek is succesvol toegepast als online methode voor real-time detectie van stoffen opgelost in een waterige productstroom aan de uitgang van een katalytische reactor. Twee testreacties, nitriet reductie met een Pt/SiO_2 katalysator en glucose oxidatie met een Pt/CNF/Ni katalysator zijn gebruikt om reactanten, tussenproducten en eindproducten semi-kwantitatief te monitoren. De ESI-MS detector is gevoelig genoeg om kwantitatief zeer lage hoeveelheden fysisch gesorbeerd nitriet te bepalen, tot op 0.5 % van een monolaag op een platina oppervlak. Nitriet reageert ook met voorgeadsorbeerd waterstof en de kwantitatieve experimentele resultaten komen overeen met het feit dat zowel stikstof als ammonia gevormd worden. Het is mogelijk om met de ESI-MS detector gelijktijdig onderscheid te maken tussen verschillende componenten, zoals is gedemonstreerd in de analyse van glucose oxidatie. Deze eigenschap vormt het meest significante voordeel van de ontwikkelde techniek ten opzichte van alternatieve technieken. De beperking van de detector ligt in het feit dat in de vloeistof opgeloste gassen niet gedetecteerd kunnen worden, doordat het bij electrospray gebruikte ionisatieproces relatief mild is.

Hoofdstuk 4 beschrijft de ontwikkeling van – en de verkregen resultaten met – een analysemethode voor opgeloste gassen in water, gebaseerd op membrane inlet mass spectrometry (MIMS). Voor de eerste keer is deze methode succesvol online ingezet aan het einde van een reactor in een transient experiment. De techniek is toegepast om de metaaldispersie van drie verschillende katalysatoren (EuroPt-1, Pt/SiO_2 and Pt/CNF/Ni) te bepalen in de vloeistoffase via H_2–O_2 titratie. De verkregen stoichiometrie (i.e. de ratio tussen H_2 and O_2 consumptie) komt overeen met de in de literatuur vermelde stoichiometrie voor titratie-experimenten in de gasfase. Bij alledrie de katalysatoren komen de waarden voor de dispersie van platina, zoals bepaald in de vloeistoffase, uitstekend overeen met die gebaseerd op waterstof chemisorptie in de gasfase. Het is duidelijk dat water de toegankelijkheid van de platina atomen niet beïnvloed, wat in tegenspraak is met enkele recente suggesties in de open literatuur. De gebruikte detector is verder universeel inzetbaar en te calibreren voor in water opgelost H_2, O_2, N_2 en Ar, zonder dat duidelijke effecten van cross-contaminatie zichtbaar worden. Ondanks de relatief langzame dynamische respons van de detector (tussen de 4 minuten voor waterstof tot 40 minuten voor zuurstof) is bewezen dat kwantitatieve experimenten in gepulseerde modus uitgevoerd konden worden, met een detectielimiet in de orde van 0.5 m^2 Pt. De analysemethode heeft verder geleid tot de verrassende observatie dat opgelost waterstof significante fysische adsorptie vertoont op gereduceerde platina katalysatoren, terwijl opgelost zuurstof geen interacties heeft met een geoxideerde katalysator.

In *Hoofdstuk 5* worden de bereiding en prestatie van katalytische polymeer membranen beschreven. Deze membranen kunnen succesvol geprepareerd worden door monodisperse Pt/SiO_2 katalysatordeeltjes te immobiliseren in een poreuze matrix van ethyleen vinyl acetaat copolymeer (EVAL). Dit mixed matrix concept is succesvol gebruikt als reactor voor de transient response techniek. De toevoeging van relatief hoge hoeveelheden katalysatordeeltjes (65 wt%) voorkomt de vorming van macrovoids in het membraan, waardoor zowel de mechanische stabiliteit als de homogeniteit van de vloeistofstromingsverdeling verbeterd worden. De katalysatordeeltje blijven intact tijdens de bereidingsprocedure en worden fysisch geimmobiliseerd door het gehele membraan. Hierdoor kan voorkeursstroming, zoals dikwijls optreedt in ondiepe vast bed reactoren, voorkomen worden. Bovendien resulteert de nieuwe morfologie, die als een soort bevroren slurrie beschouwd kan worden, in een significant lagere drukval in vergelijking met een vast bed reactor van dezelfde diameter en met dezelfde hoeveelheid deeltjes. Experimenten kunnen daardoor binnen een groter raamwerk van operationele condities uitgevoerd worden. De platinadeeltjes zijn goed toegankelijk in de gezwollen staat, i.e. in de vloeistoffase. Dit is gedemonstreerd door zowel de katalytische activiteit van de met Pt/SiO_2 beladen membranen in de oxidatie van glucose, als door de observatie in H_2–O_2 titraties dat bijna alle atomen aan het Pt oppervlak een bijdrage leveren. Deze laatste resultaten laten tevens de toepasbaarheid van de titratiemethode zien, waardoor karakterisering van het katalytische membraan in de gezwollen staat mogelijk is. Concreet betekent dit het kunnen bestuderen van het membraan onder reactie-omstandigheden.

Tenslotte wordt in *Hoofdstuk 6* een samenvatting gegeven van het werk dat beschreven staat in dit proefschrift. Hierbij blijkt duidelijk dat de transient response techniek op basis van ESI-MS en MIMS succesvol toegepast kan worden voor het bestuderen van adsorptie en katalytische reacties in de vloeistoffase. Dankzij ESI-MS en MIMS kunnen de adsorptie van reactanten, tussenproducten en specifieke testmoleculen vanuit de vloeistoffase naar het katalysatoroppervlak experimenteel worden onderzocht.

About the author

Dejan Radivojević was born on July 11th 1972 in Kraljevo, Serbia. After completing his education in Gymnasium with orientation in a natural sciences in 1991, he enrolled Chemical Engineering at the Faculty of Technology and Metallurgy at University of Belgrade. During the studies he was involved in various projects regarding the process development in oil industry. After graduation he was working in Lola Corporation (Belgrade) in the optimization of the bricks production.

In 1987 he received highly prestigious Belgrade Octobar Award for development of new telescope and student achievements in the field of astronomy.

In February 2003 he finished masters education in Catalytic Processes and Materials (CPM) group at University of Twente. Topic of his research was development of novel catalyst supports based on carbon nano fibre (CNF) to overcome mass transfer limitations in liquid phase catalytic reactions. During the same year, he started a PhD project in the same group, titled “Liquid phase heterogeneous catalysis — deeper insight; Novel transient response technique with ESI-MS as a detector”. Results of this research were presented in a number of conferences and published in top catalysis journals.

Since December 2006, he is working in SABIC Europe in Geleen. He is a member of Chemistry and Catalysis group which is the part of Research and Development. At the moment he is responsible for a number of projects which are aiming in optimization and development of catalytic processes.

List of publications and conference contributions

Journal publications

1. D. Radivojević, K. Seshan, and L Lefferts. Preparation of well-dispersed Pt/SiO_2 catalysts using low-temperature treatments. *Applied Catalysis A: General*, 301: 51–58, 2006.
2. D. Radivojević, K. Seshan, and L. Lefferts. Pt/SiO_2 catalyst preparation: High platinum dispersions by using low-temperature treatments. *Studies in Surface Science and Catalysis*,162:529–536, 2006.
3. D. Radivojević, M. Ruitenbeek, K. Seshan, and L. Lefferts. Development of a transient response technique for heterogeneous catalysis in liquid phase, Part1: Electron Spray Ionization Mass Spectrometry (ESI-MS) as detector. *Accepted for publication in Journal of Catalysis.*
4. D. Radivojević, M. Ruitenbeek, K. Seshan, and L. Lefferts. Development of a transient response technique for heterogeneous catalysis in liquid phase, Part 2: Membrane Inlet Mass Spectrometry (MIMS) as detector for dissolved gasses. *Accepted for publication in Journal of Catalysis.*
5. D. Radivojević, M. Avramescu, M. Wessling, K. Seshan, and L. Lefferts. Frozen slurry catalytic reactor; a new structured catalyst for transient studies in liquid-phase. *Submitted to Applied Catalysis A.*
6. J. de Jong, D. Radivojević, L. Lefferts, R.G.H. Lammertink, and M. Wessling. Preparation of porous polymeric coatings in micro channels. *In preparation.*

Conference presentations

- **2008**
  - Oral presentation titled “Transient response technique for heterogeneous catalysis in liquid phase” at 14th International Congress on Catalysis (ICC), Seoul, Korea
- **2006**
  - Oral presentation titled “New approach to follow transients in liquid phase - Application to heterogeneous catalytic systems” at Nederlands Chemistry and Catalysis Conference VII (NCCC7), Noordwijkerhout, the Netherlands
  - Poster presentation titled “Preparation of well-dispersed Pt/SiO_2 catalysts using low-temperature treatments” at the Scientific Bases for the Preparation of Heterogeneous Catalysts 9th Int. Symposium, Louvain-la-Neuve, Belgium
- **2005**
  - Poster presentation titled “Low - temperature preparation of Pt/SiO_2 catalyst” at the Nederlands Chemistry and Catalysis Conference VI (NCCC6), Noordwijkerhout, the Netherlands

ISBN 978-90-365-2667-8